FRA-81-1

REPORT NO. FRA/ORD-81/11

RAIL PASSENGER VEHICLE TRUCK DESIGN METHODOLOGY

D. Wormley
K. Hedrick
D. Horak
C. Bell

MASSACHUSETTS INSTITUTE OF TECHNOLOGY
DEPARTMENT OF MECHANICAL ENGINEERING
Cambridge MA 02139

JANUARY 1981

FINAL REPORT

Prepared for

U.S. DEPARTMENT OF TRANSPORTATION
FEDERAL RAILROAD ADMINISTRATION
Office of Research and Development
Washington DC 20590

Technical Report Documentation Page

1. Report No.	2. Government Accession No.	3. Recipient's Catalog No.
FRA/ORD-81/11		

4. Title and Subtitle	5. Report Date
RAIL PASSENGER VEHICLE TRUCK DESIGN METHODOLOGY	January 1981
	6. Performing Organization Code
7. Author(s)	8. Performing Organization Report No.
Wormley, D., Hedrick, K., Horak, D., Bell, C.	DOT-TSC-FRA-81-1
9. Performing Organization Name and Address	10. Work Unit No. (TRAIS)
Massachusetts Institute of Technology* Department of Mechanical Engineering Cambridge MA 02139	RR030/R1312
	11. Contract or Grant No.
	DOT-TSC-1471
	13. Type of Report and Period Covered
12. Sponsoring Agency Name and Address	Final Report Dec. 1978-Nov. 1979
U.S. Department of Transportation Federal Railroad Administration Office of Research and Development Washington DC 20590	14. Sponsoring Agency Code

15. Supplementary Notes

*Under contract to: U.S. Department of Transportation
Research and Special Programs Administration
Transportation Systems Center
Cambridge MA 02142

16. Abstract

A procedure for the selection of rail passenger truck design parameters to meet dynamic performance indices has been developed. The procedure is based upon partitioning the design task into three trade-off studies: (1) a vertical ride quality-secondary stroke trade-off, (2) a lateral ride quality-second stroke trade-off, and (3) a stability-curving trade-off. The procedure is illustrated with the selection of design parameters for an intercity 130-mph vehicle and an urban 80-mph vehicle.

17. Key Words	18. Distribution Statement
Rail Vehicle Dynamics Passenger Truck Design	DOCUMENT IS AVAILABLE TO THE PUBLIC THROUGH THE NATIONAL TECHNICAL INFORMATION SERVICE, SPRINGFIELD, VIRGINIA 22161

19. Security Classif. (of this report)	20. Security Classif. (of this page)	21. No. of Pages	22. Price
UNCLASSIFIED	UNCLASSIFIED	190	

Form DOT F 1700.7 (8-72) Reproduction of completed page authorized

Preface

The research described in this report was sponsored by U.S. Department of Transportation, Federal Railroad Administration. The project was directed by the Transportation Systems Center, U.S. Department of Transportation. Richard Scharr, FRA; and Raymond Ehrenbeck, TSC, How Wong, TSC, and Kevin Yearwood, TSC, provided technical direction for the research.

METRIC CONVERSION FACTORS

Approximate Conversions to Metric Measures

Symbol	When You Know	Multiply by	To Find	Symbol
	LENGTH			
in	inches	*2.5	centimeters	cm
ft	feet	30	centimeters	cm
yd	yards	0.9	meters	m
mi	miles	1.6	kilometers	km
	AREA			
in^2	square inches	6.5	square centimeters	cm^2
ft^2	square feet	0.09	square meters	m^2
yd^2	square yards	0.8	square meters	m^2
mi^2	square miles	2.6	square kilometers	km^2
	acres	0.4	hectares	ha
	MASS (weight)			
oz	ounces	28	grams	g
lb	pounds	0.45	kilograms	kg
	short tons (2000 lb)	0.9	tonnes	t
	VOLUME			
tsp	teaspoons	5	milliliters	ml
Tbsp	tablespoons	15	milliliters	ml
fl oz	fluid ounces	30	milliliters	ml
c	cups	0.24	liters	l
pt	pints	0.47	liters	l
qt	quarts	0.95	liters	l
gal	gallons	3.8	liters	l
ft^3	cubic feet	0.03	cubic meters	m^3
yd^3	cubic yards	0.76	cubic meters	m^3
	TEMPERATURE (exact)			
°F	Fahrenheit temperature	5/9 (after subtracting 32)	Celsius temperature	°C

*1 in = 2.54 (exactly). For other exact conversions and more detailed tables, see NBS Misc. Publ. 286, Units of Weights and Measures, Price $2.25, SD Catalog No. C13.10:286.

Approximate Conversions from Metric Measures

Symbol	When You Know	Multiply by	To Find	Symbol
	LENGTH			
mm	millimeters	0.04	inches	in
cm	centimeters	0.4	inches	in
m	meters	3.3	feet	ft
m	meters	1.1	yards	yd
km	kilometers	0.6	miles	mi
	AREA			
cm^2	square centimeters	0.16	square inches	in^2
m^2	square meters	1.2	square yards	yd^2
km^2	square kilometers	0.4	square miles	mi^2
ha	hectares (10,000 m^2)	2.5	acres	
	MASS (weight)			
g	grams	0.035	ounces	oz
kg	kilograms	2.2	pounds	lb
t	tonnes (1000 kg)	1.1	short tons	
	VOLUME			
ml	milliliters	0.03	fluid ounces	fl oz
l	liters	2.1	pints	pt
l	liters	1.06	quarts	qt
l	liters	0.26	gallons	gal
m^3	cubic meters	35	cubic feet	ft^3
m^3	cubic meters	1.3	cubic yards	yd^3
	TEMPERATURE (exact)			
°C	Celsius temperature	9/5 (then add 32)	Fahrenheit temperature	°F

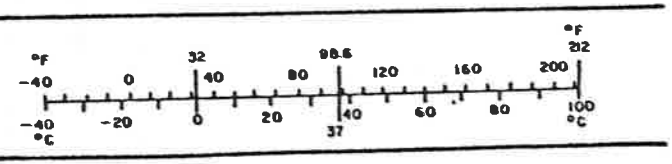

CONTENTS

CONTENTS (Concl'd)

ILLUSTRATIONS

ILLUSTRATIONS (Cont'd)

ILLUSTRATIONS (Cont'd)

ILLUSTRATIONS (Concl'd)

TABLES

NOMENCLATURE

Symbol	
a	half of wheelset contact distance
a_{11}	wheelset roll coefficient
ACC_L	average RMS lateral acceleration in the carbody, g's. (the average of the values at the leading end, the c.g. and the trailing end passenger locations) See Equation 4.6-11.
ACC_L^*	the desired value of ACC_L
ACC_v	average RMS vertical acceleration in the carbody, g's. (the average of the values at the leading end, the c.g. and the trailing end passenger locations)
ACC_v^*	the desired value of ACC_v
b	half of wheelbase
C_{px}	primary longitudinal damping (4 per truck)
C_{py}	primary lateral damping (4 per truck)
C_{pz}	primary vertical damping (4 per truck)
C_b	primary bending damping ($=d_p^2 C_{px}$)
C_s	primary shear damping
C_{sy}	secondary lateral damping (2 per truck)
C_{sz}	secondary vertical damping (2 per truck)
$C_{s\psi}$	secondary yaw damping (1 per truck)
d_p	half of primary spring spacing (lateral)
d_s	half of secondary spring spacing (lateral)
f_n	natural frequency, Hz
f_{11}	lateral creep force coefficient
f_{12}	lateral spin creep force coefficient
f_{22}	spin creep force coefficient
f_{33}	longitudinal creep force coefficient
h	distance from top of rail to vehicle cg.
h_{tp}	vertical distance from truck cg to primary springs
h_{ts}	vertical distance from truck cg to secondary springs

h_{cs}	vertical distance from carbody cg to secondary springs
I_{cx}	roll moment of inertia of carbody
I_{cy}	pitch moment of inertia of carbody
I_{cz}	yaw moment of inertia of carbody
I_{tx}	roll moment of inertia of truck frame
I_{ty}	pitch moment of inertia of truck frame
I_{tz}	yaw moment of inertia of truck frame
I_{wx}	roll moment of inertia of wheelset
I_{wy}	pitch moment of inertia of wheelset
I_{wz}	yaw moment of inertia of wheelset
K_{px}	primary longitudinal stiffness (4 per truck)
K_{py}	primary lateral stiffness (4 per truck)
K_{pz}	primary vertical stiffness (4 per truck)
K_b	primary bending stiffness ($=d_p^2 K_{px}$)
K_{sy}	secondary lateral stiffness (2 per truck)
K_{sz}	secondary vertical stiffness (2 per truck)
$K_{s\psi}$	secondary yaw stiffness (1 per truck)
ℓ_s	half of truck center pin spacing
ℓ_e	distance from car cg to car geometric center (long.)
ℓ_c	total length of carbody
M_c	mass of carbody
M_t	mass of truck frame
M_w	mass of wheelset
M_v	total vehicle mass
N_i	total load on ith axle including wheelset weight
PS	RMS primary lateral suspension stroke, inches. See Equation 4.6-5
r_o	centered wheel rolling radius
ST_L	average RMS secondary lateral suspension stroke, inches (the average of the values at the leading end and the trailing end) See Equation 4.6-13
ST_L^*	the desired value of ST_L

ST_v	average RMS secondary vertical suspension stroke, inches. (the average of the values at the leading end and the trailing end)
ST_v^*	the desired value of ST_v
$T_{s\psi}$	secondary Coulomb breakaway torque
W_v	total vehicle weight
WE	RMS wheelset excursion, inches. See Equation 4.6-7
δ_o	centered wheelset contact angle
Δ	contact angle difference coefficient
λ	wheel conicity
ξ	damping ratio
ϕ_{se}	superelevation
ϕ_d	cant deficiency.

1. INTRODUCTION

1.1 Background

In the next decade the construction of a significant number of new intercity rail passenger cars is planned to meet the projected needs of intercity passenger service [1].* Guidelines for the performance specification of these cars and for their design are needed so that meaningful specifications tailored to specific types of applications can be developed. In the past fifty years an extensive body of literature has been written related to the performance of rail cars and in recent years a number of computer aided analyses have been developed to aid in the evaluation of rail car performance [2-38]. This background literature does not contain in a single document a systematic procedure for determining first the performance capability specifications and second the primary car and truck parameters required to meet these specifications. The literature does provide a strong basis for the development of a set of initial guidelines for specification of performance and basic design parameters. The scope of this study is to develop design guidelines as outlined in the following section.

1.2 Scope and Objectives

The principal objective of this study is to develop general design procedures for conventional rail passenger cars to meet dynamic performance requirements. These performance requirements include:

---

*Numbers in [ ] refer to references listed in the References.

- Ride Quality - The acceleration environment in the passenger compartment resulting from the vehicle response to track irregularities

- Stability - The lateral stability or hunting propensity of the vehicle

- Curve Negotiation - The ability of the vehicle to negotiate a constant radius curve at constant speed without wheelslip or strong flange contact.

The general design procedures developed are applicable to powered and unpowered rail cars; however, all detailed data and specific design charts are developed for unpowered, conventional passenger cars. The study focuses upon performance in terms of the dynamic criteria listed above and results in selection of truck suspension stiffness and damping wheel profile, secondary suspension stiffness and carbody inertial parameters to meet the dynamic performance specifications.

The study is limited in scope and has not considered the design factors involving braking systems and car couplers. The detailed considerations involving motor mounting and drivetrains for powered cars have not been addressed in this study. While the study has considered conventional truck configurations, the general procedures developed including the use of specific design charts may be extended directly to general types of radial truck configurations as described in reference [39].

In Chapter 2 of this report general passenger vehicle configurations considered are described in detail and the basic para-

meters which are established in the design procedure are identified. The dynamic performance measures and methods used to compute these measures are described in Chapter 3. Vehicle dynamic performance is determined using computer simulations models and data derived from these models. These models have been derived as described in reference [39] using state-of-the-art information from the rail dynamics literature. The models employed are primarily linear and thus are useful for establishing the overall levels of performance for rail passenger vehicles and for developing general levels of design specifications. For highly detailed analysis of a specific vehicle's performance, nonlinear models are more appropriate and are recommended. None of the linear or the nonlinear models cited in the literature have been fully validated with experimental data for rail passenger vehicles. While the models used in this study have been developed specifically to represent the dominant physical characteristics of rail passenger trucks and carbodies, they also have not been validated with experimental data. Development of validated rail passenger vehicle models is recommended as a high priority research task.

The methodology used to develop design and performance guidelines is described in Chapter 4. It is based upon the use of design charts and requires calculations which can be performed with desk-top calculators. The procedure results in the determination of truck and carbody parameters required to meet specified dynamic performance specifications. It can also be utilized to determine if a set of dynamic performance specifications cannot be met with a conventional truck design. The procedure is illustrated in Chapter 4 with several design examples.

2. PASSENGER CAR-TRUCK CONFIGURATIONS

2.1 Introduction

The passenger truck embodies the suspension system of a rail vehicle and conventionally consists of the complete assembly of wheels, axles, truck frame and suspension elements. Track inputs drive the wheelsets which in turn excite the primary suspension elements, the truck frame, the secondary suspension elements and the carbody. The direct and feedback force paths are shown in Figure 2.1.1 while the primary suspension components are illustrated in Figure 2.1.2.

The performance functions a suspension must provide include:

1) Vehicle support under a variety of operational conditions

2) Guidance of the vehicle on both tangent and curved track with good tracking capability

3) Transmission of braking and traction forces from the track to the carbody

4) Dynamic stability on tangent, curved and spiral track

5) Effective isolation of the carbody from vibration induced by track irregularities

6) Control of wheel-rail forces in order to minimize wear and damage to the track and vehicle components.

These performance functions often place conflicting demands upon rail truck design since design parameters which may be altered to improve performance in one area may simultaneously reduce performance in another area. To identify the design parameters which are available in conventional trucks to meet performance requirements, a review of truck design is conducted in the section below.

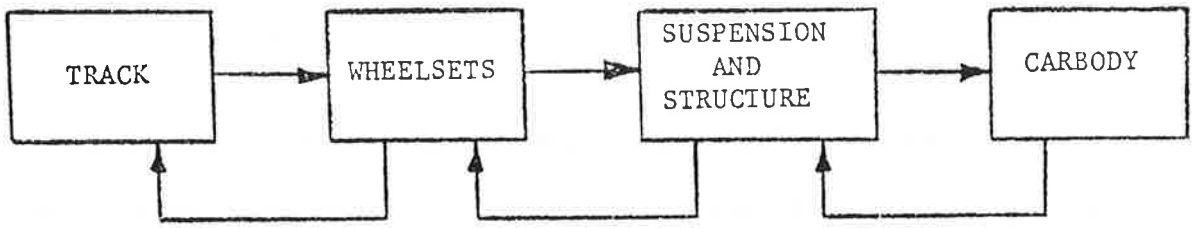

FIGURE 2.1.1: LOAD PATHS OF A TRUCK

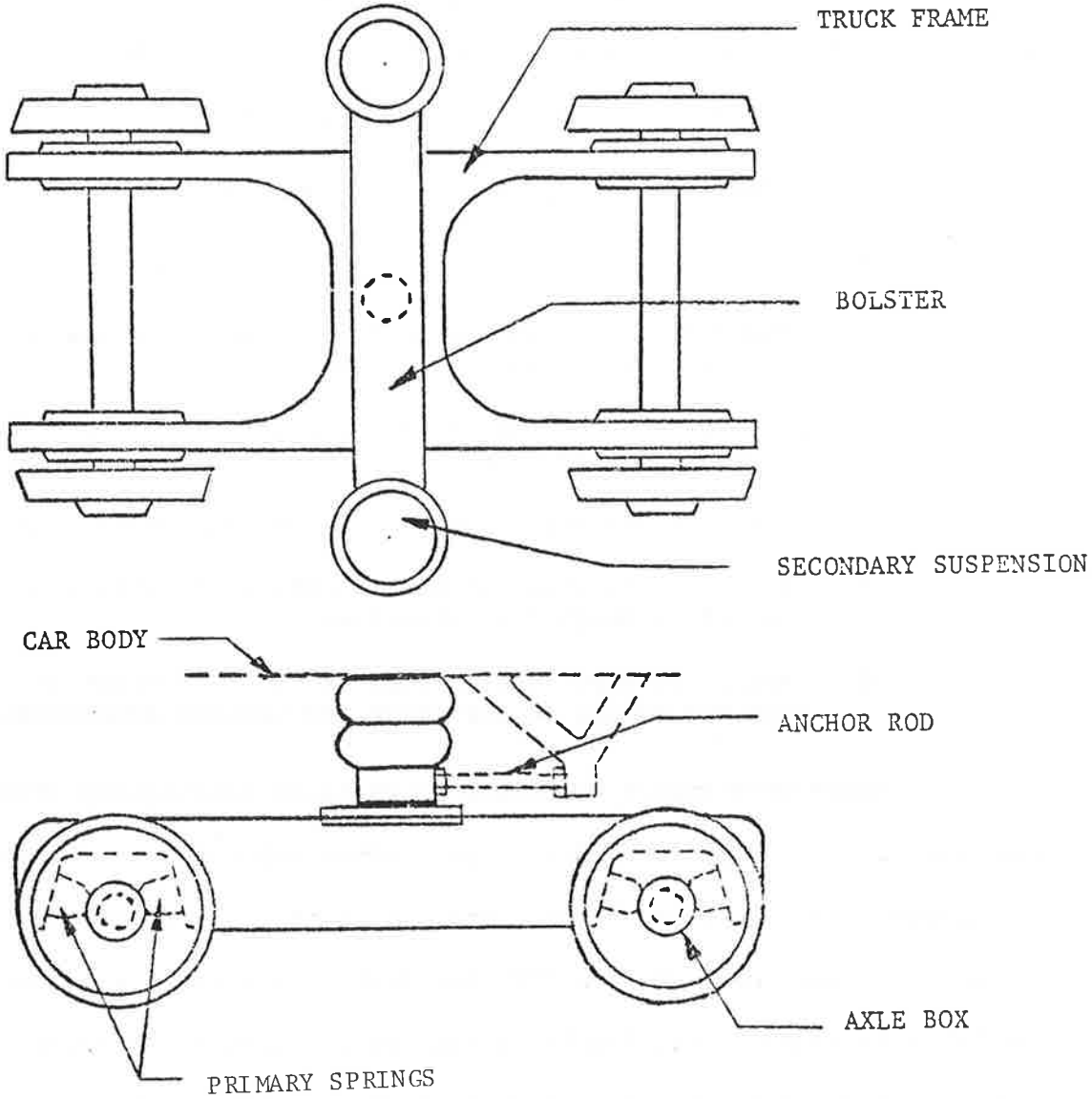

FIGURE 2.1.2: PASSENGER TRUCK CONFIGURATION

2.2 Description of Conventional Trucks

2.2.1 Unpowered Trucks

The main components of a conventional unpowered truck are wheelsets, primary suspension elements, truck frame and secondary suspension elements as shown schematically in Figure 2.1.2.

a) Wheelsets:

The wheelset is the fundamental, common component of all rail vehicles. In the usual configuration profiled wheels are rigidly connected to the axle, ensuring that both wheels rotate at the same angular velocity. The kinematics and dynamics of wheel/rail interactions have a strong influence on the dynamic performance of trucks. The wheelset is connected to the truck frame through the primary suspension elements.

b) Truck Frame

The truck frame is the main structural member of the truck. In most conventional truck designs an H-shaped frame is used and the wheelsets are connected directly to the frame through primary suspension elements. Wheel load equalization is usually achieved by using a split or "articulated" H-frame, or if the H-frame is rigid, by allowing sufficient compliance in the primary vertical suspension. Some trucks employ a separate equalizer sub-frame which consists of two equalizer bars connected directly between the wheelset bearing boxes along each side of the truck. The subframe is connected to the truck frame through primary suspension elements.

c) Primary Suspension

The suspension between the wheelsets and the truck frame is the primary suspension. The elements are generally quite stiff and often take the form of rubber rings or Chevron-shaped rubber mounts which encase the axle bearing boxes and provide longitudinal, lateral, and vertical support. In some trucks such as those employing equalizer bars, coil springs are used to connect the wheelsets to the truck frame. Vertical primary dampers are also sometimes employed in primary suspensions, particularly in conjunction with the coil springs.

d) Secondary Suspension

The secondary suspension generally consists of the springs, dampers, and the bolster assembly which connects the carbody to the truck frame; the bolster is a structural member which straddles the truck and carries the load of the carbody from the secondary springs to the centerplate and side pads of the truck frame. In contrast to the primary suspension elements, secondary lateral and vertical elements are relatively soft to provide adequate vibration isolation between the truck and the carbody.

Secondary vertical stiffness is often provided by coil springs, air springs, or a combination of the two. Secondary lateral stiffness is often provided by the transverse stiffness of the vertical springs in combination with the lateral contribution from the anchor rod bushings. On some trucks swing links or rubber pads are used for the lateral stiffness.

Damping is achieved with either hydraulic or air orifice dampers in the vertical direction and with hydraulic dampers or rubber dissipation in the lateral direction.

The secondary longitudinal suspension consists of anchor rods, one on each side of the truck, which carry longitudinal loads between stiff rubber bushings on the carbody and the bolster; and the centerpin, which carries the longitudinal loads from the bolster to the truck frame. Curve negotiation is achieved by allowing the truck frame to rotate in yaw with respect to the bolster against the frictional resistance provided by the centerplate and side pads. The stiff longitudinal suspension of a rail vehicle requires no special damping elements. However, longitudinally oriented hydraulic dampers are sometimes used to provide viscous damping in yaw between the bolster and the truck frame either to supplement or as an effective alternative to the frictional damping.

Finally, special secondary suspension elements are sometimes used to constrain carbody motion in roll, such as anti-roll bars or tilting mechanisms.

A summary of the primary and secondary suspension elements used in an international sample of conventional truck designs is given in Table 2.2.1. The superscript (*) indicates that the stiffness in the lateral or longitudinal direction is provided by the vertical suspension element.

TABLE 2.2.1: TRUCK SUSPENSION ELEMENTS

Train or Truck		PRIMARY SUSPENSION			SECONDARY SUSPENSION		
		Vertical	Lateral	Longitudinal	Vertical	Lateral	Longitudinal
GERMAN	ET 403	Coil Spring & Hydr. Damper	Elastic Links	Elastic Links	Air Spring & Hydr. Damper	Rubber Blocks & Hydr. Damper	Rubber Rod Bushings
GERMAN	Minden Deutz	Coil Spring & Hydr. Damper	Rubber Blocks	Rubber Bushings	Coil Spring & Hydr. Damper	Swing Links & Rubber Stops	Rubber Rod Bushings
JAPAN	DT 200	Coil Spring & Hydr. Damper	Rubber Blocks	Rubber Bushings	Air Spring & Orifice Damping	Air Spring* & Hydr. Damper	Anchor Rod Bushings
CANAD.	LRC	Chevron-Spring & Hydr. Damper	Chevron Spring	Chevron Spring	Air Spring	Rubber Pads & Hydr. Damper	Anchor Rod Bushings
BRITISH	BT-10	Coil Spring & Hydr. Damper	Rubber Bushings	Rubber Bushings	Air Spring & Hydr. Damper	Swing Links & Hydr. Damper	Rubber Rod Bushings
RUSSIAN	ER 200	Coil Spring & Flexible Conn. & Hydr. Damper	Coil Spring* & Flexible Conn.	Coil Spring* & Flexible Conn.	Air Spring & Hydr. Damper	Air Spring* & Hydr. Damper	Anchor Rod Bushings
U.S.A.	Budd Corp. PIII	Rubber Rings	Rubber Rings	Rubber Rings	Air Coil Spring & Hydr. Damper	Air & Coil Spring* & Stabilizer Rubber Spacers and Hydr. Damper	Anchor Rod Bushings Air & Coil Spring* & Dry Friction
U.S.A.	GSI Comp. G-70	Coil Spring	Coil Spring*	Coil Spring*	Air Coil Spring & Hydr. Damper	Air & Coil Spring* & Hydr. Damper	Anchor Rod Bushings & Dry Friction

TABLE 2.2.1 (Concl'd)

Train or Truck		PRIMARY SUSPENSION			SECONDARY SUSPENSION		
		Vertical	Lateral	Longitudinal	Vertical	Lateral	Longitudinal
FRENCH	Y-28	Coil Spring & Rubber Blocks	Rubber Blocks	Rubber Blocks	Coil Spring & Hydr. Damper	Swing Links & Hydr. Damper	Rubber Connections
	Y-32	Coil Spring & Hydr. Damper	Rubber Connections	Rubber Connections	Coil Spring & Hydr. Damper	Coil Spring* & Hydr. Damper	Anchor Rod Bushings
	Y-224	Coil Spring & Hydr. Damper	Rubber Bush Links	Rubber Bush Links	Coil Spring & Rubber Hydr. Damper	Coil Spring* & Rubber Hydr. Damper	Rubber Bushed Rods & Hydr. Damper
	Y-225	Coil Spring & Rubber Hydr. Damper	Rubber Bush Links	Rubber Bush Links	Sumiride Air Spring & Damper	Metal Rubber Sandwich & Hydr. Damper	Rubber Bushed Rods
	Y-226	Coil Spring & Hydr. Damper	Steel & Rubber Rings	Steel & Rubber Rings	Coil Spring & Hydr. Damper	Coil Spring* Rubber Conn. & Hydr. Damper	Coil Spring & Rubber Conn.* Hydr. Damper
ITALIAN	Fiat Eurofa	Coil Spring & Hydr. Damper	Rubber Connections	Rubber Connections	Coil Spring & Hydr. Damper	Coil Spring* Rubber Bushing & Hydr. Damper	Coil Spring* & Rubber Busings
	Z-1040	Coil Spring & Rubber Arrangement	Coil Spring & Rubber Arrangement	Coil Spring & Hydr. Damper	Coil Spring & Hydr. Damper	Swing Links & Hydr. Damper	Rubber Rod Bushings

2.2.2 Powered Trucks

a) Configuration

A powered truck contains electric motors, reduction gears and driving gears in addition to the components of an unpowered truck. The powered trucks used today may be divided into three groups, according to the way the traction equipment is attached to the truck frame and to the wheelsets.

b) Trucks with Axle-Hung Traction Units

This design is shown schematically in Figure 2.2.1. The motor, the reduction gear and the driving gear are one rigid unit. The unit is supported on the axle on bearings, and hung from the truck frame at several points, through rubber. Since traction motors are sensitive to rail-induced vibrations, many high speed trucks have vibrational isolators between the elements through which track forces can propagate. In the most general case there are rubber isolators between the axle and the driving gear, and between the driving gear and the motor, in addition to the rubber suspension between the motor and the truck frame.

c) Truck with Frame-Mounted Motors

This design is shown in Figure 2.2.2. The driving gear is supported on the axle on bearings, and hung from the truck through rubber. The motor is supported from the truck frame at several points. The driving torque is transmitted from the motor to the gear through a flexible coupling, which is capable of operation under misalignment

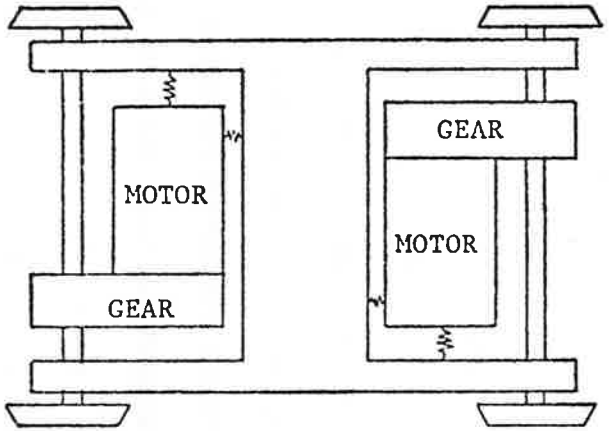

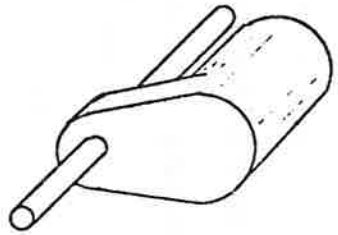

FIGURE 2.2.1: TRUCK WITH AXLE-HUNG TRACTION UNIT

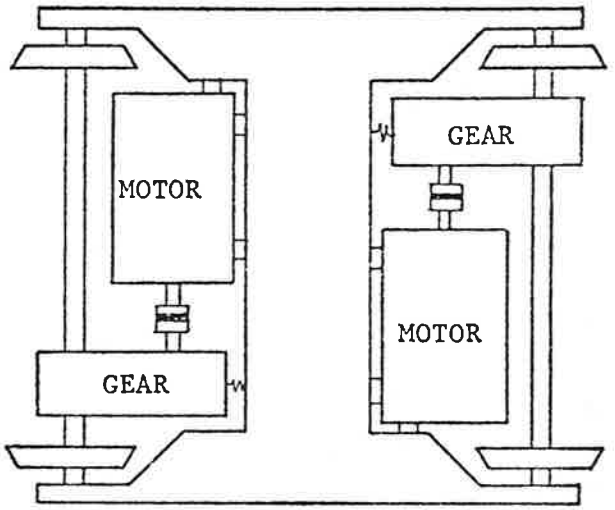

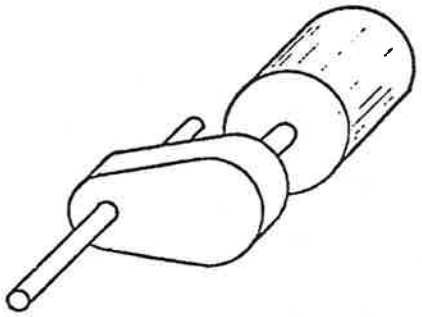

FIGURE 2.2.2: TRUCK WITH FRAME-MOUNTED UNIT

of several degrees. The flexible coupling reduces the rail-induced vibrations transmitted to the motor through the gear. Trucks with a frame mounted motor minimize the axle mass of the truck and, therefore, are suitable for high speed operation. However, in some cases they cannot be used because of space limitations and most inside-frame trucks have axle-hung traction units.

d) Monomotors

Monomotors are trucks in which a single truck frame mounted motor drives both axles, by means of two driving gears. They are usually symmetric. Very few current trucks are monomotors.

2.3 Passenger Truck Representation in Terms of Fundamental Design Parameters

The fundamental design parameters of a passenger truck may be identified by developing a conceptual model of the truck from the general characteristics described above. A model is developed in the following paragraphs to predict the dynamic performance criteria cited above. The model represents a compromise between the requirements for simplicity so that results may be easily interpreted for use in design studies and complexity so that detailed performance characteristics may be represented accurately. The model developed has been shown to be useful in previous truck parametric studies and can be extended directly to new types of radial truck configurations [39]. The model described below is representative of conventional, unpowered truck configurations. Addition of degrees of freedom to represent motor motions, would permit the model to be extended directly to powered trucks.

The basic truck model used in the design study is illustrated in Figure 2.3.1. Two rigid wheelsets are connected to the truck frame with lateral, longitudinal and vertical stiffness and damping elements. In the model these primary suspension elements are assumed to be linear stiffness and damping elements. Secondary suspension longitudinal suspension is represented as a linear stiffness and damper for small motions which occur if the centerplate and bolster do not breakaway while if the forces are sufficient to result in breakaway, a dry friction representation is used.* The relationship of the model to a specific passenger truck is illustrated in Table 2.3.1.

TABLE 2.3.1: CORRESPONDENCE BETWEEN MODEL AND PIONEER III PASSENGER TRUCK

	VERTICAL	LATERAL	LONGITUDINAL
Primary Suspension System	Stiffness of rubber ring around the axle boxes	Stiffness of rubber ring around the axle boxes	Stiffness of rubber ring around the axle boxes
Secondary Suspension System	Vertical stiffness of air and coil springs, vertical stiffness of side bearer pads, and vertical hydraulic damper	Lateral stiffness of air and coil springs, stiffness of stabilizer rod rubber spacers, hydraulic damper and lateral stiffness of anchor rods	Longitudinal stiffness of anchor rod bushings and longitudinal stiffness of air and coil springs, friction at side bearers and at center pivot

*A detailed discussion of the effects of breakaway is included in Chapter 4.

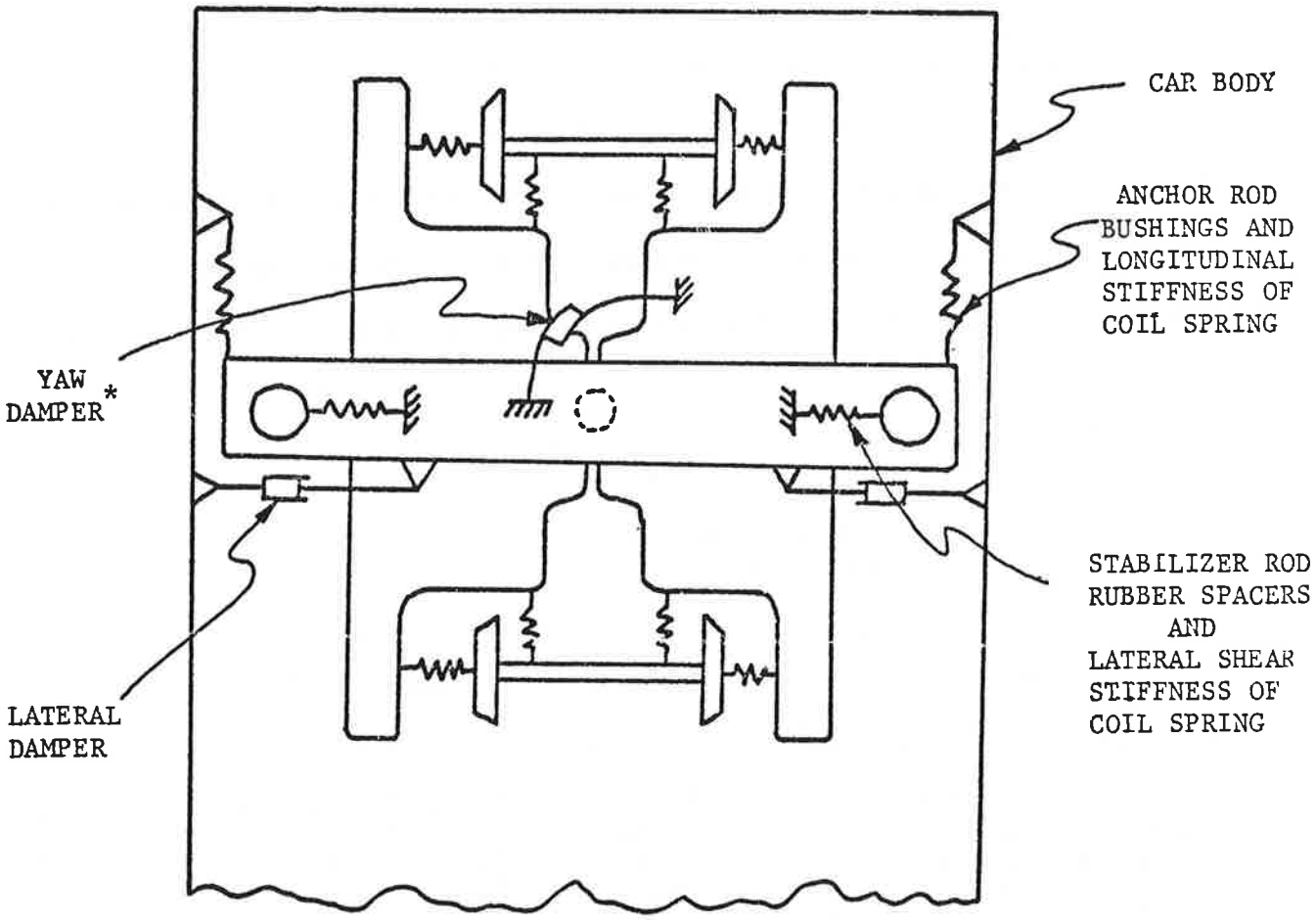

*Yaw damper represents dry friction at centerplate and side bearings

FIGURE 2.3.1: PASSENGER TRUCK MODEL

3. PASSENGER VEHICLE PERFORMANCE MEASURES AND CONSTRAINTS

3.1 Introduction

The design performance of rail passenger vehicles is broadly defined in terms of safety and productivity. Safety as it relates to the vehicle-track system is considered primarily in terms of derailment. Derailments result from a variety of sources including equipment failure, poor track conditions, train operation and make-up as well as dynamic conditions such as hunting and curving. In this study, safety in terms of derailment is considered in terms of train lateral dynamic motions which lead to wheel climb and represent conditions with a high propensity for the wheel to climb over the rail head.

The productivity of a rail passenger vehicle is a function of its revenue and operation, maintenance and capital costs. These are directly influenced by vehicle operating speed, passenger ride quality and wheel-track forces which result in wear and degradation of vehicles and track.

In this development of design guidelines, the issues of safety and productivity as they relate to vehicle dynamic performance are addressed by defining a set of dynamic performance indices and a set of associated dynamic constraints. The specific performance indices which have been selected are described in detail in the following section and include quantitative measures of:

- ride quality
- vehicle curve negotiation capability
- vehicle stability.

The performance indices are evaluated as a function of variations in vehicle design parameters while the following constraints, which are described quantitatively in a following section, are satisfied:

- maximum allowable clearance between the vehicle and wayside fixed structures
- minimum allowable level of wheel load equalization
- maximum allowable suspension stroke
- maximum allowable wheelset excursion
- maximum allowable lateral/vertical force.

3.2 Performance Indices

3.2.1 Ride Quality

The passengers' perception of ride comfort is a subjective evaluation of many factors including vibration, noise, temperature, and passenger compartment features. In this study the dynamic vibration environment is considered primarily and in particular the vibration resulting from excitation of the vehicle due to track irregularities. These are numerous quantitative descriptors [26,27] that have been used to describe rail passenger ride quality. In this study two measures have been adopted for design goals: the root mean square (r.m.s.) acceleration levels and the distribution of the r.m.s. acceleration in one third octave frequency bands are described in the I.S.O. guidelines [28] for vertical and lateral motion and in [29] for roll motion.

Figure 3.2.1 illustrates the I.S.O. recommended limits for the vertical and lateral 1 hour reduced comfort boundaries. When the vehicle vibration environment is broad band, i.e., has a frequency content over a wide range, the recommended procedure is to compute the r.m.s. accel-

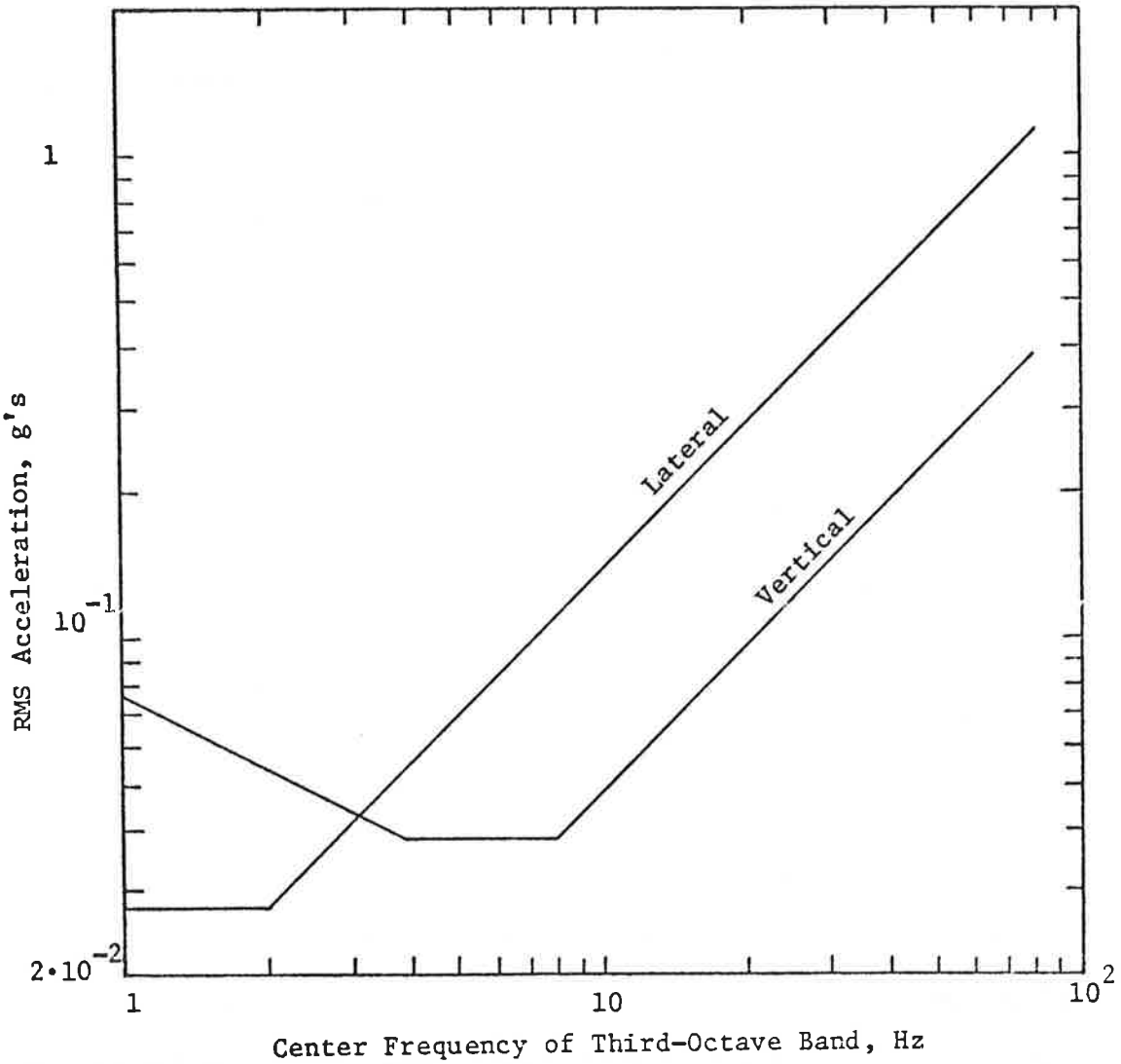

FIGURE 3.2.1: LATERAL AND VERTICAL ACCELERATION LIMITS AS A FUNCTION OF FREQUENCY FOR 1 HOUR EXPOSURE TIME; "REDUCED COMFORT BOUNDARY" (Reference 28)

eration in 1/3 octave frequency bands and to compare it to Figure 3.2.1 at the 1/3 octave center frequency.

Figure 3.2.2 [29] shows roll equal discomfort curves where DISC = 1 corresponds to the threshold of discomfort and DISC = 2 provides twice the level of discomfort as DISC = 1. In the Figure r.m.s. roll angular acceleration (rad/sec^2) is computed as a function of frequency for sinusoidal excitation.

The ride quality criteria adopted in this study have been general passenger acceptance levels. The parametric study data are presented in terms of these criteria; however, the data can also be expressed in terms of alternate criteria should other criteria prove to be more appropriate for a specific situation.

3.2.2 Vehicle Stability

Vehicle running stability or hunting is a phenomena associated with conically shaped steel wheel/steel rail vehicles. The conical wheels provide a lateral guidance or centering action which tends to force the wheels into the tread region away from the flanges. The friction or creep forces between the wheel and the rail are a function of the vehicle speed. As the speed increases, a value can be reached at which the vehicle-truck-wheelset system has zero effective damping and a sustained periodic oscillation is set up. This state is called hunting and the speed at which it occurs is called the critical speed.

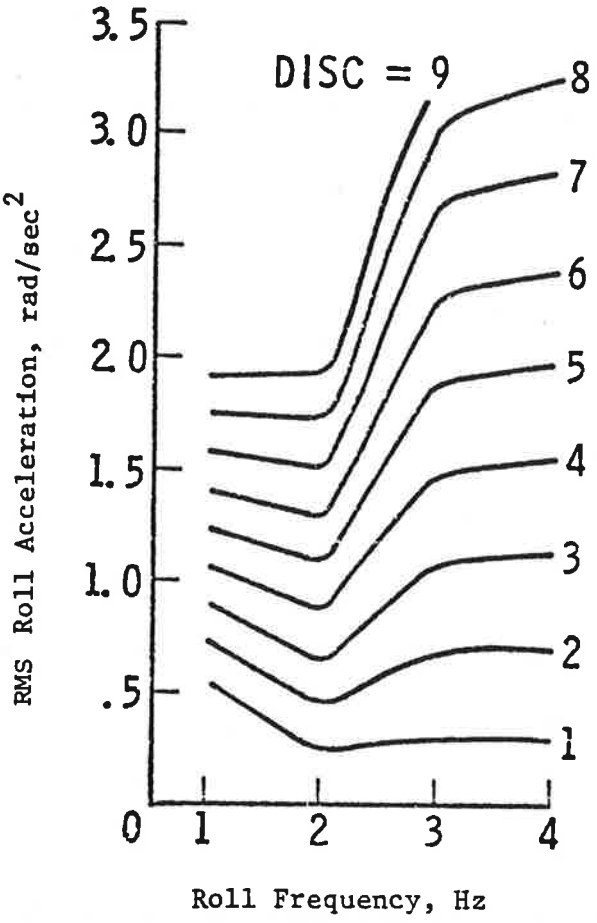

FIGURE 3.2.2: ROLL EQUAL DISCOMFORT CURVES [29]

Rail vehicles exhibit several different modes of hunting, commonly classified as carbody hunting and truck hunting. Carbody hunting generally occurs at relatively low speeds and as speed is increased the vehicle usually passes through this condition and can be operated successfully above the carbody hunting speed. Truck hunting occurs at higher speeds and is of direct importance in evaluating stability at primary vehicle operating speeds. In this study the truck critical speed at which hunting occurs is evaluated and compared with the vehicle operating speed. The margin between operating speed and critical speed is adopted as a design performance measure.

A vehicle can have a good margin between operating speed and critical speed and still have a tendency to oscillate with low damping after a disturbance. To obtain a measure of the inherent damping in the principal modes of vibration, the damping ratios of the principal modes of vibration are computed for the operating speed range of the vehicle. The value of the least damped mode of vibration is used as a performance measure to reflect the need, not only to be stable, but also to have adequate damping in a response to a disturbance. The higher the value of this performance measure, the more damped is the mode of vibration.

3.2.3 Curve Negotiation

The majority of wheel profile and rail wear results from high force levels that occur as the vehicle negotiates a curve. Most current conventional passenger vehicles rely on flanging to limit wheelset excursions during curve negotiation. Wheel flanging

creates noise and increased stress levels.

It would be desirable if flange guidance could be avoided, and creep guidance achieved [12] at least for mainline intercity curves (≈1°-3°). To evaluate curving, the performance region over which the passenger vehicle can traverse a specified curve without flanging is computed. To achieve curve negotiation using creep guidance, two conditions must be avoided: (1) wheel slippage or the condition where the required friction force exceeds that available and (2) flange contact due to excessive wheelset excursions.

Two independent factors can cause excessive wheelset excursions in curves; track curvature and lateral unbalance. Section 4.5.2 analyzes in detail vehicle response to track curvature.

The lateral unbalance aspect of curving performance may be illustrated in a plot of cant deficiency versus degree curve where:

$$\phi_d(\text{cant deficiency}) = \frac{V^2}{Rg} - \phi_{S.E.} \qquad (3.2\text{-}1)$$

where V = constant forward speed (kmh)

R = radius of curve (kilometers)

$\phi_{S.E.}$ = radians

g = acceleration due to gravity.

The superelevation $\phi_{S.E.}$ is defined in Figure 3.2.3. The maximum superelevation considered in this study is $\phi_{S.E.} = 6.14°$ (Δ = 6 inches) [30]. The curve is also defined in terms of degrees as shown in Figure 3.2.4.

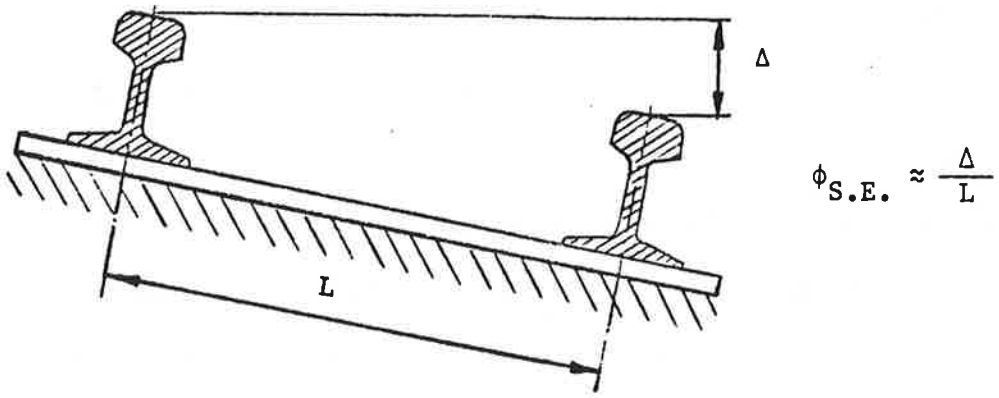

FIGURE 3.2.3: DEFINITION OF SUPERELEVATION

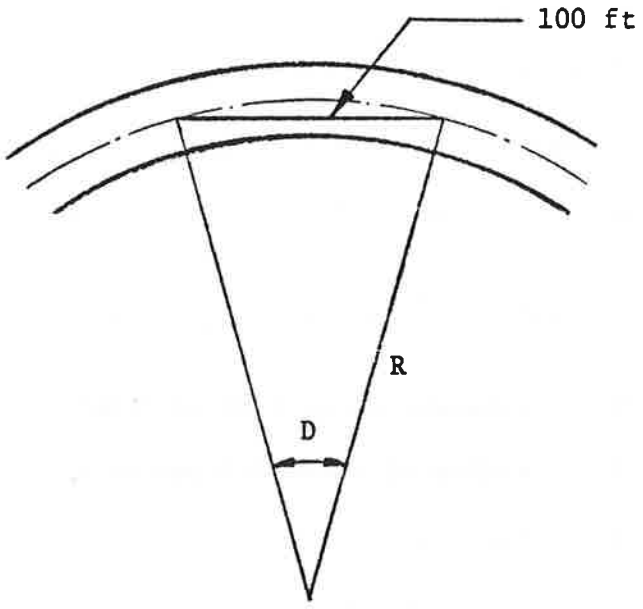

FIGURE 3.2.4: DEFINITION OF DEGREE CURVE, D

For design purposes curving performance will be considered as illustrated in Figure 3.2.5. This figure illustrates the constraints on curving performance. The FRA Track Safety Standards [30] specifies that the following relation must be satisfied:

$$V_{max} = \sqrt{\frac{\Delta + 3}{.0007D}} \qquad (3.2\text{-}2)$$

where V_{max} = maximum allowable operating speed, mph

Δ = superelevation in inches

D = degree of curve (°).

The two cant deficiency boundaries shown in the figure are computed by substituting equation (3.2-2) into (3.2-1) and setting Δ to its maximum value of 6 inches. These boundaries indicate the primary operating regions of interest for design.

3.3 Performance Constraints

In this study, the three performance indices discussed in the previous sections are optimized subject to a set of constraints described in this section. The constraints considered include vehicle wayside clearance, wheel load equalization, wheel/track forces during curves, suspension stroke lengths, and wheelset excursions.

3.3.1 Wayside Clearance

In a vehicle design, an overall dynamic motion body envelope is established which limits maximum permissible body excursions so that track wayside clearance constraints are met as described in reference [31]. These constraints are typically met as described in [31],

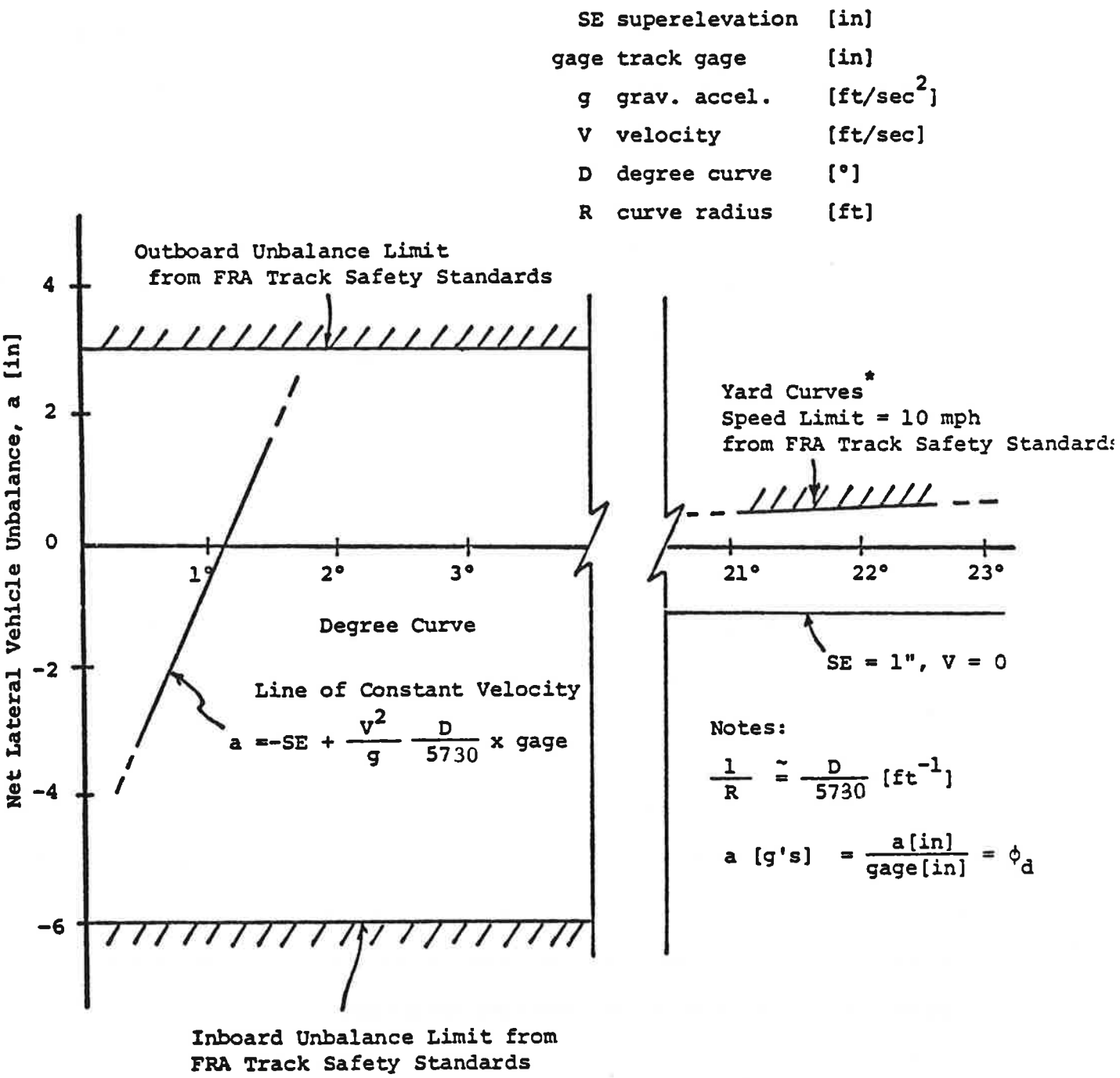

FIGURE 3.2.5: LIMITS OF LATERAL UNBALANCE WHICH BOUND THE REGION OF ACCEPTABLE STEADY-STATE CURVING CONDITIONS ASSUMING NO TRACK IRREGULARITIES

*Boundary shown corresponds to an assumed 1" superelevation for yard curves.

using bump stops to limit suspension travel. In preliminary design these constraints are considered indirectly by requiring suspension strokes to have infrequent contact with bump stop limits.

3.3.2 Wheel and Load Equalization

Specifications have been used for passenger trucks which require that the load be maintained equal on each truck wheel as the track disturbs the wheels. These specifications take the form of a test in which the maximum percent deviation for any wheel is restricted as one wheel is raised a specified amount. A typical specification is that less than 25% load change is required as the wheel is raised 5cm. Wheel load equalization specifications are usually met as basic part of truck design using, for example, equalizer bars and/or split frames. The influence of the elements employed in truck design to achieve wheel load equalization is represented in the dynamic models used for performance evaluation.

3.3.3 Wheel-Track Interaction Forces

During curve negotiation substantial wheel track forces are generated. The following relationships have been cited in the literature [32] as approximate static guidelines. These values are:

1. Lateral to vertical wheel load ratio $(L/V) \leq .9$ at the leading outer wheel to prevent wheel climb.
2. Lateral to vertical wheel ratio (L/V) for one side of an entire truck $(\frac{L_1 + L_2}{V_1 + V_2}) \leq .5$ to prevent rail rollover.

3. Net lateral axle load $\leq$ 40% of the vertical axle load to prevent track shift on poor track

In this study wheel L/V and truck L/V ratios are computed and limited in parametric studies of curving behavior. Dependence of L/V limits on such factors as time duration or tonnage is not considered.

3.3.4 Suspension Stroke Lengths

In general, vertical and lateral ride quality is improved by softening the suspension stiffnesses and allowing increased suspension strokes. These strokes must be limited to meet wayside clearance requirements. The suspension strokes for the vehicle operating over tangent track disturbed by the random track irregularities are computed by calculating the rms stroke value and then assuming that the peak stroke is three times the rms stroke as is consistent with the linear vehicle model excited by Gaussian random track disturbances. The peak deflections which occur during a steady state curve are calculated directly. A nominal set of suspension peak stroke lengths typical of conventional passenger trucks [4] are:

- primary suspension stops (zero to peak)
  - lateral $\leq$ 0.95 cm
  - longitudinal $\leq$ 0.95 cm
  - vertical $\leq$ 0.95 cm
- secondary suspension stops (zero to peak)
  - lateral $\leq$ 3.8 cm
  - vertical $\leq$ 3.8 cm.

3.3.5 Wheelset Excursions

In order to avoid frequent flange contact on tangent track or curves the wheelset excursion (lateral displacement of the wheel with respect to the rail at the contact point) must be limited to zero-to-peak values of 0.76 cm. This constraint is interpreted for operation on tangent track by computing the rms wheel set excursions and assuming the peak values are three times the rms values. In curving it is computed directly.

3.4 Computation of Vehicle Performance Indices

3.4.1 Use of Computer Models

The design process requires identification of vehicle parameters which provide performance that satisfies the indices and constraints cited in the preceeding section. The suspension, geometric and inertial parameters are related in rather complex fashion to the performance indices, thus computer simulation models have been employed to generate tabular data for design. Several factors have played a central role in the development of models for use in design;

1) The requirement that random track disturbances due to crosslevel, alignment and vertical irregularities be accomodated to compute ride quality.

2) The requirement that many simulation runs be permitted so that important ranges of parameter values can be evaluated places a premium on computational efficiency.

3) The emphasis on generating parametric data which illustrates results for generic passenger trucks as opposed to a highly detailed investigation of a specific passenger truck design.

4) The availability of state-of-the-art computer models as described in the literature.

These factors have led to the use of primarily linear models which represent the dominant physical characteristics of rail passenger vehicles. State-of-the-art models are available based upon linear analysis techniques which can accept random track inputs and provide efficient computation of the performance indices. These models are appropriate for computing general trends in performance and useful for initial determination of truck design parameters. For evaluating the detailed performance of a specific truck design, models which include suspension and wheel-rail nonlinearities are appropriate and recommended. However, nonlinear computation models for evaluating random response are not currently available which are efficient for large numbers of parametric runs. Thus, consistent with the current state-of-the-art in computer models, primarily linear models are used in this study.

At the present time no dynamic computational model exists for passenger trucks which has been validated in detail with test data. While the models used have not been validated with test data, they are generally accepted by the technical community as providing useful information to guide in truck design and preliminary performance evaluation. However, development of validated models would provide a much stronger basis for the type of study discussed in this report and is strongly recommended.

The computational models used in the study are discussed in the following sections. First, the description of the track is given. Tangent track is represented as containing random irregularities which are defined in terms of their statistical properties. The track models are developed based upon experimental data measured for track and provide distinct models for vertical, cross-level and lateral irregularities. Each of these models is assumed to be statistically independent of the other models. In addition to the tangent track model, representations of curved, but nominally smooth track have been developed which include superelevation.

Three principal vehicle models have been developed:

a) A linear vertical dynamic model in which carbody heave, pitch and roll motion are excited by track vertical and cross level disturbances acting through the wheelsets and trucks.

b) A linear lateral dynamic model in which carbody lateral, yaw and roll motion are excited by track lateral and cross-level disturbances acting through the wheelsets and trucks.

c) A lateral steady-state curving model in which the wheel-track and suspension forces and relative excursions are determined for a vehicle running at constant speed on a fixed radius curve.

The first two dynamic models represent a decoupling of vehicle motion primarily into vertical-roll motion resulting from vertical and crosslevel disturbances and into a lateral-roll motion resulting from lateral and crosslevel disturbances. This decoupling of motions is convenient in terms of computational efficiency and is appropriate since each of the inputs is statistically independent and

the dynamic models are linear. These models allow computation of the ride quality in the passenger compartment, of the suspension strokes, wheelset excursions and wheel-track forces resulting from track disturbances. In addition, the lateral model allows computation of the vehicle hunting speed.

The steady-state curving model is used to determine wheel-track forces in curves and suspension strokes. It includes the friction breakaway nonlinearity between the carbody and bolster.

3.4.2 Track Representation

Track irregularities represent the primary disturbance inputs to the rail vehicle. Track irregularities are due to a combination of initial installation error and degradation due to track loads. A recently completed study [34] outlined track irregularity measurement and analytical characterization techniques.

Four irregularities are universally used to define track geometry and are shown in Figure 3.4.1 Gauge is the horizontal distance between the two rails, crosslevel is the difference between the elevations of the rails, alignment is the average of the two rail lateral positions (often referred to as centerline), and vertical profile is the average of the two rail elevations.

$$\begin{aligned} y_a(\text{alignment}) &= \frac{y_\ell + y_r}{2} \\ y_g(\text{gauge}) &= y_\ell - y_r \\ z_v(\text{vertical}) &= \frac{z_\ell + z_r}{2} \\ z_c(\text{cross-level}) &= z_\ell - z_r, \end{aligned} \qquad (3.4.2\text{-}1)$$

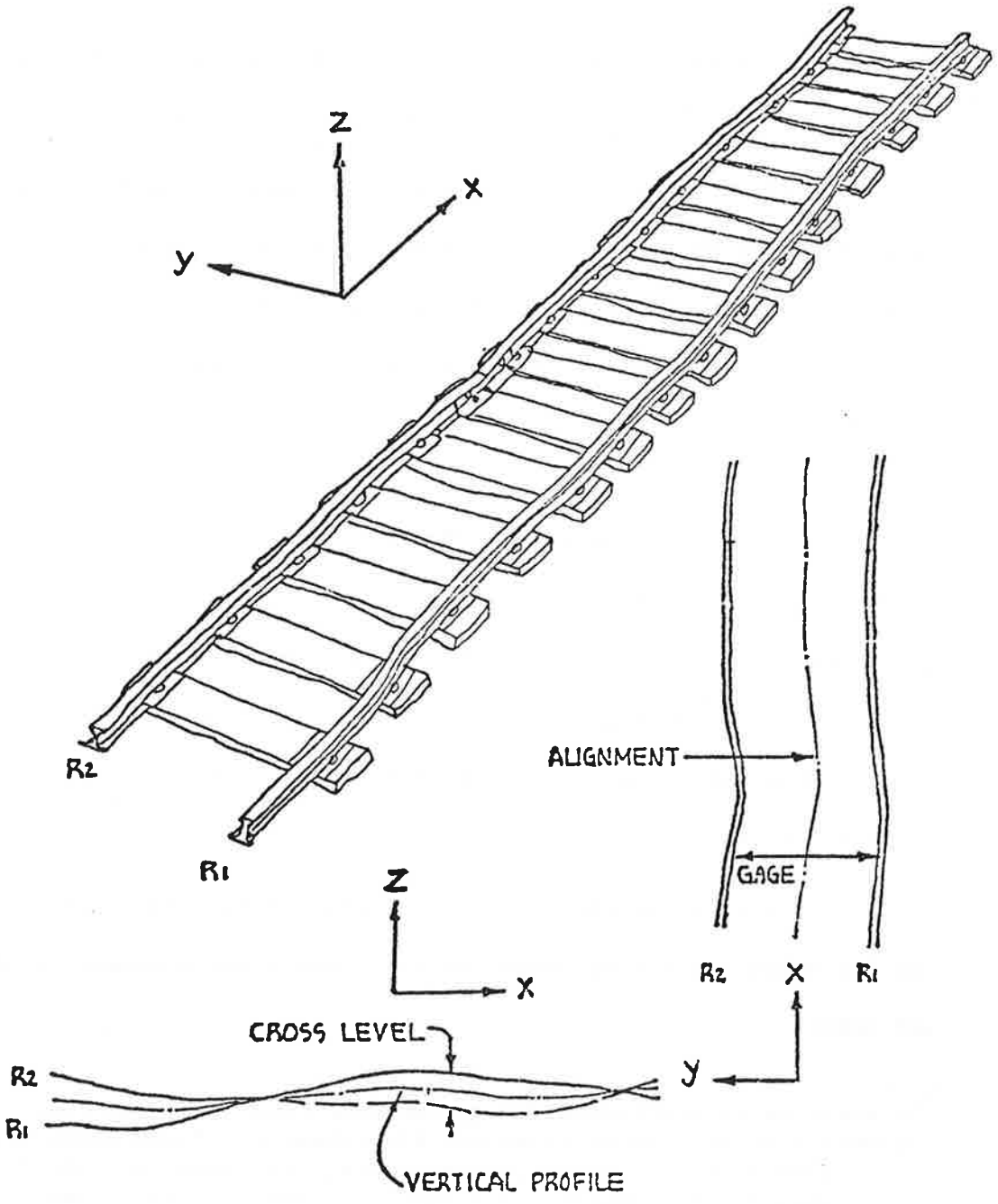

FIGURE 3.4.1: TRACK IRREGULARITY DEFINITIONS

where the subscripts ℓ and r denote the left and right rail respectively with y the lateral distance and z the vertical distance.

Track irregularity measurements taken by the F.R.A. Geometry Cars [34] have shown that the irregularities are statistical variables that are well described by their spectral density representation [34,35] (the spectral density is effectively a representation of the mean square of the variable occurring in incrementally small segments of spatial wavelength). References [34,35] describe various analytical representations of track spectral density while [4] describes the relationship between the FRA Track Safety Standard spectral densities for class 6 track. The characterization of track is based upon measurements by track geometry cars, thus the effects of dynamic track loading which may vary from measurement to measurement are not precisely evaluated.

This design study has been conducted for class 6 track and the following analytical forms for the track power spectral densities are used:*

*In addition to statistical irregularities track also contains anomalies which provide transient disturbances. These anomalies, which typically occur at switches, frogs, and crossovers should be considered in a detailed analysis of truck and track component response to track disturbances.

· vertical $\left(\frac{z_\ell + z_r}{2}\right)$

$$S_v(\Omega) = \frac{A_v \Omega_c^2}{\Omega^2 (\Omega^2 + \Omega_c^2)} \qquad (3.4.2\text{-}2)$$

·cross-level $(z_\ell - z_r)$

$$S_c(\Omega) = \frac{4A_v \Omega_c^2}{(\Omega^2 + \Omega_c^2)(\Omega^2 + \Omega_s^2)} \qquad (3.4.2\text{-}3)$$

·alignment $= \left(\frac{y_\ell + y_r}{2}\right)$

$$S_a(\Omega) = \frac{A_s \Omega_c^2}{\Omega^2 (\Omega^2 + \Omega_c^2)} , \qquad (3.4.2\text{-}4)$$

where S_v, S_c, S_a are spectral densities (in^2/rad/ft), Ω is the wavelength (rad/ft), Ω_c, Ω_s are break wavenumbers, and A_v and A_a are roughness parameters. Reference [14] shows that for class-6 track these parameters are:

$A_v = .00159\ in^2\text{-rad/ft}$

$A_a = .00159\ in^2\text{-rad/ft}$

$\Omega_s = .1335$ rad/ft

$\Omega_c = 2\pi/25$ rad/ft.

Figures 3.4.2 and 3.4.3 show the class-6 spectral densities compared with measured data. Data for other track classes are included in reference [14].

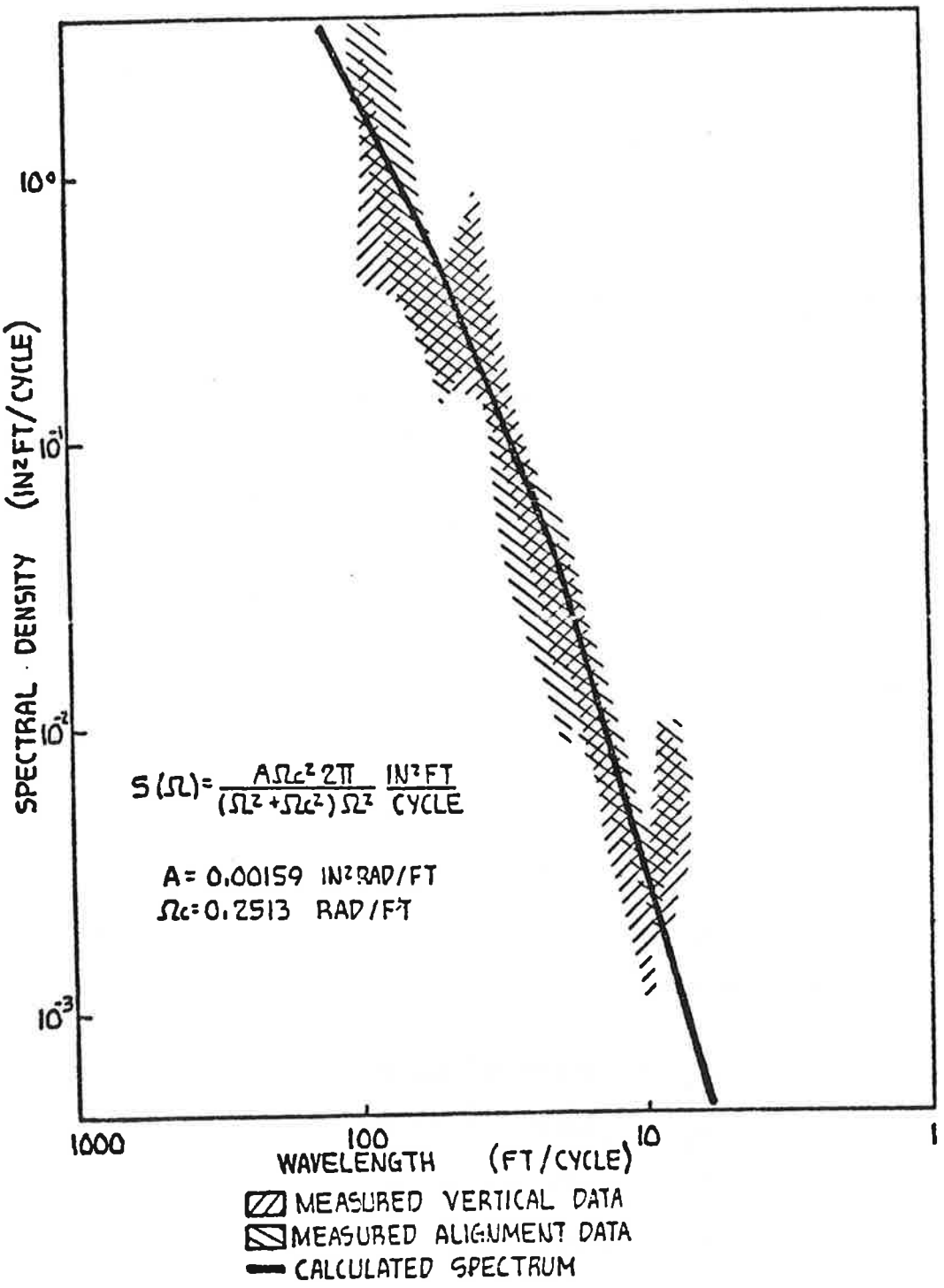

FIGURE 3.4.2: CLASS 6 VERTICAL PROFILE AND ALIGNMENT SPECTRAL DENSITIES

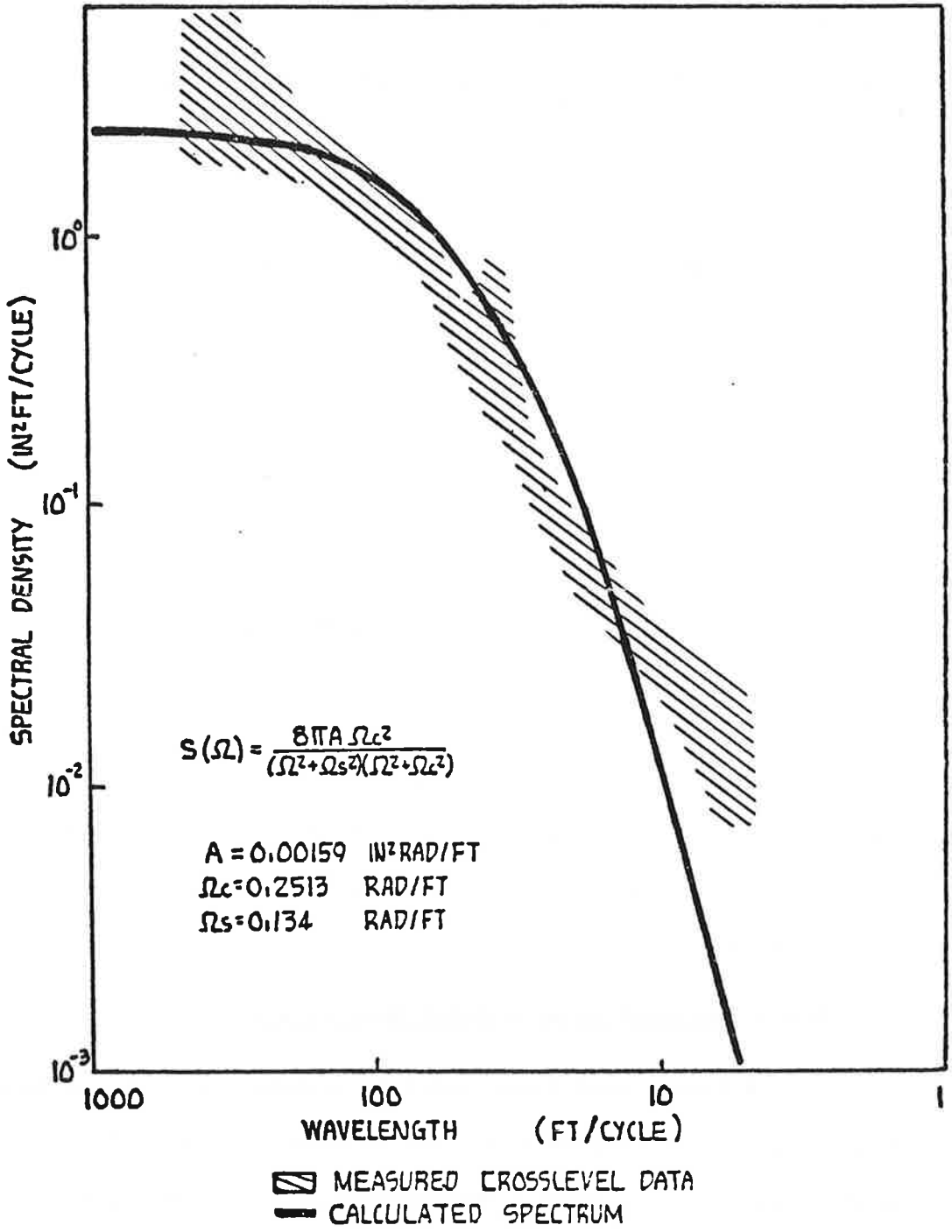

FIGURE 3.4.3: CLASS 6 CROSSLEVEL SPECTRAL DENSITY

In general, it is assumed that the cross-spectral densities between the track inputs are negligible, and thus each input is statistically independent of the other inputs. Experimental data have shown [4] that the assumption of statistical independence is appropriate.

For a vehicle traveling at a constant forward speed, V, the spatial spectral densities may be converted to temporal spectral densities which are used directly as inputs to the vehicle models by:

$$\omega = V\Omega \qquad (3.4.2\text{-}5)$$

$$f = \frac{\omega}{2\pi} , \qquad (3.4.2\text{-}6)$$

where ω = temporal frequency rad/sec

f = frequency : Hz.

Curved Track Representation: For evaluation of curving, the track is assumed to be smooth and of a constant radius of curvature, R, and also to have a constant superelevation, ϕ_{se} as described in section 3.3.

3.4.3 Vertical Dynamic Model Description

A linear analytical model describing the vertical dynamic motions of a rail passenger vehicle is used for the analysis of passenger ride comfort, subject to limitations on secondary suspension vertical stroke and vertical track force levels. The degrees of freedom represented include the heave, roll, and pitch of both trucks and

the carbody. In addition to these rigid-body modes, carbody flexibility is incorporated by including the first bending mode and first two torsion modes of the body.

The model chosen for this study is shown in Figure 3.4.4. The degrees of freedom of the carbody are:

z_c, the heave or vertical position of the carbody center of mass;

ϕ_c, the roll or rotation of the rigid carbody about the x-axis;

θ_c, the pitch or rotation of the rigid carbody about the y-axis;

$u(x,t)$, the first bending mode of the carbody; and

$w_1(x,t)$ and $w_2(s,t)$, the first and second torsion modes of the carbody.

The degrees of freedom for the leading truck are:

$z_{\ell t}$, the heave or vertical position of the leading truck center of mass

$\phi_{\ell t}$, the roll or rotation of the leading truck about the x-axis, and

$\theta_{\ell t}$, the pitch or rotation of the leading truck about the y-axis

The corresponding degrees of freedom for the trailing truck are z_{tt}, ϕ_{tt}, and θ_{tt}, respectively.

The model of Figure 3.4.4 represents a passenger vehicle equipped with a conventional secondary suspension, i.e., the secondary suspension linear spring and damper represent airspring stiffness and hydraulic damping. Alternatively, the secondary damping can be obtained

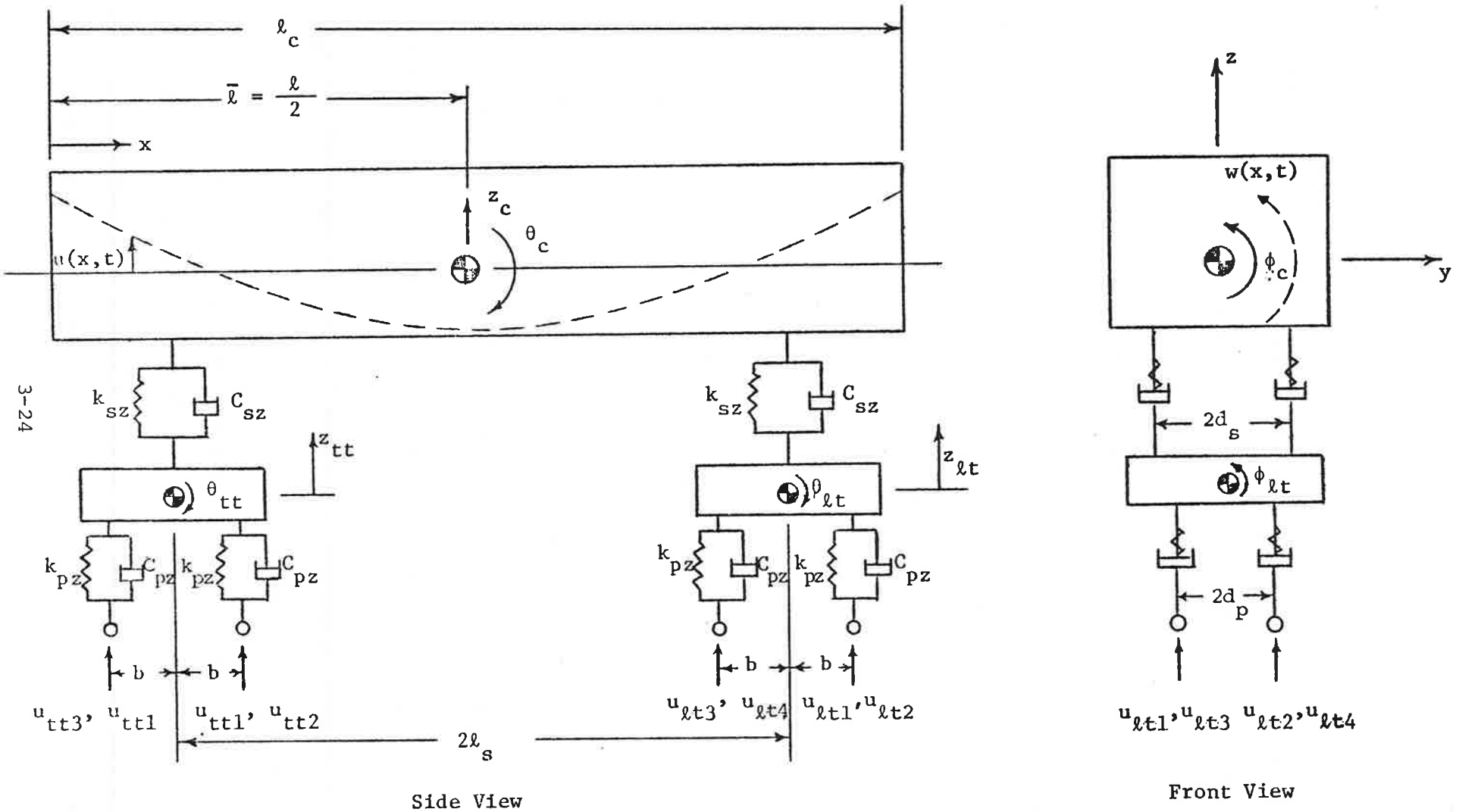

FIGURE 3.4.4: VERTICAL MODEL WITH CONVENTIONAL SECONDARY SUPENSION

by pneumatic orifice damping. In modeling such cases, the secondary suspension model of Figure 3.4.5 is used in the vehicle model [31]. For the secondary suspension model of Figure 3.4.5 four additional degrees of freedom are required in the overall model. These additional degrees of freedom are:

$z_{\ell tr}$ - the heave or vertical position of the connecting point p (see Figure 3.4.5) for the right, secondary suspension group above the leading truck,

$z_{\ell t\ell}$ - the heave or vertical position of the connecting point p for the left, secondary suspension group above the leading truck, and

z_{ttr} and $z_{tt\ell}$ - the corresponding degrees of freedom for secondary suspension above the trailing truck.

The vertical dynamics model represents the operation of a laterally and longitudinally symmetrical vehicle at constant velocity on nominally level, rigid track, with no coupler forces or aerodynamic forces acting on the vehicle. It is assumed that the wheels follow the rails exactly at all times; therefore, wheelset inertia is neglected and the wheels are modeled as massless - point followers.* It is further assumed that the actual primary and secondary vertical suspension characteristics are represented by the idealized effective linear spring and damper elements. Inherent in this use of linear suspension elements is the assumption that the linear and angular deflections of the vehicle are small.

The vertical model is used primarily to calculate the vertical acceleration response at a passenger location in the vehicle due to track vertical and crosslevel disturbances. The vertical stroke of the

*Wheelset inertia is included in the lateral model.

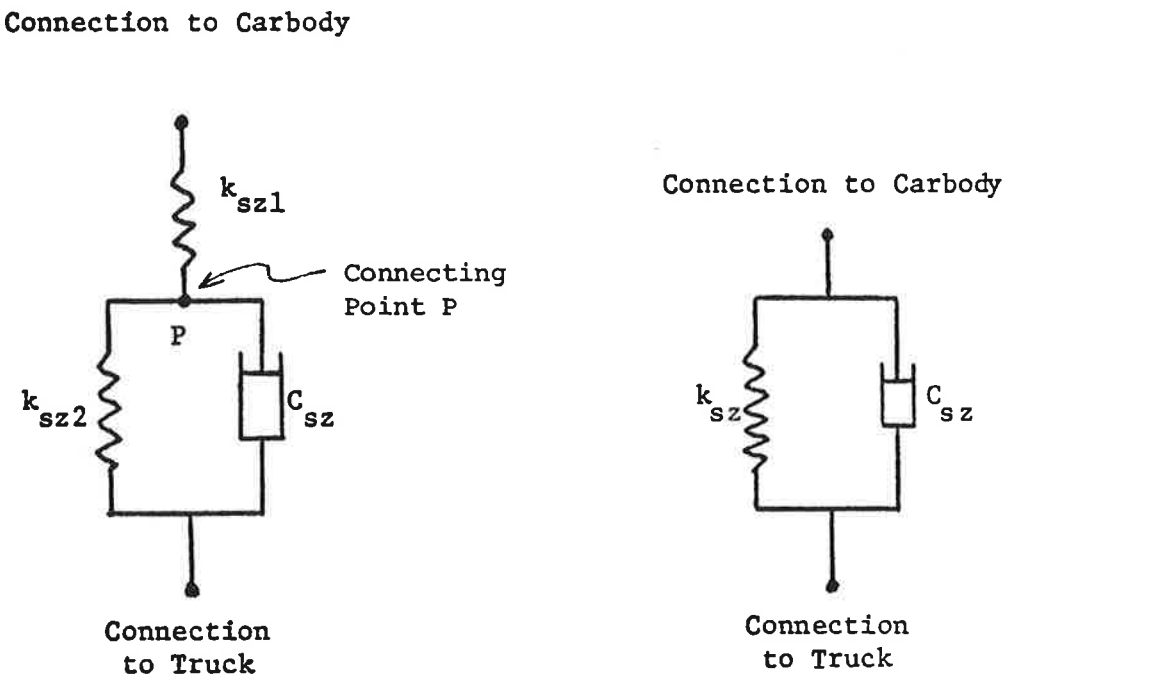

a) Secondary suspension with orifice damping

b) Secondary suspension with conventional damping

FIGURE 3.4.5: MODELS FOR SECONDARY SUSPENSIONS

secondary suspension elements is also calculated. The vertical force between a wheel and the track is estimated as the force in the primary suspension elements associated with that wheel.

The differential equations describing the vertical model are derived in reference [39].

3.4.4 Lateral Dynamic Model Description

3.4.4.1 Ride Quality: A schematic of the lateral model is shown in Figure 3.4.6. This model is an extension of the lateral model developed in reference [4]. The model is useful for computation of passenger compartment accelerations, suspension strokes and wheelset excursion due to lateral and crosslevel track disturbance inputs. The model consists of fifteen degrees of freedom including lateral and yaw motions of the wheelsets, the lateral and yaw motions of the trucks and the lateral, yaw and roll motions of the carbody. The wheelsets, trucks and carbody are modeled as rigid masses, with the assumption that internal bending is negligible. A constant vehicle velocity is assumed and aerodynamic and coupling forces neglected.

The primary and secondary suspension systems are represented by lumped linear springs and dampers, i.e., the secondary lateral stiffness represents the total lateral stiffness in the secondary, and combines the effects of rubber bushings, airsprings and anchor rods.

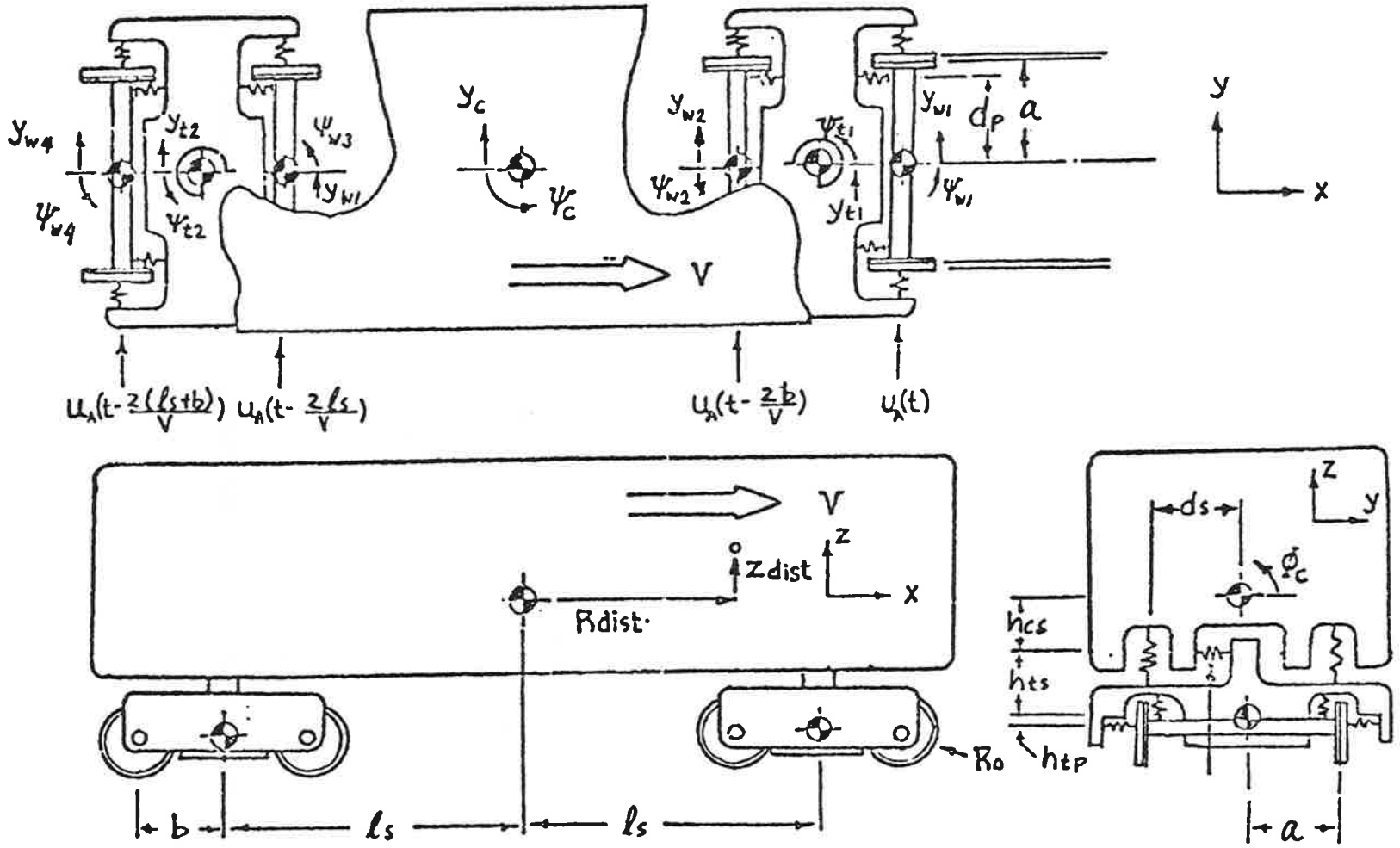

FIGURE 3.4.6: LATERAL RAILCAR MODEL

The primary difference between the model of [4] and the one used in this study is the inclusion of truck roll as a geometric constraint which provides a better representation of the effect of the track irregularities on the truck and carbody. The roll angle of the truck is analytically calculated as the instantaneous average of the roll angles of the two wheelsets under it. The wheelsets are assumed to follow the truck perfectly in the vertical direction without wheel lift. Truck roll is not considered as a dynamic degree of freedom to reduce computational complexity.

Forces which occur at the interface between the wheel and the rail are important in the lateral vehicle motion. These forces arise partly from geometric conditions in which the wheel-rail contact and rolling radii change and from creep generated at the interface. In this study the creep forces are computed using Kalker's linear creep theory and are primarily dependent upon normal force at the wheel, wheel-rail geometry, and the relative velocity between the wheel and the rail. In addition to these creep forces, gravitational stiffness forces due to the change in wheelset center of mass vertical position are computed.

The linear equations for the lateral model with lateral and crosslevel track disturbances are derived in reference [34] and can be summarized in matrix form as:

$$\bar{\underline{M}}\,\ddot{\underline{y}} + \bar{\underline{C}}\,\dot{\underline{y}} + \bar{\underline{K}}\,\underline{y} = \bar{\underline{B}}\,\underline{u} \qquad (3.4.4\text{-}1)$$

where $\underline{y}$, is a 15x1 vector of position degrees of freedom

$\underline{u}$, is a 15x1 matrix of alignment and cross-level inputs

$\bar{\underline{M}}$, $\bar{\underline{C}}$, and $\bar{\underline{K}}$ are the 15x15 inertia, damping and stiffness matrices

$\bar{\underline{B}}$, is a 15x15 input distribution matrix.

This model is used in computing the forced response of the vehicle.

3.4.4.2 Stability: The motion of a rail vehicle can be defined in terms of a sum of its independent modes of motion, e.g. wheelset modes, coupled wheelset-truck modes, and carbody modes. The character of these modes change with forward speed. Vehicle critical speed can be defined as the speed at which one of these modes has zero damping and exhibits a sustained (oscillation) motion. The character and effective damping of these modes of vibration are independent of the track input irregularities in the linear models used, thus the ride quality model described above may be directly used for stability studies with the track inputs set to zero. Therefore the model described in section 3.4.4.1 with $\underline{u} = 0$ is used to calculate vehicle critical speed.

$$\bar{\underline{M}}\,\ddot{\underline{y}} + \bar{\underline{C}}\,\dot{\underline{y}} + \bar{\underline{K}}\,\underline{y} = 0. \qquad (3.4.4\text{-}2)$$

In order to analyze the various dynamic modes of vibration of the system defined by Equation (3.4.4-2), it is necessary that the eigenvalues and vectors of Equation (3.4.4-2) are computed.

3.4.5 Steady-State Curving Model

A steady-state curving model with 15 degrees of freedom is used to evaluate the curving performance of passenger rail vehicles. The model is an extension of the 15 D.O.F. lateral dynamic model discussed in Section 3.4.4, and incorporates the same degrees of freedom:

4 wheelsets; lateral, yaw

2 trucks; lateral, yaw

1 carbody; lateral, yaw, roll.

As in the lateral dynamic model, truck and wheelset roll are included kinematically in that the roll angle of a truck is set equal to the average of the two wheelset roll angles for that truck at all times. Sketches of the curving model components, degrees of freedom, and geometry are shown in Figures 3.4.7 and 3.4.8.

The development of the curving model closely follows the Newland/Boocock approach to linear curving [12,13]. Some of the smaller effects such as gravitational stiffness and spin creep forces, which are often left out of a linear curving analysis are retained in this development for completeness. The four creep force coefficients established by the Kalker theory of creep [36] are included in the development, as well as the influence of centrifugal loading and the resulting differential wheel loading on creep forces and component displacements. The wheel/rail geometry parameters of contact angle, rolling radius, and wheelset roll angle are assumed to vary linearly

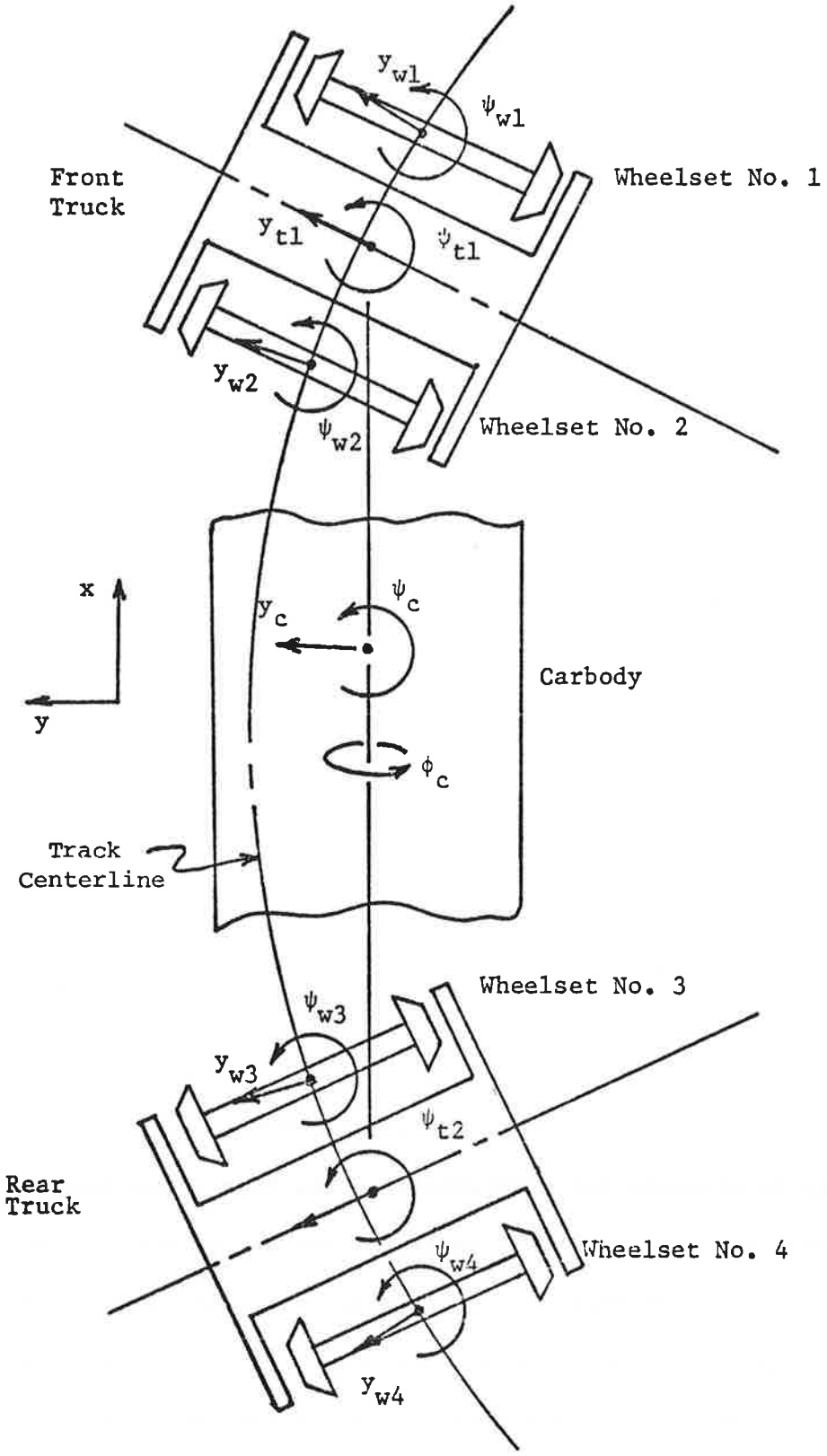

FIGURE 3.4.7: CURVING MODEL COMPONENTS AND DEGREES OF FREEDOM

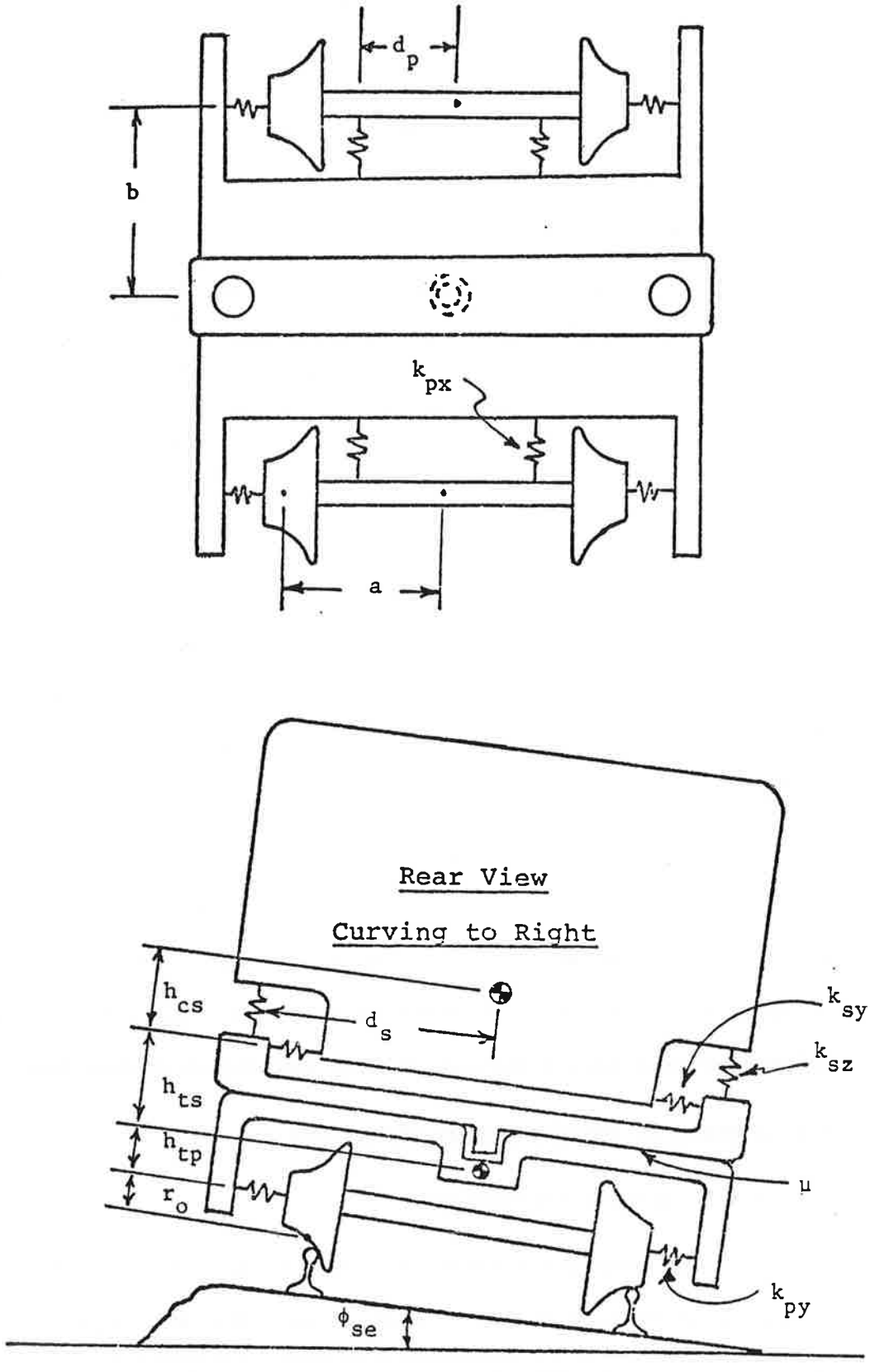

FIGURE 3.4.8: CURVING MODEL DETAILS

with lateral wheelset displacement. A nonlinearity is included in the steady-state curving model to allow for secondary Coulomb yaw breakaway between the truck and the carbody. The associated torque vs. yaw characteristic (Figure 3.4.9) dictates a modification of some of the curving equations each time the discontinuity is crossed.

In the development of the steady-state curving model, linear wheel-rail geometry is assumed and all angles are assumed to be small. The model is described in detail in reference [39].

The curving model is used in this study to map out wheel slip and flange contact boundaries or other trajectories in the cant deficiency vs. degree curve plane, while the associated loci of vehicle displacements are plotted. The displacement curves obtained encompass the full range of vehicle response to inputs bounded by the input trajectory, and the relative dependence of each solution variable on cant deficiency and curve radius can be seen. Knowledge of the range of primary strokes required for acceptable curving, for example, is important in determining what tolerances, if any, should be incorporated into a certain primary suspension system design.

3.5 Summary of Vehicle Design Parameters

3.5.1 General Parameters

The computer simulation models permit the evaluation of the influence of vehicle design parameters upon the design performance indices. The models described in the previous sections are sufficiently complex to require computer assistance in their solution. A number of

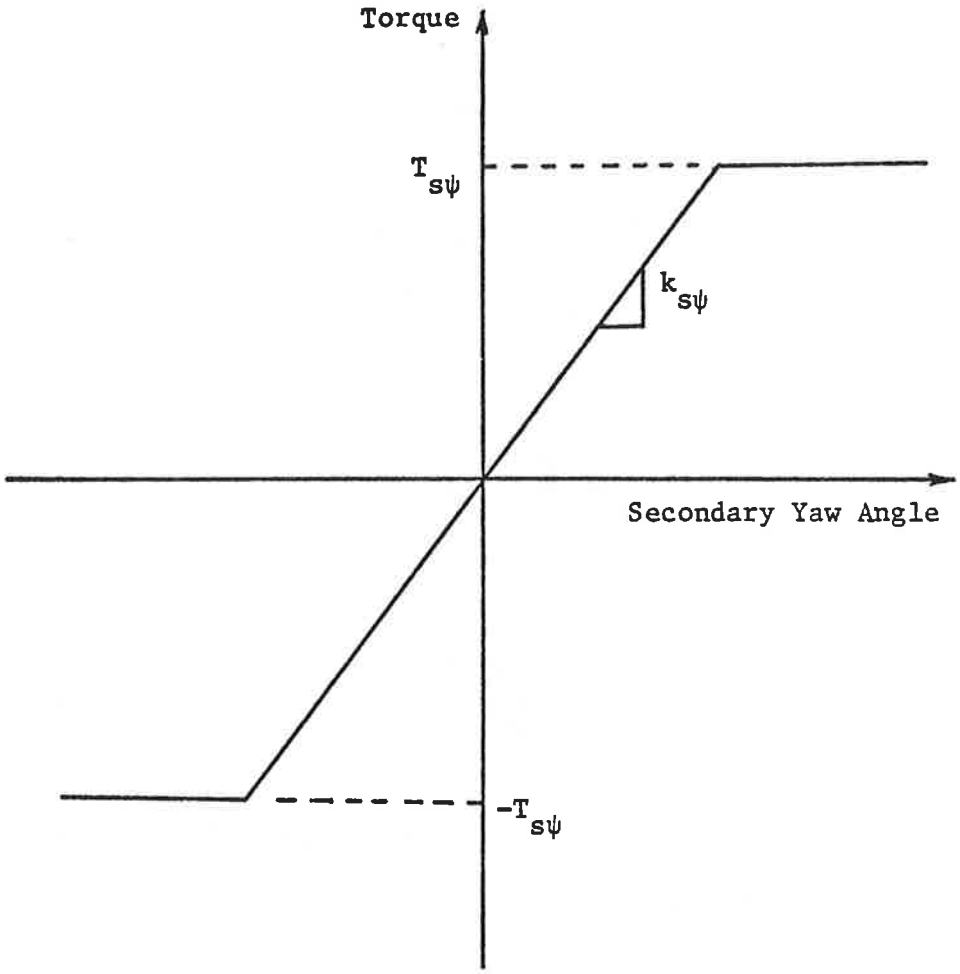

FIGURE 3.4.9: SECONDARY BREAKAWAY TORQUE CHARACTERISTIC

useful guidelines illustrating the influence of design parameters on performance indices can be derived from relatively simple models. These models are described in the following paragraphs and provide a starting point of a design procedure.

3.5.2 Kinematic (Hunting) Models

a) Unrestrained, massless wheelset

The simplest model is that of an unrestrained, massless wheelset moving at a constant speed V. It can be shown that the wheelset will move along a sinusoidal trajectory of wavelength

$$L = 2\pi\sqrt{\frac{ar_o}{\lambda}} \qquad (3.5\text{-}1)$$

and frequency

$$f = \frac{V}{2\pi}\sqrt{\frac{\lambda}{ar_o}} \quad (\text{Hz}). \qquad (3.5\text{-}2)$$

Since the oscillations neither decay nor grow with time, the wheelset is a marginally stable system.

b) Restrained wheelset with inertia and creep

The characteristic equation of this model is of fourth order and its terms depend on V. It is found that as V is increased

from zero the wheelset will pass from region of stability, through the point of marginal stability, to the region of instability. An approximate expression for the critical speed, above which the wheelset is unstable, is

$$V_c = \left[\frac{2ar_o[d_p^2 F_{11} K_{px} + a^2 F_{33}(K_{py} + \frac{Na_{11}}{2a})]}{(a^2 F_{11} M_w + F_{33} I_{wz})\lambda} \right]^{1/2} . \qquad (3.5\text{-}3)$$

The wavelength and frequency at the critical speed are the same as those given by Equations 3.5-1 and 3.5-2, respectively.

c) A rigid truck with two wheelsets

The equations of motion of a rigid truck have the same form as those of a wheelset and, therefore, a rigid truck behaves similarly. An unrestrained, massless rigid truck has a wavelength of

$$L = 2\pi \sqrt{\frac{ar_o}{\lambda} \left(\frac{a^2 + b^2}{a^2}\right)} , \qquad (3.5\text{-}4)$$

and the kinematic frequency is

$$f = \frac{V}{2\pi} \sqrt{\frac{\lambda}{ar_o} \left(\frac{a^2}{a^2 + b^2}\right)} . \qquad (3.5\text{-}5)$$

The critical speed can be approximated by

$$V_c = \left[\frac{[K_{s\psi} + \frac{2Na_{11}b^2}{a} + 2(a^2 + b^2)(K_{sy} + \frac{Na_{11}}{a})](a^2 + b^2)r_o}{[(a^2 + b^2)(M_T + 2M_w) + I_{tz} + 2I_{wz} + 2M_w b^2]a\lambda} \right]^{1/2} \qquad (3.5\text{-}6)$$

Equation 3.5-3 gives best results when K_{px} and K_{py} are very low (say, < 20000 lb/ft) since then the coupling between the wheelsets and the truck frame is weak and the mode of instability is indeed wheelset hunting, as assumed. Equation 3.5-6 gives best results when the truck is very stiff (say, K_{px}, K_{py} > $4x10^6$ lb/ft) since then the deviation from the perfectly rigid model is small compared to the rigid truck motions. A practical truck lies somewhere between the two extremes and, therefore, its critical speed cannot be computed accurately by either of the two equations. However, the effect of the parameters on the critical speed of the simple model is similar to their effect on the critical speed of complex models, so that some insight into the complex case can be gained by studying the simple cases.

3.5.3 Models of Truck Frame and Carbody Vibrations

The natural frequencies of all the rigid body motions of the truck frame for a practical passenger truck are in the range of 5 Hz - 30 Hz. The carbody secondary suspension natural frequencies are in the range of 0.5 Hz-2.5 Hz. Because of this frequency separation, and because the damping ratios are usually below 0.25, the coupling between truck (primary) natural modes and carbody (secondary) modes is weak. It has been observed that when the truck natural frequencies and damping ratios are computed without considering the carbody mass, and vice versa, the error is usually less than 10%, so that the designer can estimate most of the eigenvalues of the system without using large eivenvalue computer programs. The following equations are available.

a) Truck frame lateral motion

$$f_n = \frac{1}{2\pi}\sqrt{\frac{4K_{py} + 2K_{sy}}{M_T}} \qquad (3.5\text{-}7)$$

$$\xi = \frac{4C_{py} + 2C_{sy}}{2\sqrt{M_T(4K_{py}+2K_{sy})}} \qquad (3.5\text{-}8)$$

b) Truck frame vertical motion

$$f_n = \frac{1}{2\pi}\sqrt{\frac{4K_{pz} + 2K_{sz}}{M_T}} \qquad (3.5\text{-}9)$$

$$\xi = \frac{4C_{pz} + 2C_{sz}}{2\sqrt{M_T(4K_{pz} + 2K_{sz})}} \qquad (3.5\text{-}10)$$

c) Truck frame roll

$$f_n = \frac{1}{2\pi}\sqrt{\frac{4d_p^2K_{pz} + 2d_s^2K_{sz}}{I_{tx}}} \qquad (3.5\text{-}11)$$

$$\xi = \frac{4d_p^2C_{pz} + 2d_s^2C_{sz}}{2\sqrt{I_{tx}(4d_p^2K_{pz}+2d_s^2K_{sz})}} \qquad (3.5\text{-}12)$$

d) Truck frame yaw

$$f_n = \frac{1}{2\pi}\sqrt{\frac{K_{s\psi} + 4d_p^2 K_{px} + 4b^2 K_{py}}{I_{tz}}} \qquad (3.5\text{-}13)$$

$$\xi = \frac{C_{s\psi} + 4d_p^2 C_{px} + 4b^2 C_{py}}{2\sqrt{I_{tz}(K_{s\psi} + 4d_p^2 K_{px} + 4b^2 K_{py})}} \; . \qquad (3.5\text{-}14)$$

e) Truck frame pitch

$$f_n = \frac{1}{2\pi}\sqrt{\frac{4b^2 K_{pz}}{I_{ty}}} \qquad (3.5\text{-}15)$$

$$\xi = \frac{4b^2 C_{pz}}{2\sqrt{I_{ty}(4b^2 K_{pz})}} \; . \qquad (3.5\text{-}16)$$

f) Carbody lateral motion

$$f_n = \frac{1}{2\pi}\sqrt{\frac{4K_{sy}}{M_c}} \qquad (3.5\text{-}17)$$

$$\xi = \frac{4C_{sy}}{2\sqrt{M_c(4K_{sy})}} \; . \qquad (3.5\text{-}18)$$

g) Carbody vertical motion

$$f_n = \frac{1}{2\pi}\sqrt{\frac{4K_{sz}}{M_c}} \tag{3.5-19}$$

$$\xi = \frac{4C_{sz}}{2\sqrt{M_c(4K_{sz})}} \; . \tag{3.5-20}$$

h) Carbody roll

$$f_n = \frac{1}{2\pi}\sqrt{\frac{4d_s^2K_{sz} + 4h_{cs}^2K_{sy} - h_{cs}W}{I_{cx}}} \tag{3.5-21}$$

$$\xi = \frac{4d_s^2C_{sz} + 4h_{cs}^2C_{sy}}{2\sqrt{I_{cx}(4d_s^2K_{sz} + 4h_{cs}^2K_{sy} - h_{cs}W)}} \; . \tag{3.5-22}$$

i) Carbody yaw

$$f_n = \frac{1}{2\pi}\sqrt{\frac{2K_{s\psi} + 4\ell_s^2K_{sy}}{I_{cz}}} \tag{3.5-23}$$

$$\xi = \frac{2C_{s\psi} + 4\ell_s^2C_{sy}}{2\sqrt{I_{cz}(2K_{s\psi} + 4\ell_s^2K_{sy})}} \; . \tag{3.5-24}$$

j) Carbody pitch

$$f_n = \frac{1}{2\pi}\sqrt{\frac{4\ell_s^2 K_{sz}}{I_{cy}}} \qquad (3.5\text{-}25)$$

$$\xi = \frac{4\ell_s^2 C_{sz}}{2\sqrt{I_{cy}(4\ell_s^2 K_{sz})}} \qquad (3.5\text{-}26)$$

In the design of a vehicle these simple formulas are useful in estimating values of the system natural frequencies and damping ratios. It is generally accepted design practice to select parameters so that coupled members have a separation of a factor of two or more in natural frequencies.

4. DESIGN METHODOLOGY

4.1 Scope of Methodology

A design methodology has been developed to select values of truck parameters which significantly influence the following dynamic performance indices:

- Ride quality in terms of passenger compartment rms accelerations
- Stability in terms of vehicle critical speed
- Tracking capability
- Constant radius curve negotiation in terms of wheelset excursions (flange contact) and wheel-rail interaction forces (slip).

These performance indices are evaluated for a vehicle traveling at constant speed using the dynamic computer models described in Chapter 3, thus, the selection of design parameters is based primarily upon linear analysis. For rail passenger vehicles the use of primarily linear analyses to develop initial values of design parameters is appropriate since passenger trucks are designed for levels of motions and forces which allow elements to operate primarily in a linear range. However, after a set of initial design parameters have been selected, it is recommended that the design be analyzed with detailed nonlinear models to evaluate the performance.

The vehicle model developed in Chapter 3 includes approximately fifty parameters which define the elements in the carbody, trucks and wheelsets. These parameters may be grouped as follows:

1) Truck primary and secondary suspension stiffness and damping parameters

2) Carbody, wheelset and truck inertial properties

3) Wheel-rail interaction parameters

4) Geometric properties.

In the design methodology, all of the inertial and geometric parameters are assumed to be selected from vehicle static design and the dynamic performance indices are used to select the suspension and wheel profile parameters. A summary of the parameters which are initially fixed in the design procedure, dependent parameters fixed by other parameters and parameters determined by the design procedure is contained in Table 4.1.1. Values of all these parameters are included in the table for the prototype passenger vehicle referenced in following sections. The design methodology selects the values of the ten suspension and wheelset parameters to meet dynamic performance specifications after the approximate size, weight and other gross characteristics of a vehicle are established.

An overview of the design procedure is presented in Figure 4.1.1. The first step in the procedure is to identify vehicle performance specifications including service requirements, speed and the dynamic indices cited above. In the second major task, the overall geometric and inertial properties of the vehicle are specified from static considerations and service requirements. The details of this task are not discussed in this study, since these parameters are

TABLE 4.1.1: SUMMARY OF PROTOTYPE VEHICLE PARAMETERS

Fixed Parameter		Dimension
a	half of wheelset contact distance	2.35 ft (0.7163 m)
b	half of wheelbase	4.25 ft (1.295 m)
d_p	half of primary springs lateral spacing	2.0 ft (0.6096 m)
d_s	half of secondary springs lateral spacing	3.75 ft (1.163 m)
h_{cs}	vertical distance from carbldy c.g. to secondary lateral springs	2.94 ft (0.8961 m)
h_{tp}	vertical distance from truck c.g. to primary lateral springs	0.35 ft (0.1067 m)
h_{ts}	vertical distance from truck c.g. to secondary lateral springs	1.68 ft (0.6511 m)
ℓ_c	total length of carbody	85.0 ft (25.91 m)
ℓ_e	distance from carbody c.g. to its geometric center	0.0 ft (0.0 m)
ℓ_s	half of truck center pin spacing	29.75 ft (9.068 m)
M_c	carbody mass	2,860. slugs (41,740. kg)
M_t	truck frame mass	250. slugs (3649. kg)
M_w	wheelset mass	120. slugs (1751. kg)
I_{cx}	roll moment of inertia of carbody	76,340. slug-ft^2 (103,500. kg-m^2)
I_{cy}	pitch moment of inertia of carbody	1.764×10^6 slug-ft^2 (2.391×10^6 kg-m^2)

TABLE 4.1.1 (Cont'd)

Fixed Parameter		Dimension
I_{cz}	yaw moment of inertia of carbody	1.764×10^6 slug-ft^2 (2.391×10^6 kg-m^2)
I_{tx}	roll moment of inertia of truck frame	2058. slug-ft^2 (2,790. kg-m^2)
I_{ty}	pitch moment of inertia of truck frame	434. slug-ft^2 (588. kg-m^2)
I_{tz}	yaw moment of inertia of truck frame	2486. slug-ft^2 (3371. kg-m)
I_{wx}	roll moment of inertia of wheelset	561. slug-ft^2 (761. kg-m^2)
I_{wy}	pitch moment of inertia of wheelset	112. slug-ft^2 (152. kg-m^2)
I_{wz}	yaw moment of inertia of wheelset	561. slug-ft^2 (761. kg-m^2)
r_o	centered wheel rolling radius	1.5 ft (0.4572 m)
μ	coefficient of friction between wheels on rail	0.2
ω_{1t}	natural frequency of the carbody first torsional mode	12 Hz
ξ_{1t}	damping ratio of the carbody first torsional mode	0.05
ω_{2t}	natural frequency of the carbody second torsional mode	24 Hz
ξ_{2t}	damping ratio of the carbody second torsional mode	0.05
ω_b	natural frequency of the carbody bending mode	7.1 Hz
ξ_b	damping ratio of the carbody bending mode	0.05

TABLE 4.1.1 (Cont'd)

Parameters Determined by the Design Procedure

K_{px}	primary longitudinal stiffness (4 per truck)
K_{py}	primary lateral stiffness (4 per truck)
K_{pz}	primary vertical stiffnes (4 per truck)
K_{sy}	secondary lateral stiffness (2 per truck)
C_{sy}	secondary lateral damping (2 per truck)
K_{sz}	secondary vertical stiffness (2 per truck)
C_{sz}	secondary vertical damping (2 per truck)
$K_{s\psi}$	secondary yaw stiffness (1 per truck)
$T_{s\psi}$	secondary Coulomb breakaway torque
λ	wheel conicity

TABLE 4.1.1: (Cont'd)

Fixed values of the open design parameters used for parametric studies.

Parameter	Units	Stability/ Curving	Lateral Forced Response	Vertical Forced Response
K_{px}	lb/ft (N/m)	———	1.0×10^6 (1.46×10^7)	1.0×10^6 (1.46×10^7)
K_{py}	lb/ft (N/m)	———	5.0×10^5 (7.3×10^6)	5.0×10^5 (7.3×10^6)
K_{pz}	lb/ft (N/m)	1.935×10^6 (2.827×10^7)	1.935×10^6 (2.827×10^7)	1.935×10^6 (2.827×10^7)
K_{sy}	lb/ft (N/m)	24,000. (350,700.)	———	24,000. (350,700.)
C_{sy}	lb-s/ft (N-s/ft)	1,200. (17,530.)	———	1,200. (17,530.)
K_{sz}	lb/ft (N/m)	22,200. (324,600.)	22,200. (324,400.)	———
C_{sz}	lb-s/ft (N-s/m)	2,000. (29,200.)	2,000. (29,200.)	———
$K_{s\psi}$	ft-lb/rad (N-m/rad)	1.0×10^6 (1.36×10^6)	6.0×10^6 (8.16×10^6)	———
$T_{s\psi}$	ft-lb (N-m)	7,500. (10,180.)	———	———
λ	——— ———	———	0.05	———

TABLE 4.1.1 (Cont'd)

Dependent Parameters (fixed by other parameters)		Dimension	
C_{px}	primary longitudinal damping (4 per truck)	$\frac{K_{px}}{250.}$	lb-s/ft (N-s/m)
C_{py}	primary lateral damping (6 per truck)	$\frac{K_{py}}{250.}$	lb-s/ft (N-s/m)
C_{pz}	primary vertical damping (6 per truck)	$\frac{K_{pz}}{250.}$	lb-s/ft (N-s/m)
$C_{s\psi}$	secondary yaw damping (1 per truck)	$\frac{K_{s\psi}}{250.}$	ft-lb-s/rad (N-m-s/rad)
f_{11}	lateral creep force coefficient	lb (N)	
f_{12}	lateral/spin creep force coefficient	ft-lb (N-m)	
f_{22}	spin creep force coefficient	ft^2-lb ($N-m^2$)	
f_{33}	longitudinal creep force coefficient	lb (N)	
a_{11}	wheelset roll coefficient		
δ_o	centered contact angle		
Δ	contact angle difference coefficient		

The wheel/rail contact parameters take the following values as a function of λ. These creep coefficients correspond to full Kalker values. Field experience has led some investigators to use from 50% to 100% of the full value. The use of full Kalker values is conservative for stability calculations in most cases, and reduced creep coefficients generally result in increased critical speed.

TABLE 4.1.1 (Cont'd)

λ	f_{11}	f_{12}	f_{22}	f_{33}	a_{11}	δ_o	Δ
0.05	2,120,000. (9,440,000.)	17,500 (23,760.)	160. (66.)	2,300,000. (10,240,000.)	0.05	0.05	0.0
0.1	2,245,000. (10,000,000.)	17,525. (23,790.)	375. (155.)	2,520,000. (11,220,000.)	0.0675	0.0675	4.5
0.15	2,370,000. (10,560,000.)	17,550. (23,820.)	274. (113.)	2,760,000. (12,200,000.)	0.075	0.075	9.0
0.25	2,620,000. (11,670,000.)	17,600. (23,890.)	1,020. (422.)	3,180,000. (14,160,000.)	0.095	0.095	17.8

TABLE 4.1.1: (Concl'd)

Miscellaneous Parameters		Dimension
V	Vehicle Speed	110. mph (177. km/h)

Class 6 track

Front end passenger location: 29.75 ft ahead of carbody c.g. longitudinally

3.75 ft off center laterally

Rear end passenger location: 29.75 ft behind carbody c.g. longitudinally

3.75 ft off center laterally

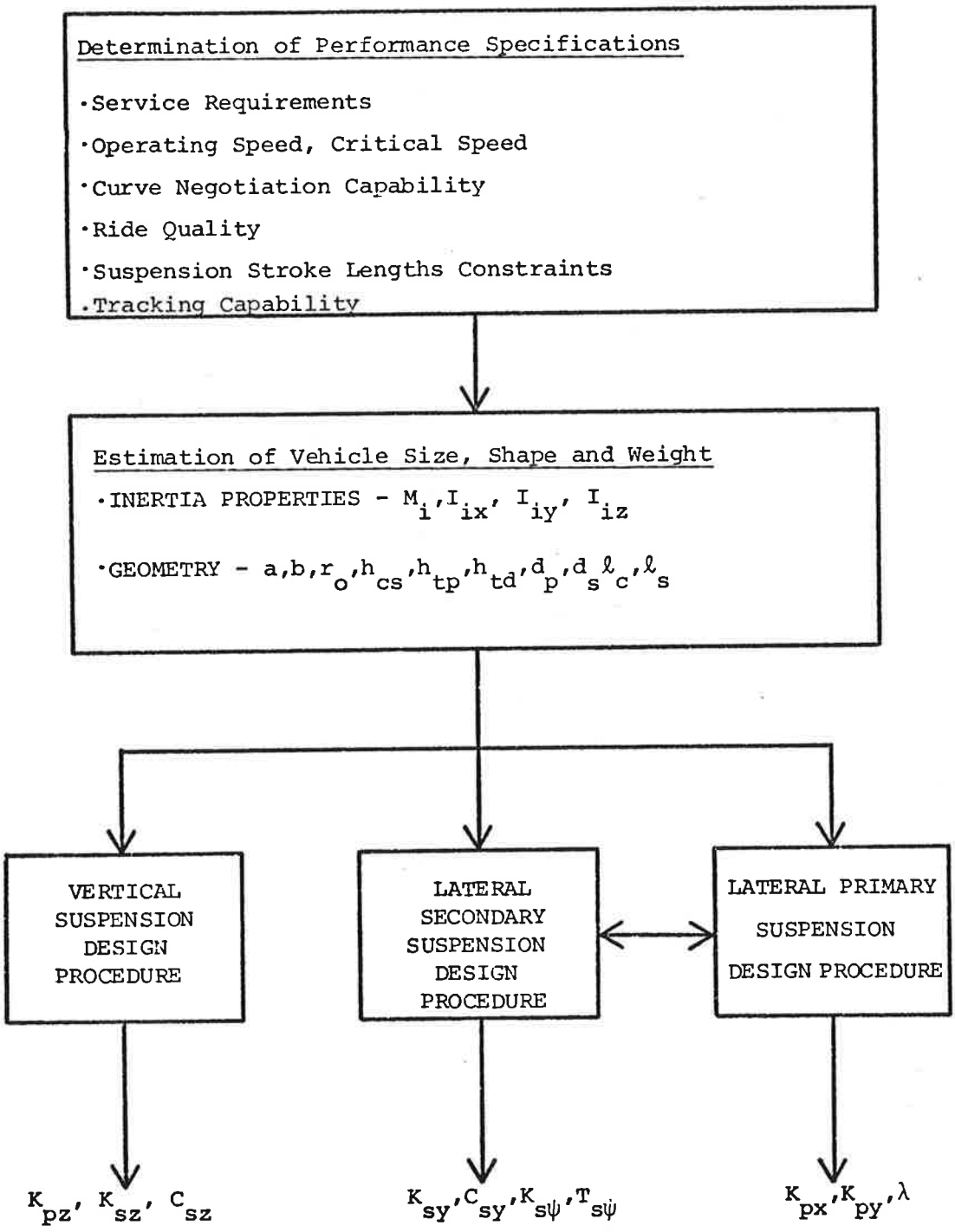

FIGURE 4.1.1: OVERVIEW OF THE DESIGN PROCEDURE

determined by service requirements primarily and are relatively fixed for a given type of intercity service. The dynamic design methodology starts with the fixed parameters and determines the free parameters by considering three factors of performance.

- Vertical ride quality to set vertical secondary suspension parameters
- Lateral ride quality to set secondary lateral suspension parameters
- Lateral stability and curving to set primary suspension and wheel profile parameters.

The bases for the detailed procedure are described in the following sections.

After the free parameters have been selected using the design procedure, the dependent parameters may be selected directly. These parameters include wheel-rail parameters which are set from a wheel-rail profile selected by establishing a design conicity. They also include primary damping values, which are assumed to be related directly to primary stiffness values for the designs which employ rubber elements in the primary suspension. These damping values are selected as 1/250 of the corresponding primary stiffness. In the analyses conducted in this study it has been found that primary suspension damping does not significantly influence performance.

4.2 Methodology Basis

The design methodology selects parameters to satisfy the performance indices which have been cited above. Based upon the work summarized in reference [39], the effects of the design parameters on performance measures may be categorized as shown in Table 4.2.1. The table identifies those parameters which strongly, moderately or weakly influence a given measure. The data show that the vertical ride quality and stroke lengths are only influenced strongly by secondary vertical stiffness and damping and moderately by primary vertical stiffness. These parameters occur in the vertical ride quality model, thus the vertical ride quality-stroke characteristics are decoupled from other performance indices and design parameters and may be considered in initial design studies independently. The selection of these vertical parameters may be considered in terms of a ride quality-stroke trade-off with respect to secondary stiffness with an optimum value of secondary damping existing to achieve the best trade-off. The primary stiffness only influences this tradeoff moderately and is selected to achieve reasonable primary vertical strokes.

Lateral stability and curving are strongly dependent on the primary lateral and bending stiffness, secondary yaw stiffness and break-away torque and wheel rail parameters. The selection of these parameters may be viewed from a stability versus curving trade-off.

TABLE 4.2.1: EFFECT OF PARAMETERS ON PERFORMANCE INDICES AND CONSTRAINTS

PARAMETER	STABILITY	CURVING	FORCED RESPONSE-LATERAL				FORCED RESPONSE-VERTICAL	
			RIDE QUALITY	SECONDARY STROKES	PRIMARY STROKES	WHEELSET EXCURSION	RIDE QUALITY	SECONDARY STROKES
K_{py}	S	M	M	M	M	M	W	W
K_{pz}	W	W	W	W	W	W	M	M
$K_b = d_p^2 K_{px}$	S	S	M	M	M	M	W	W
K_{sy}	W	W	S	S	W	W	W	W
K_{sz}	W	W	W	W	W	W	S	S
$K_{s\psi}$	S	M	W	W	W	W	W	W
$T_{s\psi}$	M	S	W	W	W	W	W	W
C_{sy}	W	W	S	S	W	W	W	W
C_{sz}	W	W	W	W	W	W	S	S
Wheel/Rail Param.	S	S	M	M	M	M	W	W
V	S	S	M	M	M	M	M	M

W - weak effect
M - moderate effect
S - strong effect

Parameters which are not listed are "W" for all indices.

In a following section detailed trade-off curves are presented to aid in selection of these primary lateral and bending stiffnesses and secondary yaw stiffness parameters. These parameters do not have a strong influence on either the vertical or lateral ride quality-stroke characteristics.

The lateral ride quality-secondary stroke performance measures are strongly dependent upon secondary lateral stiffness and damping and moderately dependent upon primary lateral suspension and wheel-rail parameters. Thus, once the primary suspension and wheel profile parameters are selected, the secondary lateral suspension parameters may be selected to achieve a good ride quality-stroke trade-off.

The integration of these three types of performance tradeoffs into a design methodology is illustrated in Figure 4.2.1. Also shown in the Figure is the coupling and iterative loop required in the lateral stability-curving and ride quality-stroke trade-off since primary suspension parameters and wheel profile parameters have a moderate influence on the ride quality-secondary stroke performance.

4.3 Vertical Ride Quality-Suspension Stroke Design

The methodology for selecting vertical suspension parameters has been developed by identifying the modes of vibration which directly influence vehicle carbody accelerations in the range of human sensitivity and contribute substantially to vehicle stroke. For the prototype baseline vehicle the natural frequencies and damping ratios of the natural modes of vibration computed with the vertical response model [39]

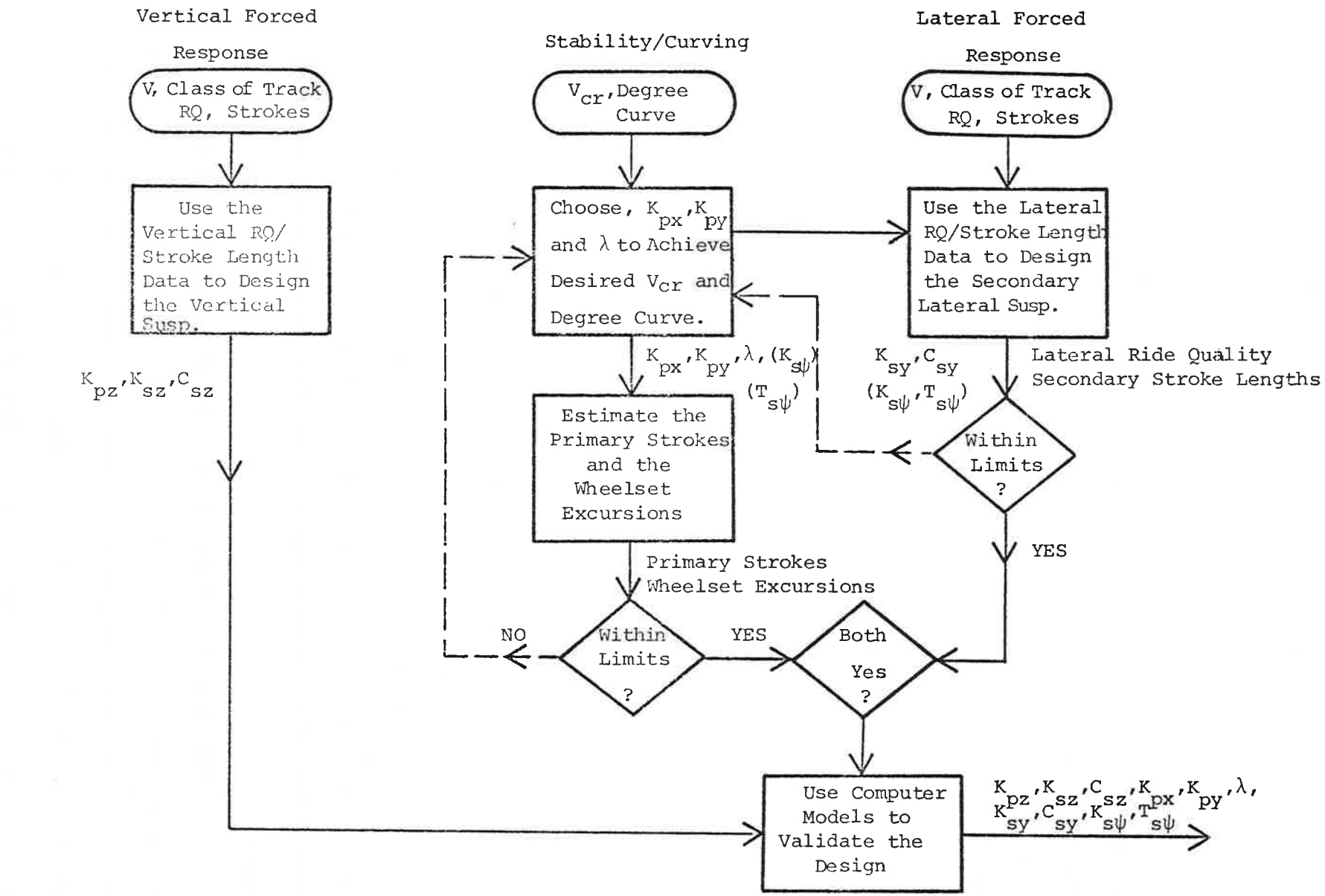

RQ means Ride Quality.

FIGURE 4.2.1: DESIGN METHODOLOGY

are summarized in Figure 4.3.1. Since all of these modes are related directly to vehicle and truck inertial, stiffness and damping properties they are independent of operating speed. The three rigid body modes (roll, heave and pitch) are in the 0.6-1.1 Hz range and are isolated from the flexible carbody bending and torsion modes in the 7-30 Hz range. These flexible carbody modes are in the truck roll and heave range of natural frequencies. The primary modes which contribute to ride quality and carbody-truck stroke are the rigid body modes near 1.0 Hz. However, the flexible modes when they are excited can also influence ride. A commonly adopted goal in truck-carbody design is to keep the truck heave and roll modes from aligning with carbody bending and torsion modes. When these separations are maintained, then the vertical ride quality-suspension stroke design task may focus upon the rigid body modes set by the secondary suspension elements and carbody inertial properties. Estimates of the truck and carbody rigid body natural frequencies and damping ratios may be computed directly from the equations summarized in Chapter 3 for comparison with flexible body modes established by carbody design. These calculations provide a basis for establishing a separation of flexible body modes and truck modes.

The acceleration generated in the prototype carbody running at 110 mph due to class 6 track irregularities is illustrated in Figure 4.3.2. These data show that the primary contributions to the total rms acceleration (a function of the area under the spectral density curve) occurs in the 0-2 Hz frequency range. Approximately 80% of the

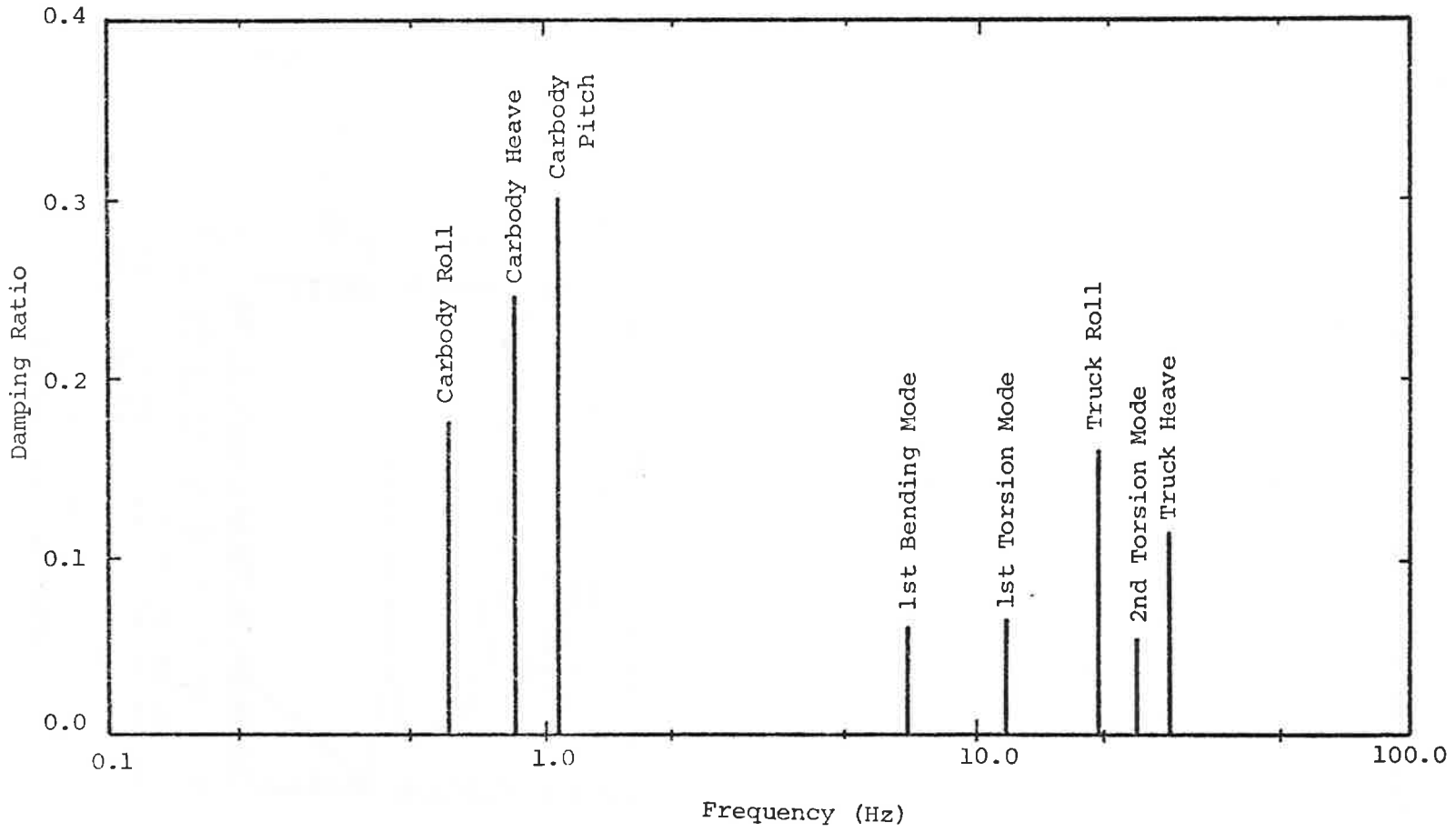

FIGURE 4.3.1: NATURAL FREQUENCIES AND DAMPING RATIOS OF THE PROTOTYPE VEHICLE-VERTICAL MODEL

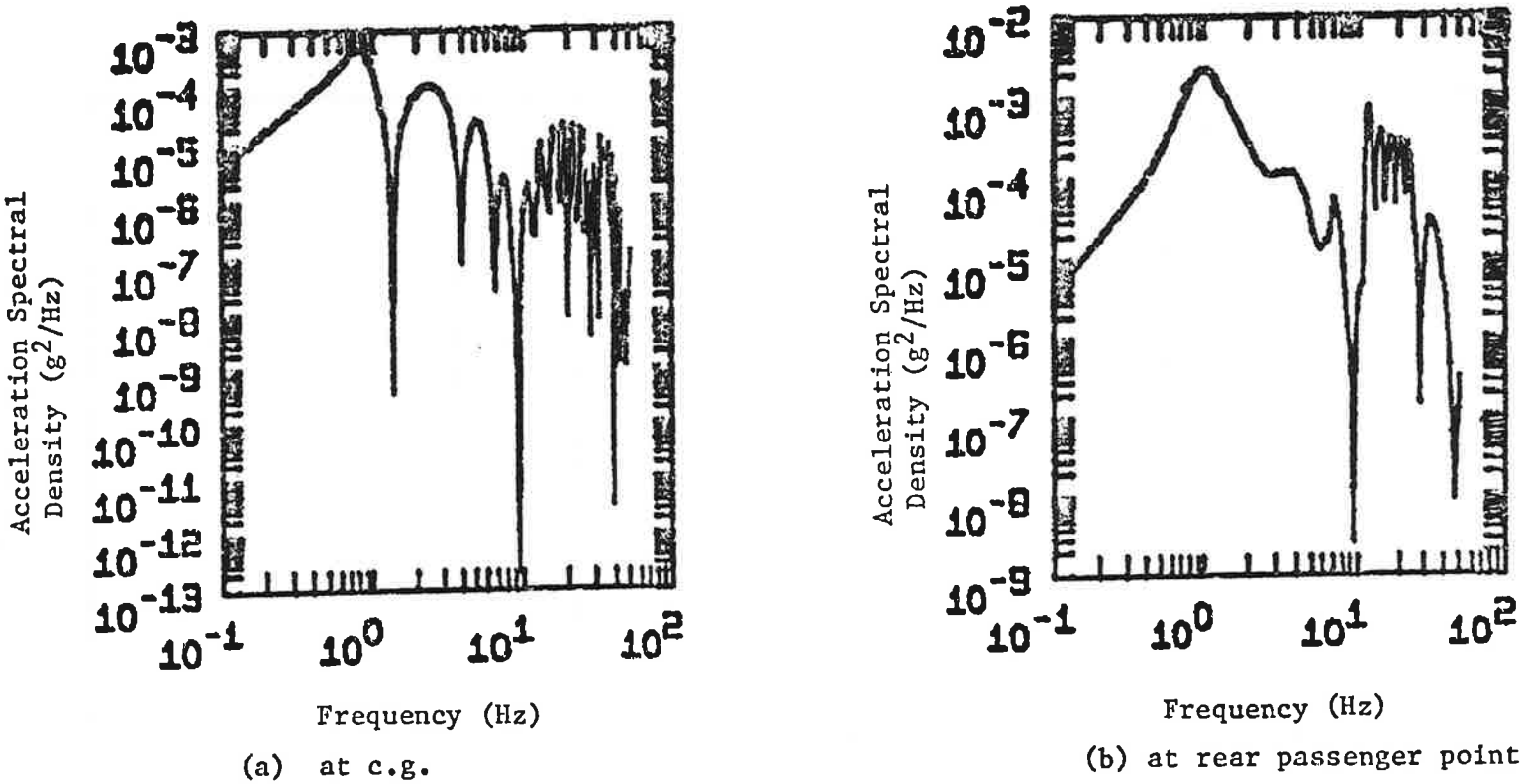

FIGURE 4.3.2: VERTICAL ACCELERATION SPECTRAL DENSITIES FOR THE BASELINE VEHICLE WITH CONVENTIONAL SECONDARY SUSPENSION

rms acceleration is represented by the acceleration in this frequency range. These accelerations are determined primarily by vehicle body motions and are thus determined by primarily the secondary suspension stiffness and damping parameters.

An individual rigid body motion z (heave, pitch or roll) excited by input u may be characterized in the frequency range near the natural frequency approximately by the following acceleration and stroke transfer functions

$$\frac{\ddot{z}}{u} = \frac{s^2(2\xi\, s/\omega_n + 1)}{\left(\frac{s^2}{\omega_n^2} + \frac{2\xi}{\omega_n} s + 1\right)} \qquad (4.3\text{-}1)$$

$$\frac{z_r}{u} = \frac{s^2/\omega_n^2}{\left(\frac{s^2}{\omega_n^2} + \frac{2\xi}{\omega_n} s + 1\right)}, \qquad (4.3\text{-}2)$$

where $\ddot{z}$ = mode acceleration

z_r = relative stroke across secondary suspension

ω_n = mode natural frequency

ξ = mode damping ratio.

These transfer functions are plotted in Figure 4.3.3 for several values of ω_n. As ω_n is reduced the stroke increases and the acceleration decreases. As the damping ratio is increased the stroke decreases, while for small ($\xi < 0.1$) or large ($\xi > 0.8$) damping ratios

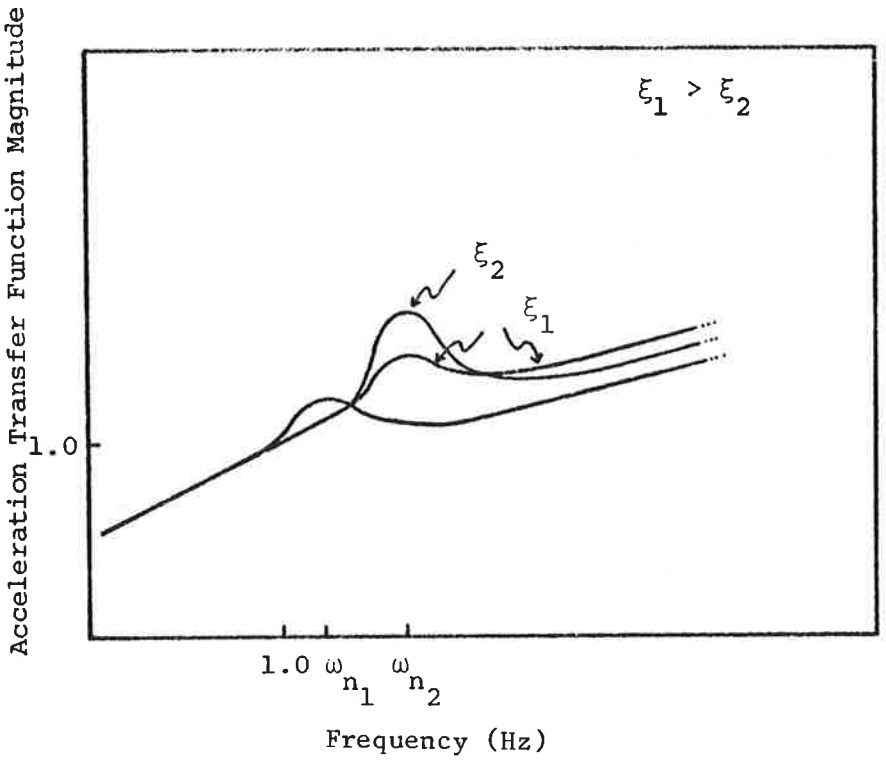

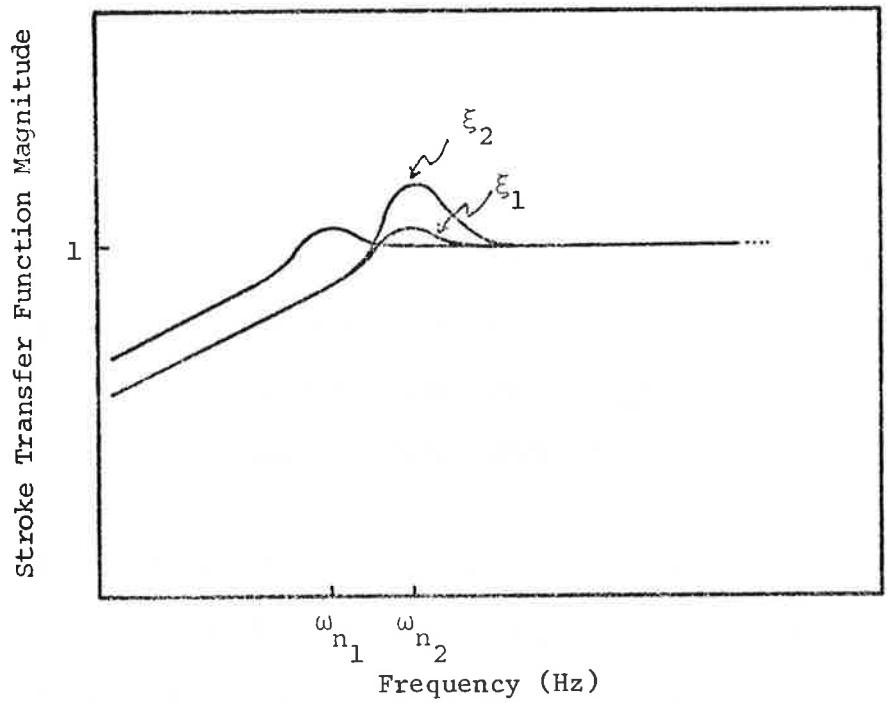

FIGURE 4.3.3: RIGID BODY MODE TRANSFER FUNCTIONS
(All coordinates logarithmic)

the acceleration transfer function increases. If ξ is very small, a large resonant peak occurs, while if ξ is too large high frequency accelerations are transmitted. The single mode model shows that a fundamental tradeoff exists between acceleration and stroke which is controlled by suspension stiffness and damping elements for a fixed mass.

This suspension trade-off is illustrated as computed with a full vertical model [39] of the prototype vehicle in Figure 4.3.4 where rms acceleration and rms stroke for a 110 mph operation on class 6 track are plotted for the vehicle center of mass and the rear passenger point. These data illustrate the specific trade-off between acceleration and stroke. They illustrate that once an allowable stroke is selected, a damping ratio and natural frequency may be selected to achieve a minimum acceleration level. For a given carbody then suspension stiffness and damping values may be directly computed since

$$\omega_n = \sqrt{\frac{K}{M}}$$

$$\xi = \frac{1}{2} \frac{C}{\sqrt{KM}} ,$$

where: ω_n = natural frequency

ξ = damping ratio

K = total stiffness of mode

M = mass

C = damping parameter.

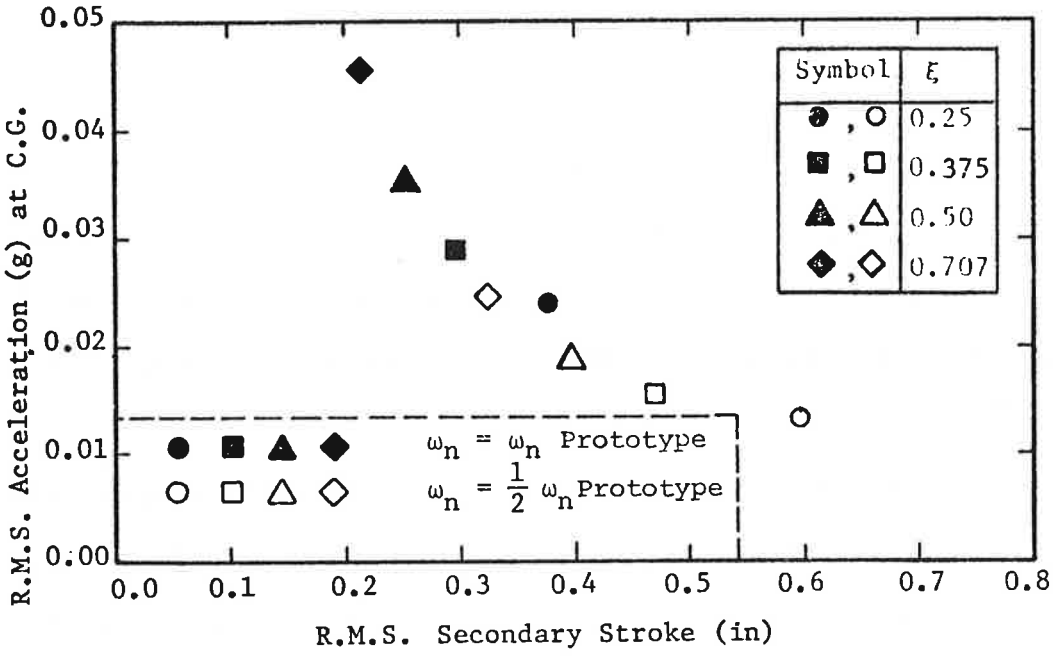

(a) at c.g.

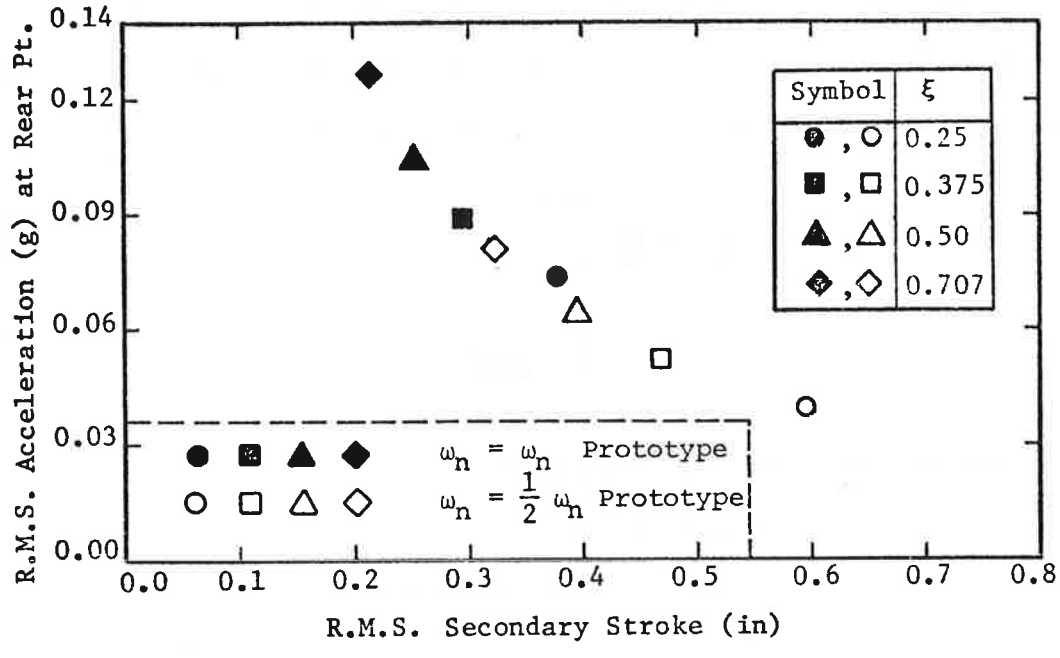

(b) at rear passenger point

FIGURE 4.3.4: VERTICAL RIDE QUALITY-SUSPENSION STROKE TRADE-OFFS FOR THE PROTOTYPE VEHICLE AT 110 MPH

For a 110 mph vehicle traveling on class 6 track, the curves in Figure 4.3.4 are relatively general for fixed truck spacing length. The resulting accelerations and strokes are strongly dependent only upon the secondary suspension natural frequency and damping ratio.

It is also noted that while not discussed here, trade-off data for pneumatic-orifice type suspensions have been prepared [39] and may be used in place of the conventional suspension discussed above.

In the design methodology, rms acceleration-secondary stroke trade-off curves are provided for conventional forms of secondary suspension. These curves are used directly to select the secondary suspension vertical stiffness and damping parameters in the design procedure. Since the design procedure is based upon linear analysis the stroke length may be characterized as remaining within three times the rms value for 99.7% of the time. In practice bump stops are employed to provide hard limits to overall excursions and guarantee an overall envelope. If the suspension design is selected so that the rms stroke is one third of the total travel available, these stops will only rarely be encountered and linear design provides a good basis for selection of parameters.

The ride quality-stroke trade-off establishes values for the secondary vertical suspension parameters. The trade-off is to first order independent of the primary vertical suspension parameters. The recommendation for selection of the primary suspension stiffness is to achieve a primary natural frequency of approximately 10 Hz. This primary

stiffness may be set then using the formula for primary natural frequency cited in Chapter 3. The primary damping is related directly to stiffness for rubber types of primary elements and is selected as 1/250 of the primary stiffness. For practical values of primary damping, this parameter has little influence on performance.

4.4 Lateral Ride Quality - Suspension Stroke Design

The response of the carbody to lateral track irregularities results in accelerations that set the overall levels of ride quality in the carbody and in motions which establish the carbody-truck strokes. Vehicle response mode natural frequencies and damping ratios which contribute to this response are illustrated in Figure 4.4.1 for the prototype vehicle. The figure corresponds to operation at 110 mph. The first three modes are rigid body (roll-lateral, lateral-roll, lateral-yaw) motions modes between 0.4 and 1.1 Hz. These mode natural frequencies and damping ratios are relatively independent of vehicle speed and depend upon carbody inertial parameters and secondary suspension stiffness and damping elements. The fourth mode at 2.16 Hz is the truck-wheelset lateral kinematic mode. This mode is strongly influenced by speed and as speed increases for a typical vehicle, the damping associated with the mode decreases and reaches zero at the truck critical speed. This mode is strongly influenced by wheel profile (conicity) and primary suspension design as is mode 5 at 6.16 Hz a wheelset-truck lateral mode. The remaining modes are above 10 Hz and relate directly to truck and wheelset motions. All the wheelset and truck modes (4-9) are influenced primarily by primary

FIGURE 4.4.1: NATURAL FREQUENCIES AND DAMPING RATIOS OF THE PROTOTYPE VEHICLE-LATERAL MODEL (V=110 mph)

suspension and wheel profile design. The selection of these design parameters to insure adequate damping at operating speed is addressed specifically in the stability-curving trade-off. If these higher frequency modes are adequately damped, then they have only a secondary influence on ride quality and the secondary suspension parameters may be considered as the primary design parameters influencing ride quality.

The acceleration spectral density and an ISO type ride quality plot for the prototype vehicle determined from the forced response model [39] for a vehicle traveling at 110 mph on class 6 track are shown in Figure 4.4.2. The spectral density data show that primary contributions to the response occur in the 0-2 Hz frequency range while the ISO plot shows the primary area of concern is near 1 Hz. The forced response in this frequency region is influenced primarily by the rigid body modes. More than ninety-five percent of the total rms acceleration in the carbody and the rms secondary suspension strokes are represented by the frequency band 0-2 Hz. Thus, the lateral ride quality-stroke trade-off may be considered primarily in terms of the secondary suspension design parameters which influence the rigid body modes.

The lateral forced response design is then conceptually similar to the vertical design in which secondary suspension parameters are selected on the basis of the acceleration-suspension stroke trade-off in which as natural frequency is increased the stroke decreases and the acceleration increases. Trade-off data for the secondary suspension parameters based on a full carbody model are illustrated in Figure 4.4.3.

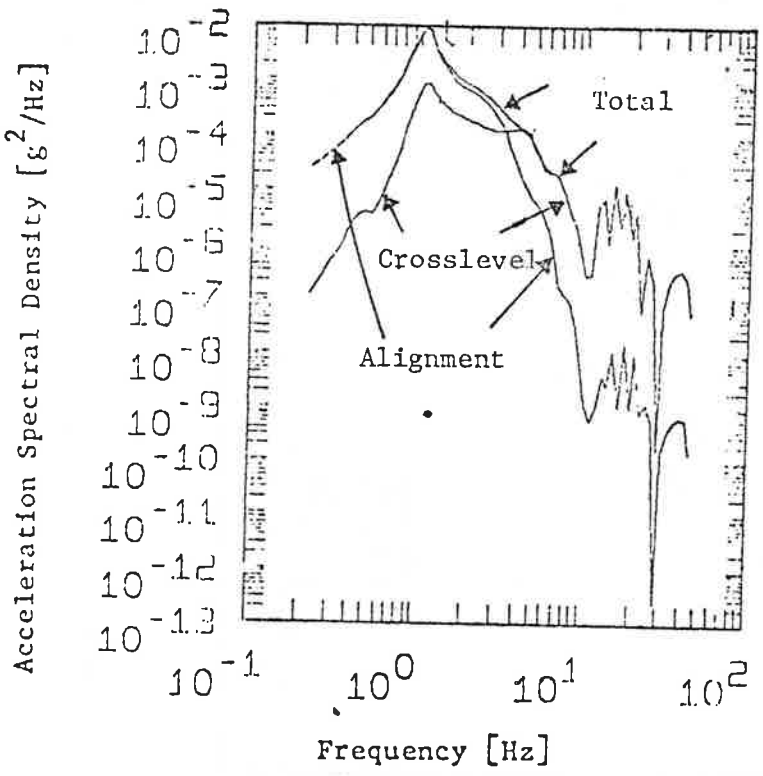

(c) Acceleration Spectral Density

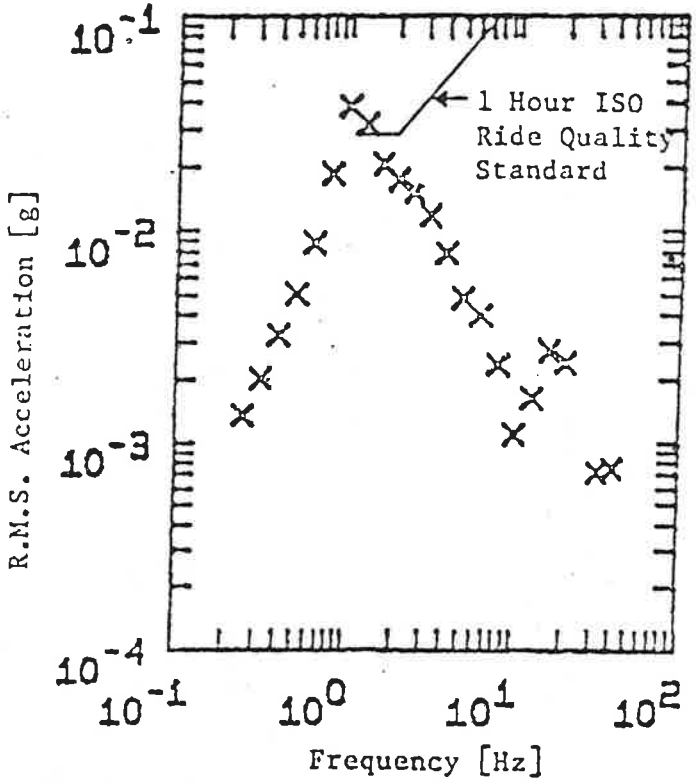

(d) One Third Octave Band R.M.S. Acceleration

FIGURE 4.4.2: FRONT PASSENGER POINT SPECTRAL DENSITY AND ONE THIRD OCTAVE BAND PLOTS

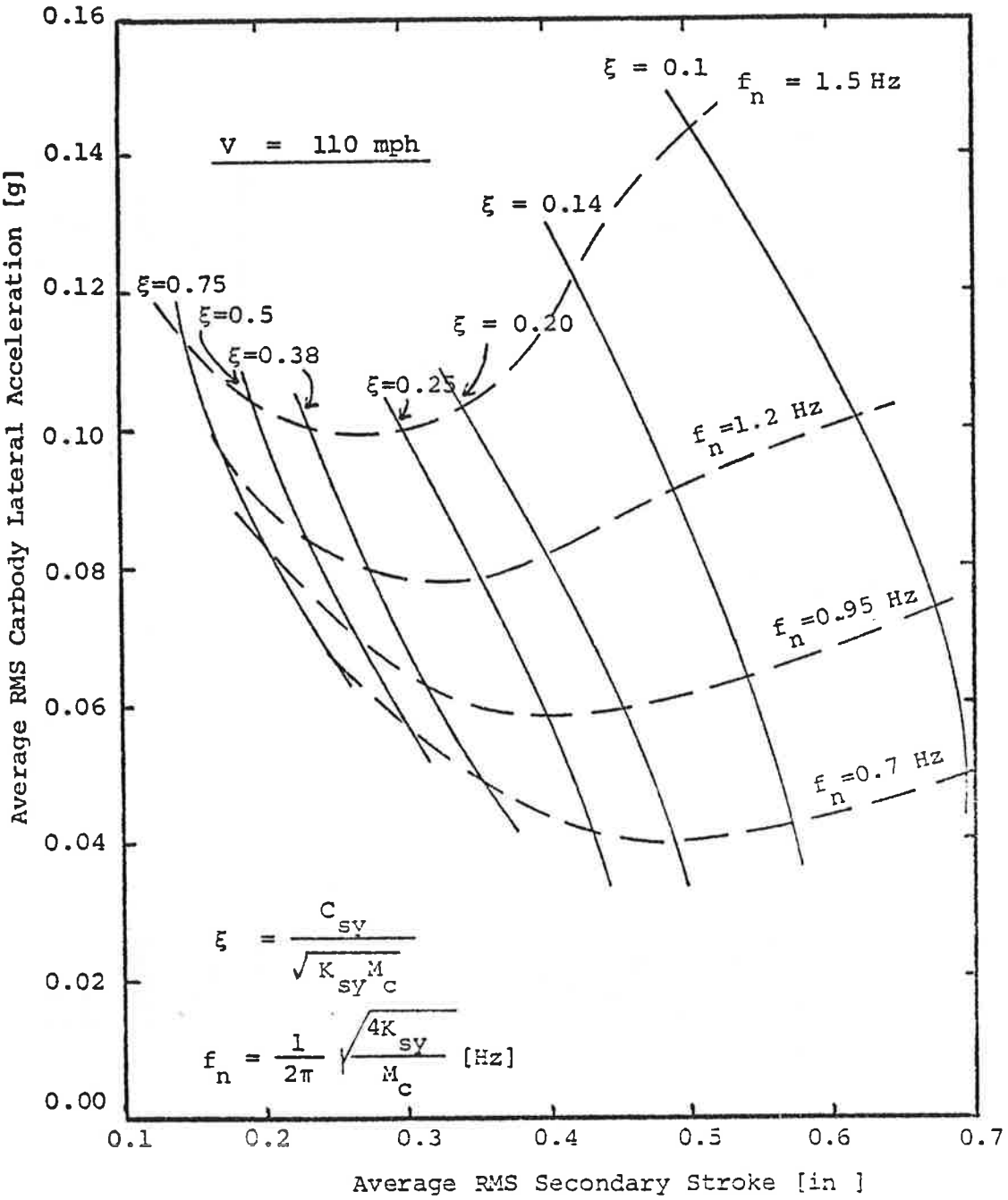

FIGURE 4.4.3: CARBODY LATERAL ACCELERATION-SECONDARY STROKE LENGTH TRADE-OFF PLOT, V=110 mph

These data show that a damping ratio in the range 0.2-0.3 provides the best tradeoff for any given suspension natural frequency. The natural frequency can then be selected to provide minimum rms acceleration for the stroke allowable. Directly from the selection of natural frequency, the secondary stiffness may be computed for the given car mass and from the damping ratio the suspension damping constant may be computed. Trade-off curves similar to those of Figure 4.4.3 are provided in the design procedure to aid selection of secondary suspension parameters.

Since the secondary suspension design is based upon linear analysis, the strokes will remain within three times the rms values 99.7% of the time; however, to provide an absolute stroke envelope, bump stops may be used to limit travel. If these stops allow motions of three times the rms stroke, they will be encountered infrequently and the performance predictions based on linear analysis will provide a good initial basis for design.

4.5 Stability-Curving Design Trade-Off

4.5.1 Fundamental Parameters

The selection of the primary suspension lateral and longitudinal stiffnesses, the secondary yaw suspension parameters and the wheel profile are governed primarily by the stability-curving tradeoff. The secondary yaw suspension plays a central role in the stability-curving trade-off. This suspension consists typically as shown in Figure 4.5.1 of anchor rods with finite stiffness between the truck and

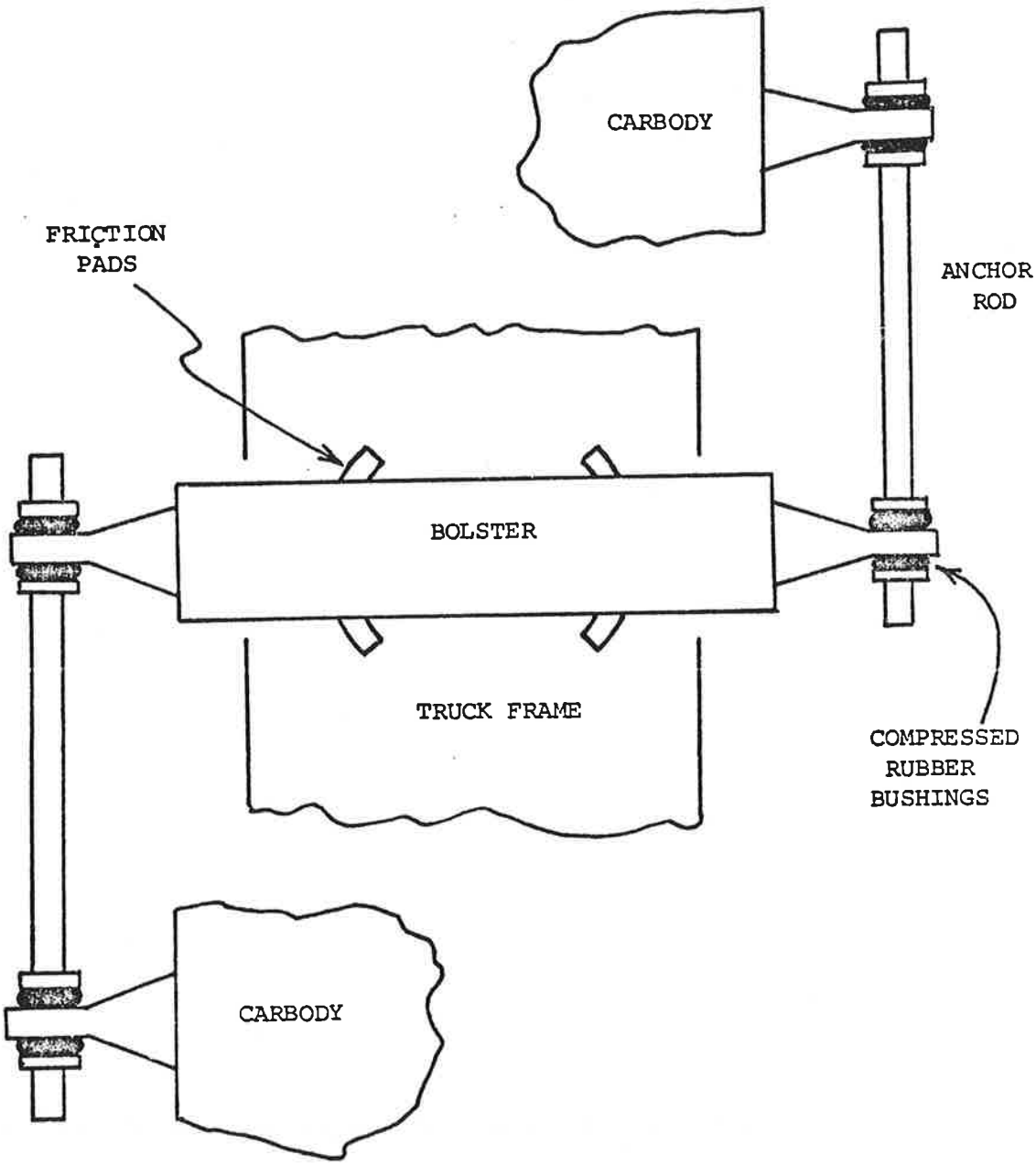

FIGURE 4.5.1: PHYSICAL ARRANGEMENT OF THE SECONDARY YAW SUSPENSION

the bolster and then a center friction plate between the bolster and carbody. When the torque carried by the friction plate is less than a breakaway torque $T_{s\psi}$, the secondary yaw suspension consists of the stiffness in the anchor rod assembly $K_{s\psi}$. In considering stability it is assumed that breakaway does not occur and the secondary yaw suspension is characterized by the stiffness $K_{s\psi}$. In considering curve negotiation, it is assumed breakaway occurs and the secondary yaw suspension is characterized by a breakaway torque $T_{s\psi}$. These assumptions provide a good basis for initial design studies and reflect the design philosophy of U.S. passenger truck design groups. Using these assumptions, the basis for design parameter selection to achieve curve negotiation and stability are described in the following paragraphs.

4.5.2 Curve Negotiation

In the design procedure curve negotiation is considered in terms of the steady-state curving response of a vehicle in a constant radius curve. The limits to curve negotiation are represented in terms of flange contact and slip. Curving ability is described in terms of the largest degree curve which can be negotiated without flanging or slip.

The geometric relationship between a wheelset and the track during curve negotiation is established by the wheel-rail forces and wheelset-truck suspension forces. Lateral and longitudinal creep forces are the dominant forces acting between the rail and the wheel, during curving, with the exception of hard flanging forces which are not considered in this study. The longitudinal creep forces, which result from

the combination of wheel conicity and solid axles, tend to steer a wheelset toward the pure rolling line, the distance of the pure rolling line from the track centerline being dictated by the given wheel conicity and curve radius. The lateral creep force on the wheelset also acts toward the pure rolling line when the wheelset is yawed or steered in that direction relative to the local perpendicular to the track. Thus, a wheelset unconstrained in yaw seeks the pure rolling line of the track, which always sits outside of the track centerline for conventional conical wheels on curved track as shown in Figure 4.5.2. The distance of the pure rolling line from the track centerline, y_o is given in terms of radius of curve, R, wheel radius, r_o, conicity λ and half gauge a by:

$$y_o = \frac{ar_o}{\lambda R} \quad . \tag{4.5-1}$$

In contrast if a pair of wheelsets is fully constrained in yaw in a rigid truck, free from secondary suspension or centrifugal forces, the wheelsets are restricted in their ability to steer toward the pure rolling line in response to the longitudinal creep forces. The resulting lateral and longitudinal creep forces, $F_{lat.}$ and $F_{long.}$ are illustrated in Figure 4.5.3 and are defined as follows from the deviation of creep forces in [39].

$$\begin{aligned} F_{lat.} &= 2\,\frac{b}{R}\,f_{11} \quad \text{(per wheelset)} \\ F_{long.} &= f_{33}\,\frac{\lambda}{r_o}\,y' \text{(per wheel)} \quad . \end{aligned} \tag{4.5-2}$$

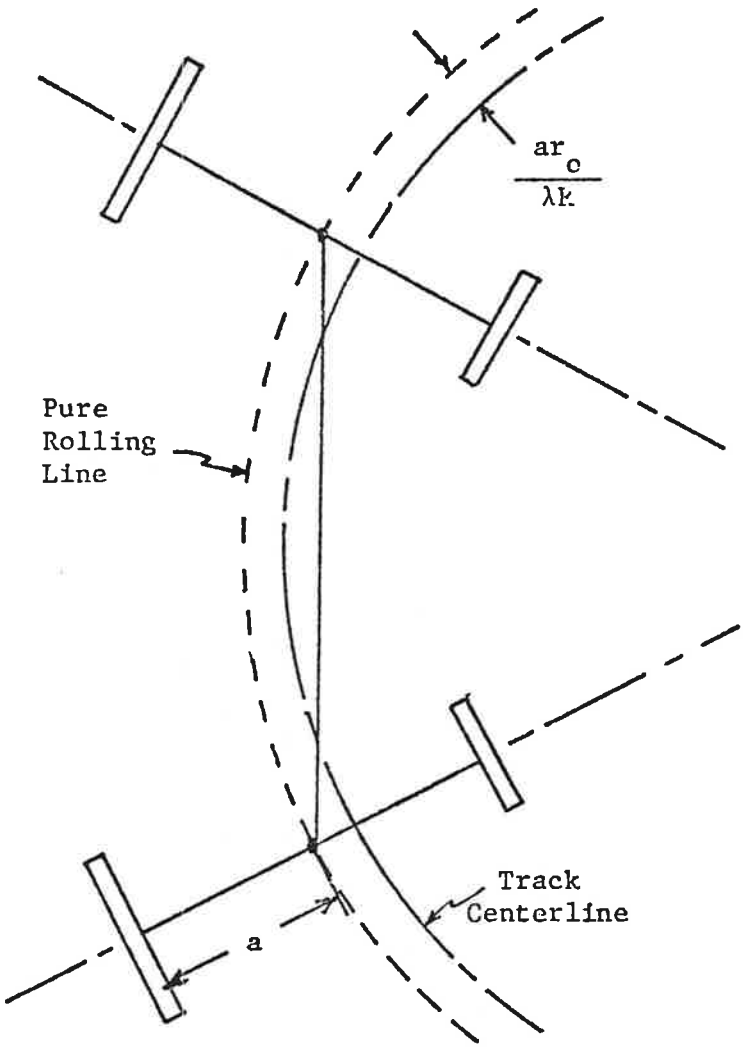

FIGURE 4.5.2: FREE TRUCK, WHEELSETS UNCONSTRAINED IN YAW, BALANCED RUNNING

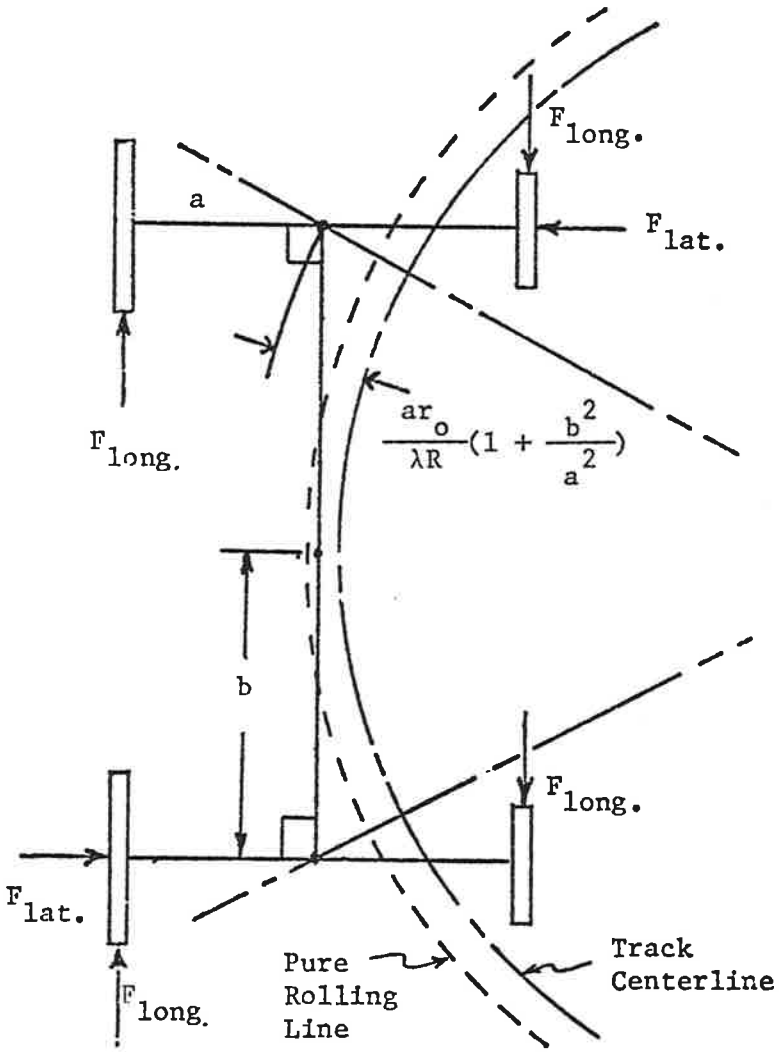

FIGURE 4.5.3: FREE RIGID TRUCK, BALANCED RUNNING

If the lateral f_{11}, and longitudinal, f_{33}, creep force coefficients are assumed equal, the result of summing moments in yaw is

$$y' = \frac{b^2 r_o}{Ra\lambda} \qquad (4.5\text{-}3)$$

or

$$y = y' + \frac{ar_o}{\lambda R} = \frac{ar_o}{\lambda R}\left(1 + \frac{b^2}{a^2}\right). \qquad (4.5\text{-}4)$$

The lateral displacement of a free truck in balanced running is thus essentially bounded by (4.5-1) and (4.5-4) over the full range of primary stiffnesses, although the displacements of the two wheelsets are no longer identical when finite primary stiffnesses are introduced.

When a full vehicle is considered, the carbody exerts secondary suspension moments on the trucks, as illustrated in Figure 4.5.4. The moments are normally similar in magnitude, but their directions are opposite; positive on the front truck, which hinders curving by turning the truck toward the outside rail, and negative on the rear truck, which tends to help curving by steering the truck toward the inside rail.

The steady-state curving performance of a rail vehicle may be evaluated in terms of the slip boundary and/or the flange contact boundary. Both the slip boundary and flange contact boundary are shown for the prototype vehicle in Figure 4.5.5. The slip boundary represents the conditions of cant deficiency discussed in 3.2.3 and degree curve for which the largest resultant creep force magnitude is equal to μN at any wheel of the vehicle. The

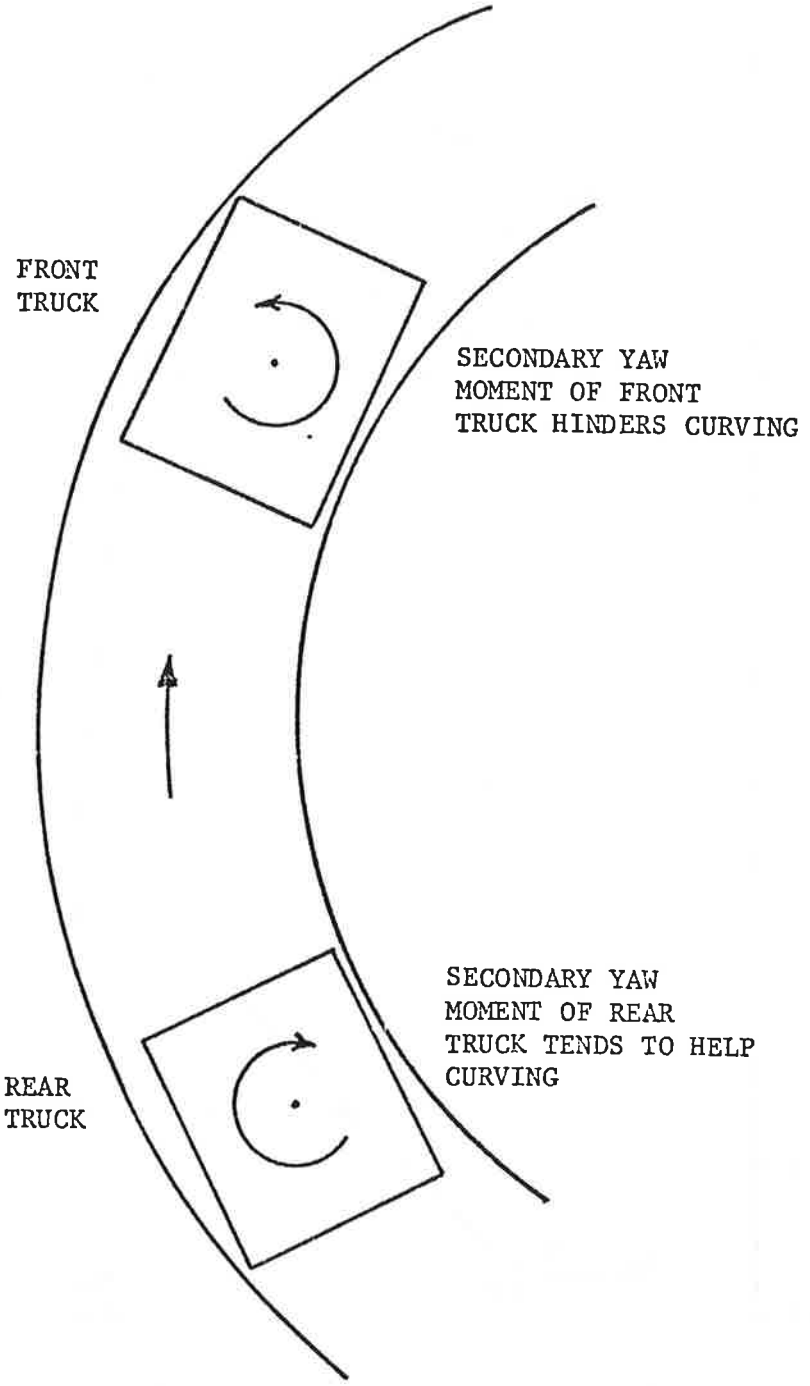

FIGURE 4.5.4: DIRECTION OF SECONDARY YAW MOMENT ON FRONT AND REAR TRUCKS DURING CURVING

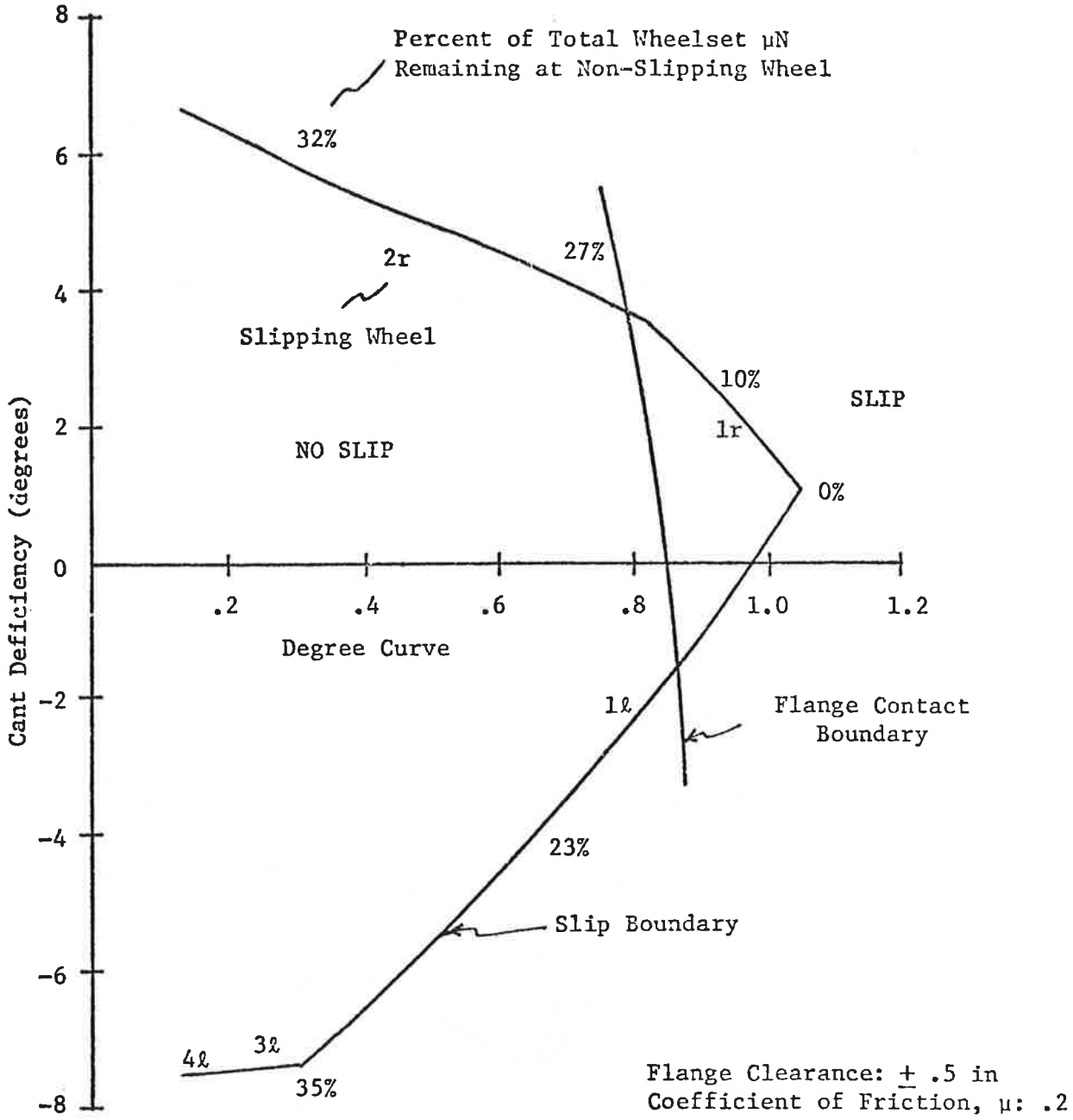

FIGURE 4.5.5: STEADY-STATE CURVING PERFORMANCE CURVE FOR BASELINE VEHICLE

flange contact boundary represents the condition of cant deficiency and degree curve for which the largest lateral displacement of any wheelset in either direction is equal to a flange clearance of 0.5 inches.

Also shown on the performance curve is the wheel which has reached the slip condition in each portion of the curve, and the fraction of μN remaining at the other wheel of the slipping wheelset. At a cant deficiency of about one degree, corresponding to the maximum degree curve negotiable without slip, the fraction of μN remaining at the other wheel goes to zero. At the FRA maximum allowable cant deficiency of 3.07 degrees, the fraction of μN remaining at the other wheel is about 20%, or 10% of the total μN for the wheelset. This figure is fairly low, which suggests that within the allowable range of operation, the slip boundary as defined herein is a relatively good measure of the performance boundary.

Flange contact is reached before slip for the baseline vehicle, at about a 0.8 degree curve. This relatively low value of curvature at which flange contact occurs is a result of the fairly stiff primary suspension adopted for the baseline vehicle. This vehicle would thus tend to flange its way around any curve greater than a 0.85 degree curve.

To provide a basis for selecting design parameters K_{px}, K_{py} and $T_{s\psi}$, steady state curve negotiation is considered with zero cant deficiency. First the influence of the secondary suspension breakaway torque is considered. Data in Appendix A show that the degree

curve which can be negotiated for various values of breakaway torque and secondary suspension longitudinal stiffness. These data indicate that for values of breakaway stiffness above 7500 ft-lb the degree curve negotiation is relatively independent of $T_{s\psi}$ for values of $K_{s\psi}$ less than 10^6 ft-lb/rad. Consistent with data in [39], a baseline value of $T_{s\psi}$ = 7500 ft-lb/rad is recommended for an initial design value.

For designs which are characterized by values of secondary yaw breakaway torque cited above, relatively simple expressions can be derived to represent curve performance as shown in Appendix A. These expressions for flange and slip limits may be summarized as:

$$D = 5730\, y_{fc}\, \frac{K_b K_s + f^2 \frac{\lambda a}{r_o}}{b^2 K_s K_b \frac{r_o}{\lambda a} + b K_b f + \frac{a r_o}{\lambda} K_b K_s + f^2 a^2} \qquad (4.5\text{-}5)$$

where D = degree curve negotiated

y_{fc} = flange limit excursion

for the flange limited case, and

$$D = 5730 \frac{\mu N}{bf} \sqrt{\frac{\left(1 + \frac{f^2 \lambda a}{k_b k_s r_o}\right)^2}{\left(\frac{b}{a} + \frac{f\lambda}{k_s r_o}\right)^2 + 1}} \qquad (4.5\text{-}6)$$

for the slip limited case.

The stiffness K_b is the net bending stiffness

$$K_b = d_p^2 K_{px} \qquad (4.5\text{-}7)$$

and the stiffness K_s is the net shear stiffness

$$K_s = \frac{d_p^2 K_{px} K_{py}}{b^2 K_{py} + d_p^2 K_{px}} \quad . \tag{4.5-8}$$

When flange contact occurs the flanging force may be estimated by setting $y_1 + y_o = y_{fc}$ to yield:

$$F_f = 4f\left[\frac{\frac{1}{R}(b^2 K_s K_b \frac{r_o}{\lambda a} + bK_b f + \frac{ar_o}{\lambda} K_b K_s + a^2 f^2)}{b^2 f K_s + K_b f + bK_s K_b (\frac{r_o}{\lambda a} - 1)}\right.$$

$$\left. + \frac{\frac{F_c}{4f}(b^2 f K_s - bK_s K_b) - y_{fc}(K_b K_s + f^2 \frac{\lambda a}{r_o})}{b^2 f K_s + K_b f + bK_s K_b (\frac{r_o}{\lambda a} - 1)}\right] \quad . \tag{4.5-9}$$

For fixed geometry a, b, r_o and a fixed friction coefficient, the degree curve which can be negotiated depends upon the bending stiffness K_b, the shear stiffness K_s and the wheel conicity λ. Plots of the degree curve which can be negotiated as a function of K_{py}, K_b and λ are summarized in Figure 4.5.6. These data show that the degree curve negotiated increases directly as the bending stiffness K_b is reduced and is relatively insensitive to K_{py} the shear stiffness. As the conicity is increased the degree curve which can be negotiated increases. Thus, in maximizing curving performance, the value of

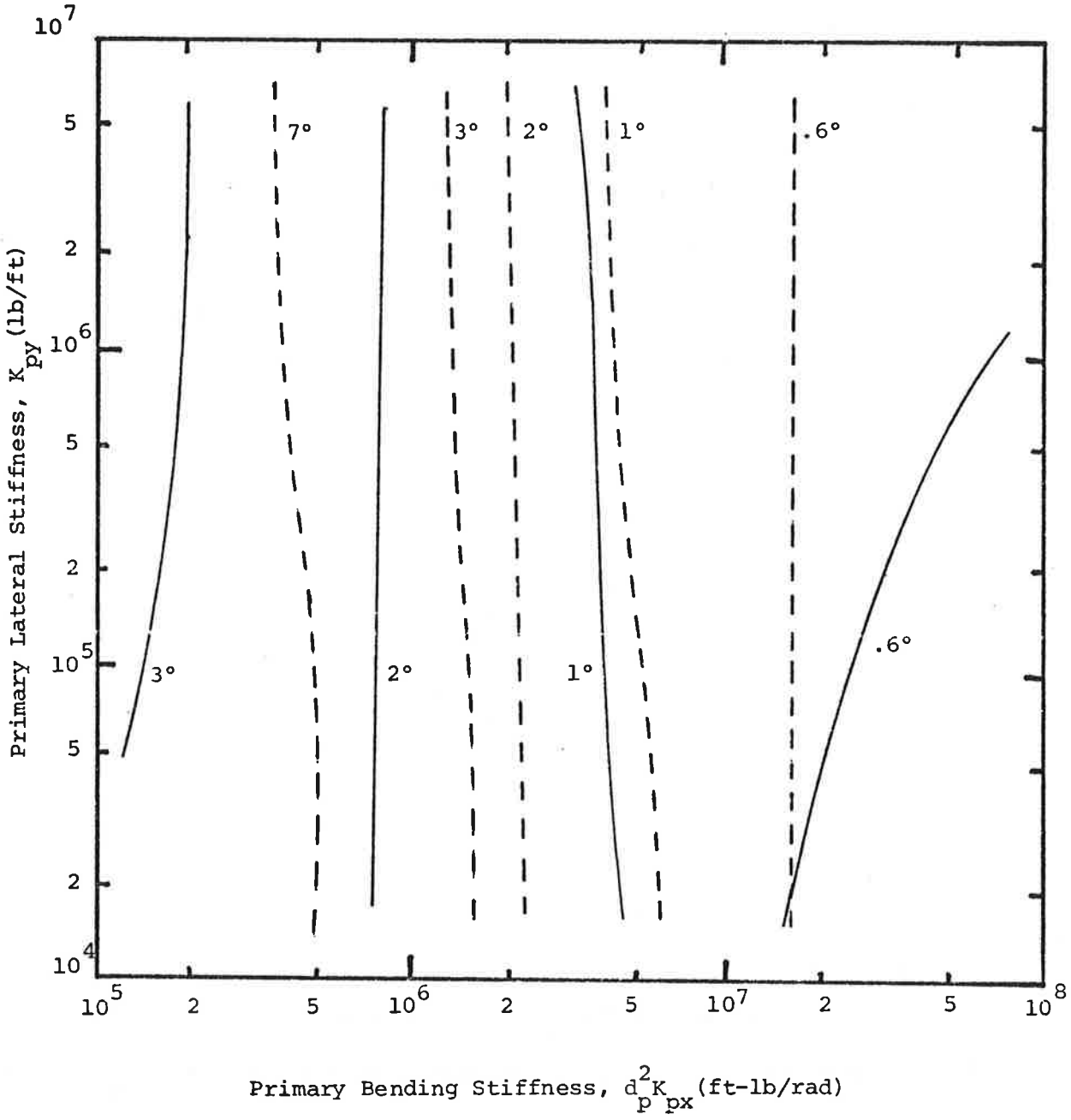

FIGURE 4.5.6: LINES OF CONSTANT CURVING PERFORMANCE FOR TWO VALUES OF CONICITY

longitudinal stiffness $K_{px} = K_b/d_p^2$ is reduced and conicity λ increased. The range over which these parameters can be varied is limited by stability as described in the following section.

4.5.3 Lateral Stability

Lateral stability requirements have a strong influence on primary suspension stiffness design parameters and secondary suspension yaw stiffness. Lateral instability or hunting results directly from wheel-rail forces generated by two wheels connected by a rigid axle. A single unconstrained wheelset is neutrally stable and will undergo sinusoidal oscillation at a kinematic frequency determined by wheel geometry and operating speed.

$$\omega = V \sqrt{\frac{\lambda}{a r_o}} \quad . \tag{4.5-10}$$

Thus primary suspension lateral and longitudinal stiffnesses are utilized to constrain and stabilize wheelsets with respect to the frame. As these stiffness are increased the natural motion of the wheelset is decreased and coupling between wheelsets and the wheelsets and truck frame increases. If the stiffnesses are increased to achieve a rigid primary suspension, then the complete truck will tend to undergo a sinusoidal motion at the kinematic frequency:

$$\omega = V \sqrt{\frac{\lambda}{a r_o}\left(\frac{1}{(1+b^2/a^2)}\right)} \quad , \tag{4.5-11}$$

which is lower than the wheelset kinematic frequency. In practice, the primary suspension stiffnesses are set at values "high enough" to stabilize wheelsets yet "low enough" to allow motion to facilitate curve negotiation. Thus, wheelset-truck coupling occurs and the principal hunting mode which limits rail vehicle stability is a coupled wheelset-truck mode.

The truck is constrained through the secondary suspension to the carbody. An important element used in the suspension is the secondary yaw stiffness. As this stiffness is increased, the truck motion is more strongly coupled to the carbody and as $K_{s\psi}$ increases the complete carbody has a kinematic frequency of:

$$\omega = V\sqrt{\frac{\lambda}{ar_o}\;\frac{1}{(1+\frac{b^2}{a^2})\left(1+\frac{\ell^2}{a^2\,(1+b^2/a^2)^2}\right)}}\;. \qquad (4.5\text{-}12)$$

The carbody kinematic frequency is lower than the truck frequency. In practice the secondary yaw stiffness is limited to values which allow only partial coupling between the trucks and the carbody.

As vehicle speed is increased, first the carbody kinematic frequency is reached, second the truck kinematic frequency and finally the wheelset kinematic frequency is reached. As speed increases the basic damping generated by wheel-rail interaction forces decreases. Thus while a tendency for carbody hunting can occur at relative low speeds (20-50 mph for typical passenger car designs), it is usually controlled by secondary suspension damping and is reflected by low

damping and not instability. As the speed increases and the inherent damping decreases for typical passenger truck design, a coupled truck wheelset mode is reached at which point damping is reduced to zero. This mode usually occurs at speeds below the pure wheelset hunting mode and is the primary hunting mode which occurs in typical passenger vehicles. The speed at which zero damping is reached is the vehicle critical speed.

A plot of the natural frequency and damping ratio associated with the two critical wheelset-truck modes of vehicle lateral response are shown in Figure 4.5.7 computed with the analysis of [39] as a function of velocity.

As speed increases, the damping of both modes decreases, however, the major mode with the lower natural frequency decreases until at the critical speed of 280 mph zero damping is reached. All other modes of vehicle behavior have damping ratios which are relatively independent of velocity.

The influence of suspension primary stiffness parameters and wheel conicity on vehicle critical speed computed using the analysis of [39] are illustrated in Figures 4.5.8 and 4.5.9. These data show that as the primary lateral stiffness K_{py} is increased, the critical speed increases sharply in a limited region of, K_{py} and as K_{py} is increased above 8×10^5 lb/ft critical speed is less sensitive to further increases in K_{py}. For very low values of K_{py} the wheelsets are not strongly coupled to the truck frame and the wheelset mode is

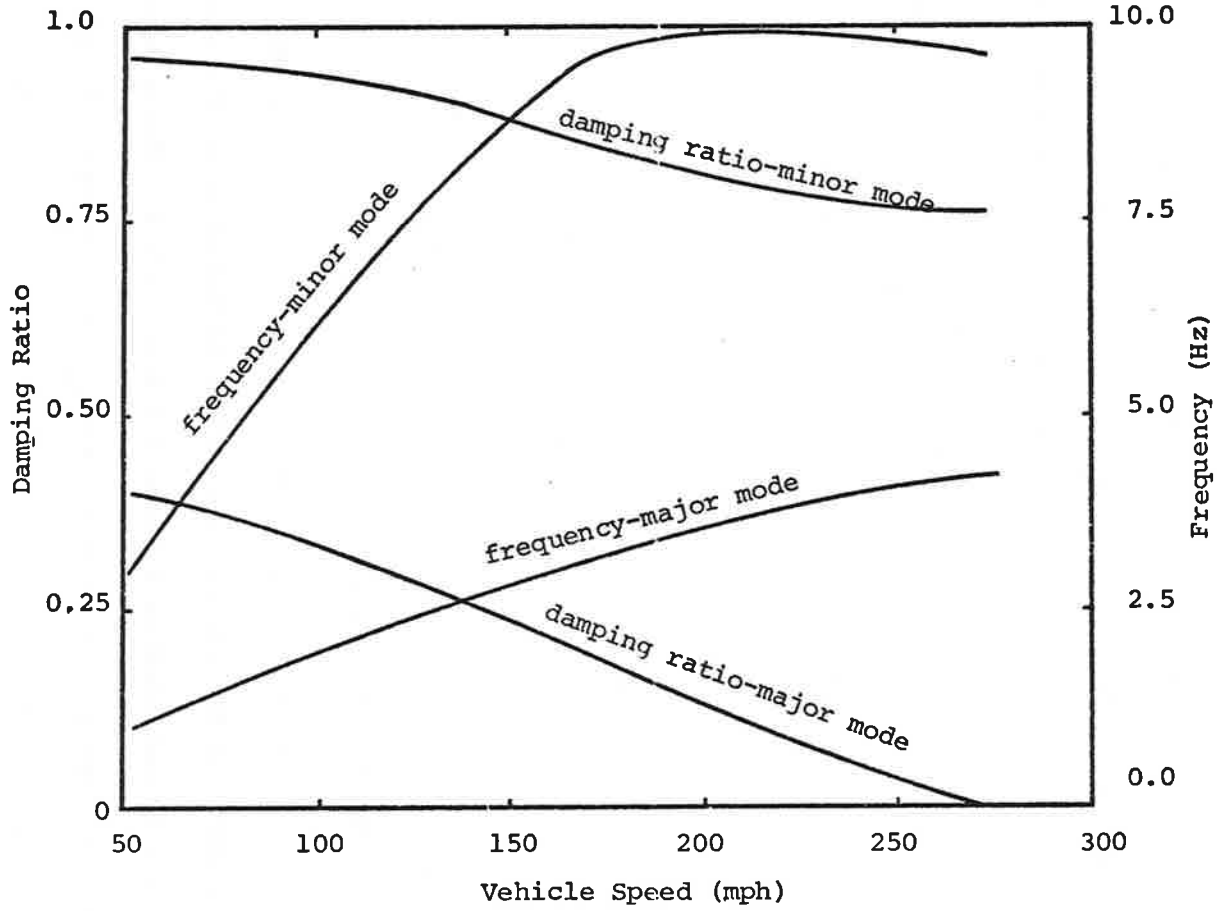

FIGURE 4.5.7: FREQUENCIES AND DAMPING RATIOS OF THE PROTOTYPE VEHICLE KINEMATIC MODES

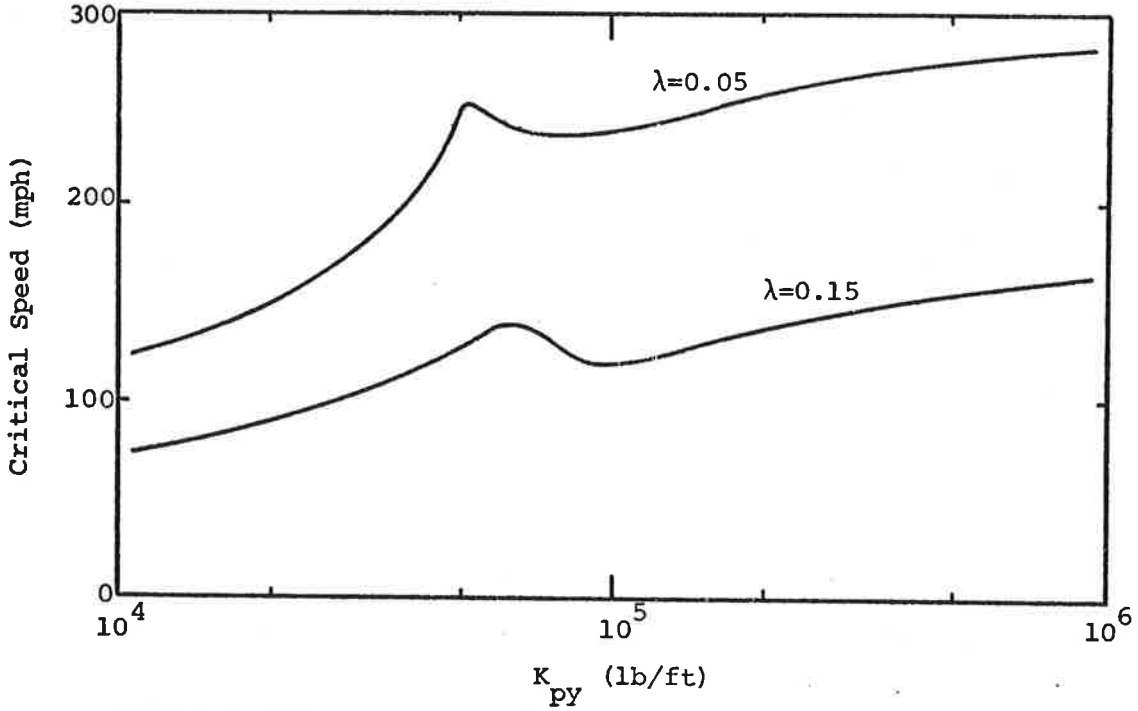

FIGURE 4.5.8: INFLUENCE OF PRIMARY LATERAL STIFFNESS ON THE CRITICAL SPEED OF THE PROTOTYPE VEHICLE

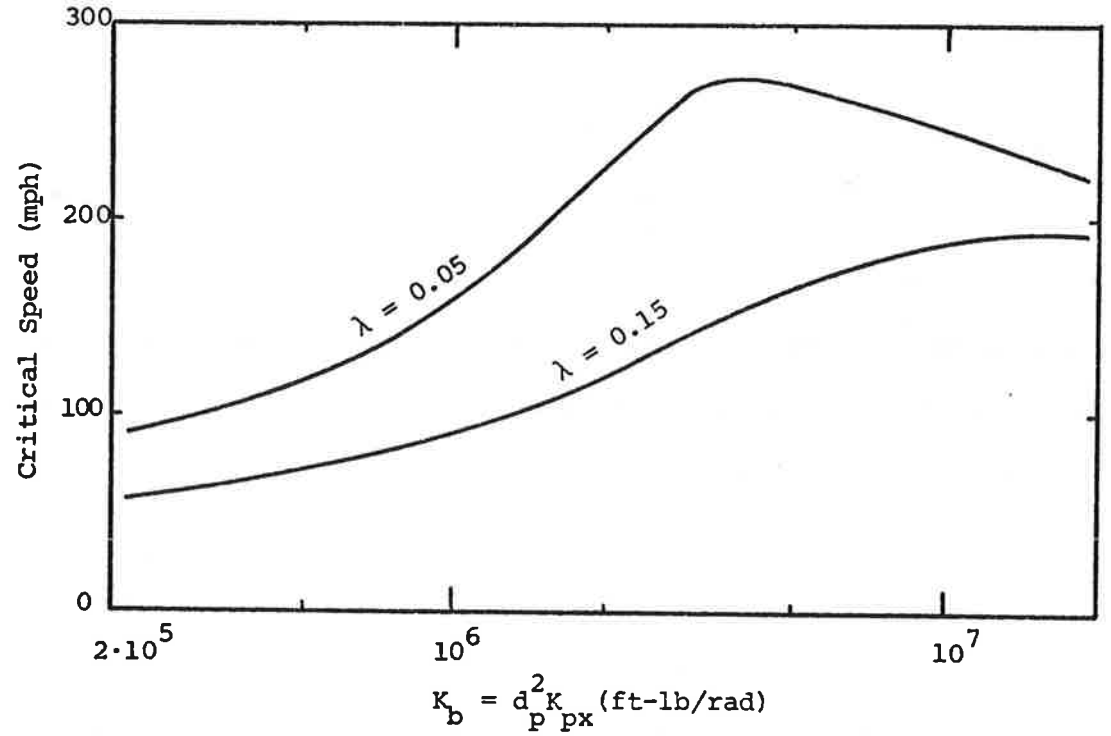

FIGURE 4.5.9: INFLUENCE OF PRIMARY BENDING STIFFNESS ON THE CRITICAL SPEED OF THE PROTOTYPE VEHICLE

important and as K_{py} is increased, the wheel-truck coupling increases and stabilizes the wheelset mode. Once a sufficiently high value of stiffness is reached, a rigid track configuration is approached and further increases in stiffness do not increase the critical speed.

The primary longitudinal bending stiffness $K_b = d_p^2 K_{px}$ has a strong influence on stability. For small values K_b the critical speed is below vehicle operating speed and the wheelset is relatively unconstrained. As K_b is increased the wheelsets are stabilized through yaw coupling to the truck. At sufficiently high values of K_b, the critical speed decreases as K_b is increased. In this range a rigid track mode is approached and the truck secondary suspension is used to stabilize the vehicle. In design it is desirable to select K_b so that a high critical speed is achieved but a rigid truck configuration is not approached.

The data for both parametric studies show that as wheel conicity λ is increased the critical speed decreases.

The influence of secondary suspension yaw stiffness on critical speed is shown in Figure 4.5.10. The critical speed is relatively insensitive to values of yaw stiffness less than 5×10^6 ft-lb/rad. In this range the truck is stabilized substantially through the primary suspension. Above this value the critical speed increases with increasing yaw stiffness. In practice, it is difficult to achieve effective values of yaw stiffness greater than 5×10^6 ft-lb/rad since values greater than this amount lead to torques which exceed the yaw

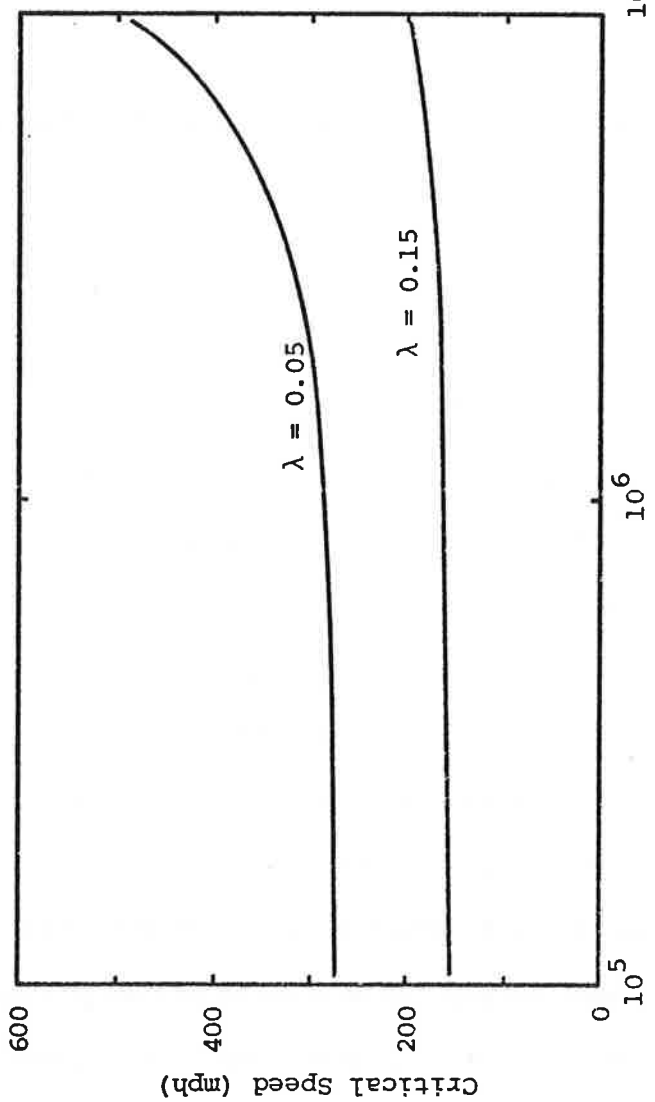

FIGURE 4.5.10: INFLUENCE OF THE SECONDARY YAW STIFFNESS ON THE CRITICAL SPEED OF THE PROTOTYPE VEHICLE

torque breakaway value. In a study of the effective value of yaw stiffness which can be achieved [40] for a typical rail passenger vehicle operating on class 6 track at 110 mph, an effective value of $1x10^6$ ft-lb/rad was determined. For the purpose of preliminary design, a value of $1x10^6$ ft lb/rad is adopted as a value which can be effectively achieved. Also for a value in this range, stability is not highly sensitive to changes in the effective secondary yaw stiffness.

4.5.4 Stability - Curving Trade-Off

This stability and curve negotiation performance of a rail vehicle has been shown to be a strong function of primary suspension lateral and longitudinal stiffnesses and wheel conicity. With recommended values of secondary yaw suspension stiffness and breakaway torque, performance is relative insensitive to these parameters. The stability-curving tradeoff may be summarized in plots of constant critical speed and degree curve negotiation with primary suspension stiffnesses as parameters. Trade-off plots for wheel conicities of λ = 0.05 and 0.15 are shown in Figures 4.5.11 and 4.5.12. With this type of plot, a set of values for primary suspension stiffness design parameters can be selected to achieve a desired critical speed with a maximum curve negotiation capability. Using plots of this type design parametric values for several critical speeds have been selected to maximize the degree curve possible. Data for five wheel conicities are summarized in Table 4.5.1. These data show for a given conicity that as critical

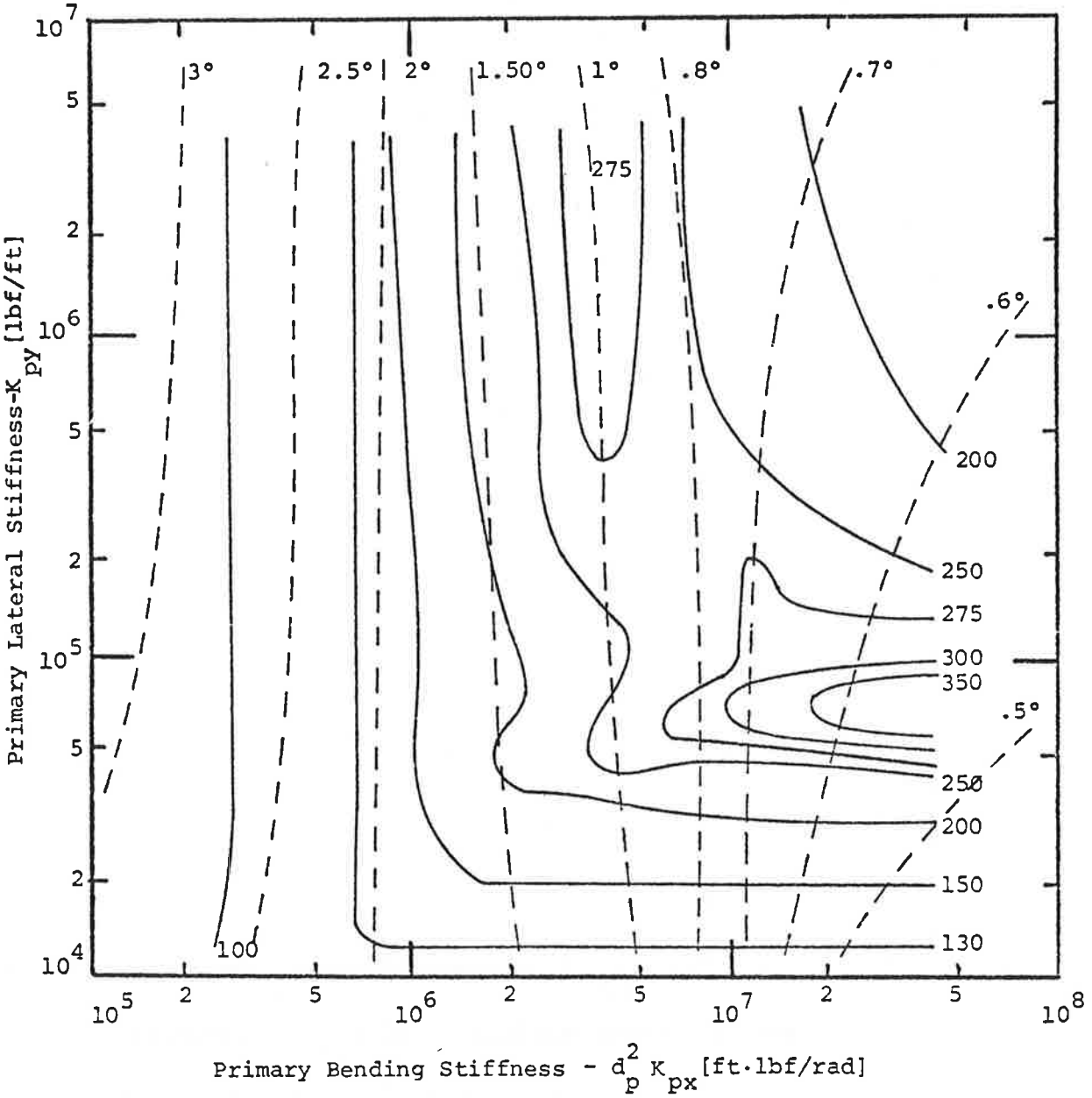

——— Lines of Constant Critical Speed [mph]
- - - -Lines of Constant Curving [Degrees]

FIGURE 4.5.11 : LINES OF CONSTANT CRITICAL SPEED AND CURVING FOR A CONVENTIONAL TRUCK WITH CONICAL WHEELS OF CONICITY $\lambda = 0.05$

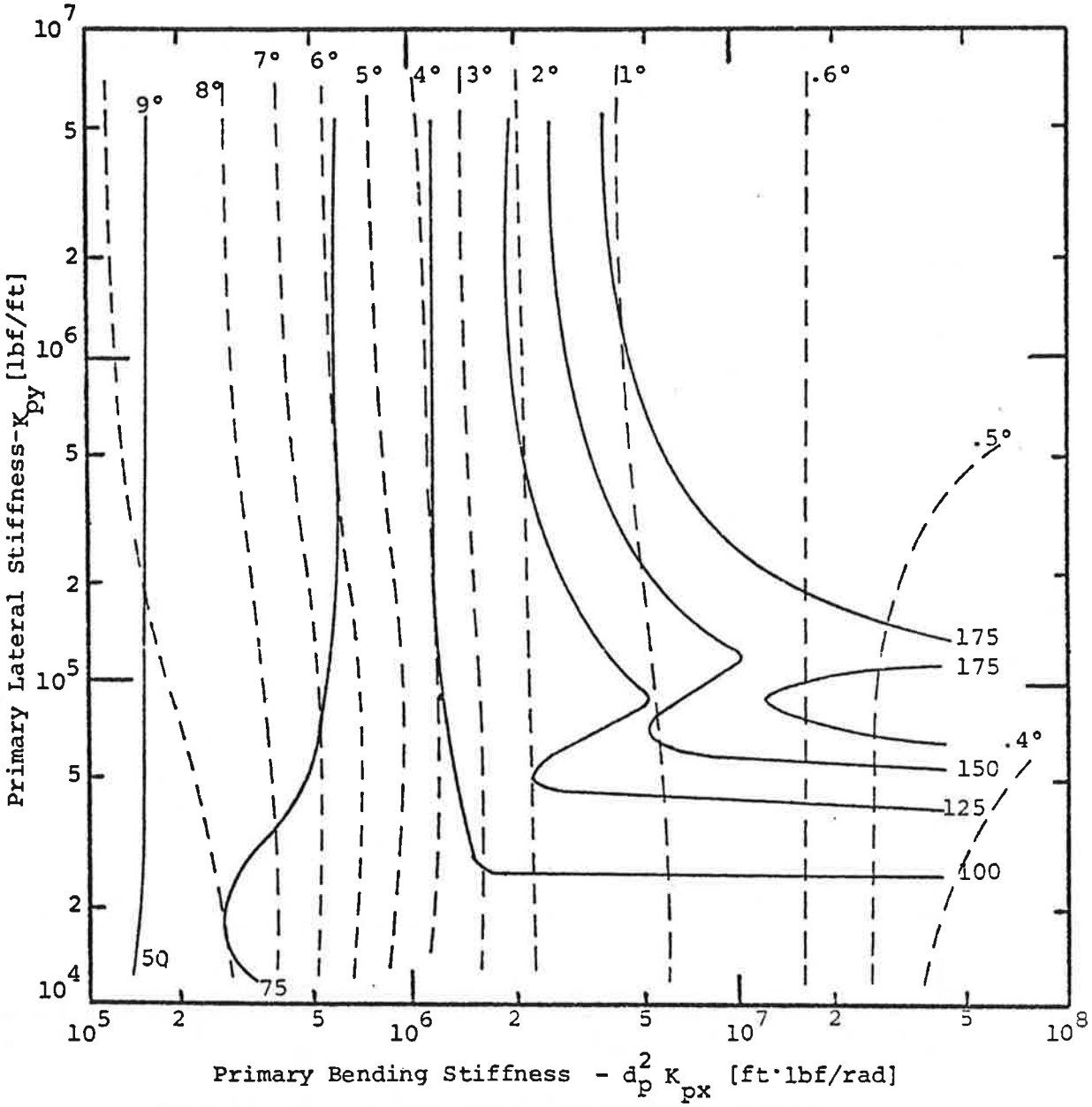

——— Lines of Constant Critical Speed [mph]

- - - -Lines of Constant Curving [Degrees]

FIGURE 4.5.12 : LINES OF CONSTANT CRITICAL SPEED AND CURVING FOR A CONVENTIONAL TRUCK WITH PROFILED WHEELS OF CONICITY $\lambda = 0.15$

TABLE 4.5.1: OPTIMUM STIFFNESS DESIGNS FOR CONVENTIONAL TRUCK

λ	V_{crit} (m.p.h.)	Curvature (Deg.)	$K_b = d^2 K_{px}$ (ft-lbf/rad)	K_{py} (lbf/ft)
0.025 (conical)	150	1.3	3.5×10^5	5×10^5
	200	1.0	7×10^5	5×10^5
	300	0.7	1.3×10^6	5×10^5
0.05 (conical)	100	2.7	3×10^5	5×10^5
	150	1.9	1×10^6	5×10^5
	200	1.6	1.5×10^6	5×10^5
	250	1.3	2.5×10^6	5×10^5
0.10 (profile)	100	4.5	9×10^5	5×10^5
	150	2.3	1.8×10^6	1×10^6
	200	1.3	3.4×10^6	1.5×10^6
	250	0.95	5×10^6	5×10^6
0.15 (profile)	100	4	1.2×10^6	2.5×10^5
	150	1.7	2.8×10^6	1.5×10^6
	175	1	4×10^6	1.5×10^6
0.25 (profile)	75	6	7×10^5	4×10^4
	100	2	2.5×10^6	5×10^5
	150	0.9	7×10^6	1×10^6
	175	0.7	1.2×10^7	2.2×10^6

speed is increased, an increased bending stiffness is required and the curve negotiation capability decreased. They also show as conicity is increased bending stiffness must be increased to maintain a constant critical speed. These data indicate that for a given critical speed, optimum values of wheel conicity and suspension parameters exist to maximize curving performance. Data are summarized in Figure 4.5.13 which show the maximum degree curve that can be negotiated without flanging and slipping for a given critical speed with conicity as a parameter. These data show that for critical speeds greater than 175 mph, a conicity of 0.05 yields the maximum curving capability, for critical speeds between 100 and 175 mph a conicity of 0.1 yields the maximum curving capability and for less than 100 mph, conicities of 0.15 and 0.25 yield maximum curving capability. As critical speed is lowered a larger conicity may be used to improve curving performance by using an appropriate value bending stiffness. Once an optimum point is selected from Figure 4.5.13 and the conicity specified, plots similar to 4.5.11 and 4.5.12 may be used to determine the values of primary suspension stiffness parameters. These types of plots are provided with the design procedure. In each case the full Kalker values for creep coefficients are assumed. This is usually conservative for stability calculations. In steady state curving, reduction of the creep coefficients tends to improve the slip performance but degrade the flange contact performance. A final design based on full Kalker values should be checked using 50% of Kalker values.

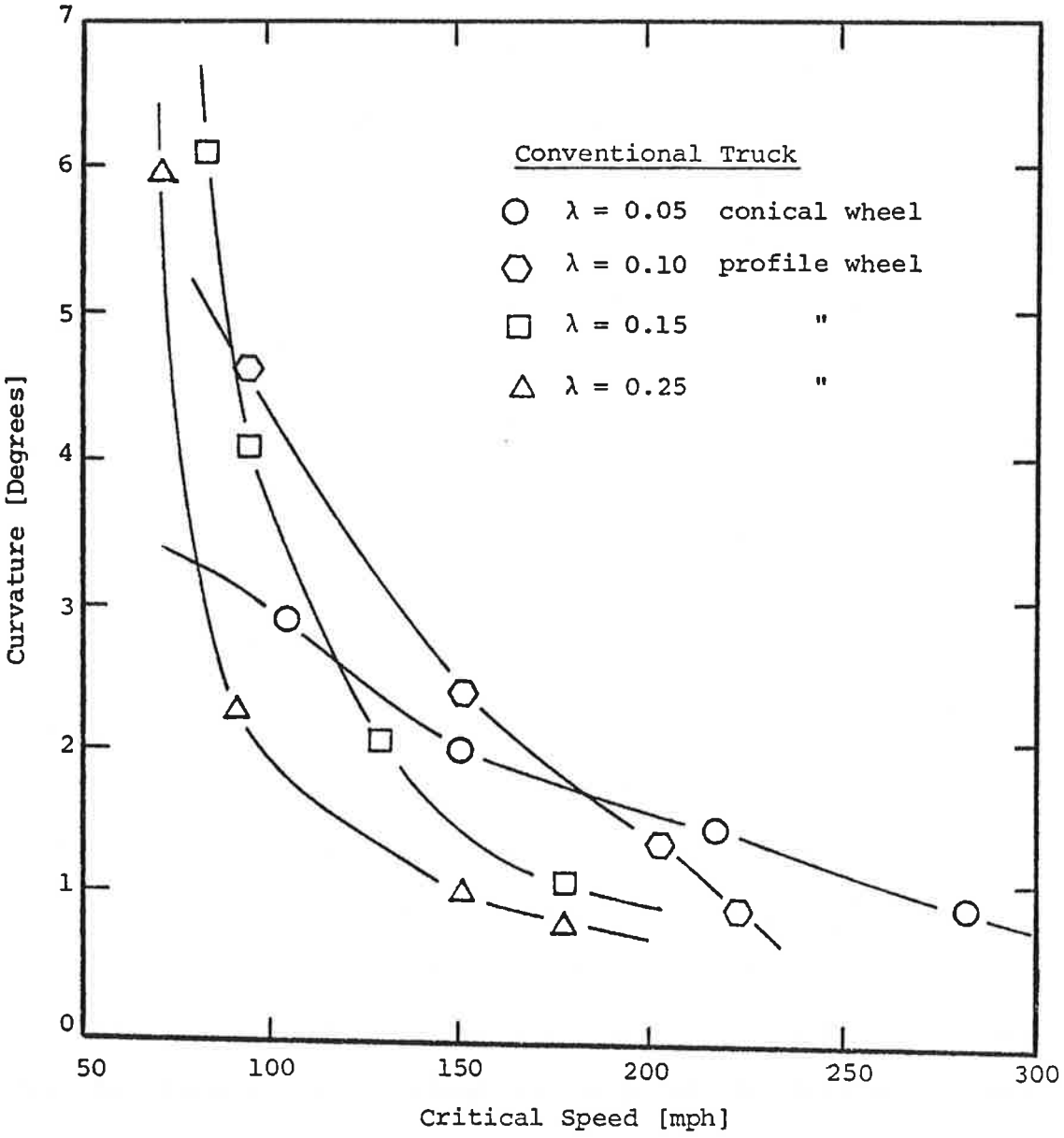

FIGURE 4.5.13 : OPTIMUM STABILITY/CURVING TRADE-OFF ENVELOPES FOR CONVENTIONAL TRUCK

4.6 Description of Design Procedure

A step-by-step procedure has been developed to establish the values of the critical design parameters. The procedure is summarized as the steps in Table 4.6.1. The detailed steps are described in the following paragraphs. The data used to illustrate the procedure are based upon operation on class 6 welded track at a nominal operating speed of 110 mph.

Steps 1, 2, 3

Enter data in Table 4.6.1 as requested to initiate the design procedure.

Step 4

In this step, the stability curving-trade-off is considered. The procedure may be summarized as follows. Given the desired critical speed or the desired curving performance a combination of primary stiffness, K_{py}, K_b, and wheel profile is determined by locating a point on one of Figures 4.6.1 through 4.6.4, at which the specified performance index is satisfied and the unspecified index is optimized. If both the desired critical speed and degree curve are specified, and it is possible to satisfy both indices, in general the designs will have one or both indices better than desired. If an optimum solution is sought, first, the wheel conicity may be selected from Figure 4.5.13 and then the appropriate Figure of 4.6.1-4.6.4 may be used to determine the suspension parameters. If the wheel profile is specified, then the design is based on the trade-off which corresponds to the profile.

Figures 4.6.1 to 4.6.4 were generated for wheelset and truck frame parameters as specified in Table 4.1.1. The maximum expected variation in wheelset and truck frame mass from the prototype values are $\pm$ 40%. This range includes both the lightest unpowered trucks and the heaviest powered truck. A relatively accurate correction for this deviation is based on the observation that most of the analytical formulas for estimating critical speed of wheelsets or rigid trucks are of the form:

$$V_{cr} = C\sqrt{\frac{1}{M}}, \qquad (4.6\text{-}1)$$

where C = a constant

M = wheelset (or rigid truck) mass.

Since typical trucks approach rigid truck behavior near the point of instability, the following correction formula is proposed for relatively stiff trucks ($K_{py} > 150000$ lb/ft, $K_b > 1000000$ ft-lb/rad)

$$V_{cr,corrected} = V_{cr}\sqrt{\frac{(2M_w + M_t)_{baseline}}{(2M_w + M_t)_{used}}}, \qquad (4.6\text{-}2)$$

where V_{cr} is read from Figures 4.6.1 thru 4.6.4

$V_{cr,corrected}$ is the value to be used for design purposes.

The value of the secondary yaw stiffness used to generate Figures 4.6.1 to 4.6.4 is $K_{s\psi} = 1.0 \times 10^6$ ft-lb/rad. The critical speed is relatively independent of $K_{s\psi}$ for this low value.

If a higher stiffness is used, the new critical speed can be estimated using Equation (4.6-3).

$$V_{cr,corrected} = V_{cr}\left[\frac{V_{baseline}(K_{s\psi})}{V_{baseline}(1.0x10^6)}\right], \quad (4.6\text{-}3)$$

where

V_{cr} is read off Figures 4.6.1 through 4.6.4

V_{cr} corrected is the value used for design purposes

$V_{baseline}(K_{s\psi})$ is the critical speed of the baseline vehicle, with primary stiffnesses approximately corresponding to the design values, and with $K_{s\psi}$ corresponding to the design value. This value is taken from Figure 4.6.5.

$V_{baseline}(1.0x10^6)$ is same as above, except for $K_{s\psi} = 1.0 \times 10^6$ ft-lb/rad.

Step 5

Follow the instructions in Table 4.6.1.

Step 6

Estimation of Primary Suspension Stroke Lengths

For typical vehicle parameters the primary stroke lengths* may be expressed as:

$$PS = PS(\lambda, K_{py}, V) \quad . \quad (4.6\text{-}4)$$

Equation (4.6-4) can be approximated as:

$$PS = PS(\text{Baseline}, \lambda) + \Delta PS(\text{Baseline}, K_{py}) + \Delta PS(\text{Baseline}, \lambda, V), \quad (4.6\text{-}5)$$

*PS means the RMS value of the stroke length.

where:

PS(Baseline, λ) is the PS of the baseline vehicle for a given λ, as determined from Figure 4.6.6.

ΔPS (Baseline, K_{py}) is the increase in PS of the baseline vehicle due to change in K_{py}, as determined from Figure 4.6.7.

ΔPS(Baseline,λ, V) is the increase in PS of the baseline vehicle with the chosen λ due to change in speed, as determined from Figure 4.6.8.

Equation (4.6-5) may be used to estimate the primary suspension stroke lengths of a vehicle for class-6 track.

Step 7

The wheelset excursions* may be expressed as:

$$WE = WE(\lambda, K_b, V) . \qquad (4.6\text{-}6)$$

Equation (4.6-6) may be approximated as:

$$WE = WE(Baseline,\lambda) + \Delta WE(Baseline, K_b)+\Delta WE(Baseline,\lambda, V) \qquad (4.6\text{-}7)$$

where:

WE(Baseline,λ) is the WE of the baseline vehicle for a given λ, as determined from Figure 4.6.9

ΔWE(Baseline, K_b) is the increase in WE of the baseline vehicle due to change in K_b, as determined from Figure 4.6.10

ΔWE(Baseline, λ,V) is the increase in WE of the baseline vehicle with the chosen λ due to change in speed, as determined from Figure 4.6.11.

---

*WE means the RMS value of the wheelset excursion.

Equation 4.6.7 may be used to estimate the wheelset excursions of a vehicle with any set of parameters, for class 6 track.

Steps 8, 9, 10

Follow the instructions in Table 4.6.1.

Step 11

The secondary lateral suspension is designed to achieve acceptable ride quality, subject to suspension stroke lengths constraints. This trade-off design step is simplified significantly if the carbody uncoupled natural frequency, f_n, and the carbody uncoupled damping ratio, ξ, the definition of which follow, are used as parameters.

$$f_{n_L} = \frac{1}{2\pi}\sqrt{\frac{4K_{sy}}{M_c}} \quad \text{(Hz)} \qquad (4.6\text{-}8)$$

$$\xi_L = \frac{C_{sy}}{\sqrt{K_{sy} M_c}} \; . \qquad (4.6\text{-}9)$$

Values of these parameters should be selected from Figures 4.6.12, 4.6.13 to achieve desired levels of ride quality and suspension stroke. In these Figures ride quality is represented as the rms acceleration averaged at three points in the vehicle-center of gravity and the front and rear passenger points identified in Table 4.1.1.

Table 4.2.1 indicates that the lateral ride quality and the secondary stroke lengths are also dependent on the wheel/rail parameters, K_{py} and K_b, but not significantly. Although the influence of these para-

meters is not large enough to affect the choice of f_n and ξ, they must be considered when the ride quality and the secondary strokes are evaluated.

The optimal vehicle is one which has good ride quality and small stroke lengths. Examination of Figure 4.6.12 reveals that if ξ is decreased below 0.2 both indices increase and, therefore, ξ should be larger than 0.2. When ξ is increased above 0.3, the strokes decrease, but the ride quality index increases steeply. A range of $0.2 < \xi < 0.3$ is recommended for the damping ratio. The ride quality improves as f_n decreases, however, there is a lower limit on this parameter obtained from static considerations, as deflection due to wind forces, superelevation, loading, etc. For f_n = 0.7 Hz the total lateral stiffness $4K_{sy}$ is about 60,000 lb/ft, for the baseline vehicle. If the natural frequency is 0.35 Hz, the corresponding total stiffness is 15,000 lb/ft which is considered impractical for a vehicle of this size, thus a natural frequency in the 0.7 to 1.0 Hz range is usually selected by a designer.

Steps 12, 13

Once the natural frequency and the damping ratio are known, the values of stiffness K_{sy} and damping C_{sy} may then be obtained from Equations (4.6-8) and (4.6-9), respectively.

Step 14

The RMS values of the accelerations and of the stroke length can be read from Figures 4.6.12, 4.6.13, if all the parameters except

M_c, K_{sy}, C_{sy} are baseline parameters and if the speed is 110 mph or 60 mph. If the vehicle has different parameters, following Table 4.2.1 the acceleration* may be expressed as

$$ACC = ACC(f_n, \xi, \lambda, K_b, V) , \qquad (4.6\text{-}10)$$

which may be approximated as

$$ACC = ACC(\text{Baseline}, f_n, \xi, V) + \Delta ACC(\text{Baseline}, \lambda) + \Delta ACC(\text{Baseline}, K_b) , \qquad (4.6\text{-}11)$$

where:

ACC(Baseline, f_n, ξ, V) is obtained by linear interpolation between Figure 4.6.12 (110 mph) and Figure 4.6.13 (60 mph) for the chosen values of f_n and ξ. (See the formula in Table 4.6.1.) ΔACC(Baseline, λ) is the increase in ACC of the baseline vehicle due to change in λ, as determined from Figure 4.6.14. ΔACC(Baseline, K_b) is the increase in ACC of the baseline vehicle due to change in K_b, as determined from Figure 4.6.15.

Step 15

The stroke length** may be expressed as

$$ST = ST(f_n, \xi, \lambda \quad K_b, V), \qquad (4.6\text{-}12)$$

which may be approximated by

$$ST = ST(\text{Baseline}, f_n, \xi, V) + \Delta ST(\text{Baseline}, \lambda) + \Delta ST(\text{Baseline}, K_b) \qquad (4.6\text{-}13)$$

*ACC means the RMS value of the lateral acceleration

**ST means the RMS value of the secondary stroke lengths.

where:

ST(Baseline, f_n, ξ, V) is obtained by linear interpolation between Figure 4.6.12 (110 mph) and Figure 4.6.13 (60 mph) for the chosen values of f_n and ξ. ΔST(Baseline, λ) is the increase in ST of the baseline vehicle due to change in λ, as determined from Figure 4.6.15.

ΔST(Baseline, K_b) is the increase in ST of the baseline vehicle due to change in K_b, as determined from Figure 4.6.17.

Step 16, 17, 18

Follow the instructions in Table 4.6.1.

Step 19

As in the lateral case, (Step 11) the vertical suspension design procedure is simplified with the introduction of f_n and ξ, as follows:

$$f_{n_v} = \frac{1}{2\pi}\sqrt{\frac{4K_{sz}}{M_c}} \quad \text{(Hz)} \qquad (4.6\text{-}14)$$

$$\xi_v = \frac{C_{sz}}{\sqrt{K_{sz}\, M_c}} \,. \qquad (4.6\text{-}15)$$

Plots of the average RMS acceleration at the three passenger locations and average RMS vertical secondary stroke are given in Figures 4.6.18 4.6.19 , for 110 mph and 60 mph, respectively. Inspection of these plots reveals that an optimal combination of f_n and ξ exists, which

achieves relatively low values of both RMS acceleration and RMS stroke lengths, and is still stiff enough to avoid large static deflections. This range is:

$$0.15 \leq \xi_v \leq 0.4$$

$$0.7 \leq f_{n_v} \leq 1.2 \text{ Hz} .$$

Note that all the points of minimum acceleration for given stroke lengths (and vice versa) lie on one "optimal" curve, as is the lateral case. It is possible to achieve performance corresponding to points better than the "optimum" curves if the secondary suspension is comprised of air springs with pneumatic orifice dampers [39]. This suspension can easily be included in the models to generate design data, but this is beyond the scope of this report.

Steps 20, 21

Once the natural frequency and the damping ratio are known, the values of vertical stiffness and damping may be computed using Equations (4.6-14) and (4.6-15), respectively.

Steps 22, 23

The RMS values of the vertical acceleration and the secondary vertical stroke lengths are estimated by linear interpolation between Figure 4.6.18 (110 mph) and Figure 4.6.19 (60 mph), for the chosen values of f_n and ξ . (See the formula in Table 4.6.1).

TABLE 4.6.1: DESIGN PROCEDURE

1. Enter the Value of Desired V_{cr} (mph) If Not Specified Go to 2. V_{cr}=

2. Enter the Value of Desired D(degrees) If Not Specified Go to 3 D =

3. If the Wheel Profile is Specified, Enter the Following Wheel/Rail Parameters' Values

λ = Δ =

δ = a_{11}=

F_{11}= F_{12}= F_{22}= F_{33}=

4. Use Figures 4.6.1 throught 4.6.4 and Equations 4.6-2,4.6-3 to find K_{py} and K_b which satisfy or exceed V_{cr} and/or D, and enter the values. If only one index is specified, maximize the unspecified one. Complete the entries in lines 1 and 2. If the parameters in line 3 are not specified use the profile as a design parameter, i.e. choose values for the parameters in line 3. (Use Table 4.1.1)

K_{py}=

K_b=

5. Compute $K_{px} = K_b/d_p^2$ Enter the Value

K_{px}=

---

6. Estimate the primary suspension stroke lengths (use wheelset #4)*

a. Determine the value of PS(Baseline,λ) from Figure 4.6.6

b. Determine the value of ΔPS(Baseline,K_{py}) from Figure 4.6.7 +

c. Determine the value of ΔPS(Baseline,λ,V) From Figure 4.6.8 +

d. Add entries a, b and c

PS=

---

*The wheelsets are numbered in order, from the leading to the trailing end of the vehicle.

TABLE 4.6.1: (Cont'd)

7. Estimate the wheelset excursions (use wheelset #1)

   a. Determine the value of WE(Baseline,λ) from Figure 4.6.9 | |

   b. Determine the value of ΔWE(Baseline, K_b) from Figure 4.6.10 | |

   c. Determine the value of ΔWE(Baseline,λ,V) from Figure 4.6.11 | |

   d. Add entries a,b, and c | WE = |

---

8. If entries 6d and 7d within reasonable limits, go to 9.
   If not repeat steps 4 thru 8.

9. Enter the value of desired rms lateral acceleration | ACC_L^* =

10. Enter the value of desired rms secondary lateral strokes.
    If not specified go to 11. | ST_L^* =

11. Choose f_{n_L} and ξ_L to satisfy entries 9 and 10. Interpolate between Figure 4.6.12 (110 mph) and Figure 4.6.13 (60 mph) to get approximate values for speed V. | f_{n_L} =
    | ξ_L =

12. Compute the secondary lateral stiffness
    $K_{sy} = \pi^2 f_n^2 M_c$ | K_{sy} =

13. Compute the secondary lateral damping
    $C_{sy} = \xi \sqrt{K_{sy} \cdot M_c}$ | C_{sy} =

---

14. Estimate the rms lateral acceleration

    a. Compute

    $$ACC(Baseline, f_n, \xi, V) = ACC(110) + \left(\frac{V-110}{50}\right) [ACC(110) - ACC(60)]$$

TABLE 4.6.1: (Cont'd)

where ACC(110) is taken from Fig. 4.6.12

and ACC(60) is taken from Fig. 4.6.13

b. Determine the value of $\Delta ACC(Baseline,\lambda)$ from Figure 4.6.14 +

c. Determine the value of $\Delta ACC(Baseline,K_b)$ from Figure 4.6.15 +

d. Add Entries a,b and c ACC_L=

---

15. Estimate the rms secondary lateral strokes

a. Compute

$$ST(Baseline, f_n, \xi, V) = ST(110) + \left(\frac{V-110}{50}\right)[ST(110)-ST(60)]$$

where ST(110) is taken from Figure 4.6.12
and ST(60) is taken from Figure 4.6.13

b. Determine the value of $\Delta ST(Baseline,\lambda)$ from Figure 4.6.16 +

c. Determine the value of $\Delta ST(Baseline\ K_b)$ from Figure 4.6.17 +

d. Add entries a,b, and c ST_L=

---

16. Compare entry 14d to entry 9, and entry 15d to entry 10. If the actual indices exceed the desired values, repeat steps 11 through 15.

17. Enter the value of desired rms vertical acceleration. If not specified to to 18. ACC_v*=

TABLE 4.6.1: (Cont'd)

18. Enter the value of desired rms secondary vertical stroke. If not specified go to 19. ST_v*=

19. Choose f_{n_v} and ξ_v to satisfy entries 17 and 18. Interpolate between Figure 4.6.18 (110mph) and Figure 4.6.19 (60 mph) to get approximate values for speed V. f_{n_v}= ξ_v =

20. Compute the secondary vertical stiffness K_{sz}=

$$K_{sz} = \pi^2 f_n^2 M_c$$

21. Compute the secondary vertical damping C_{sz}=

$$C_{sz} = \xi_v \sqrt{K_{sz} \cdot M_c}$$

22. Estimate the rms vertical acceleration

$$ACC_V = ACC\ (110) + \left(\frac{V-110}{50}\right)[ACC\ (110) - ACC(60)]$$

where ACC (110) is taken from Figure 4.6.18

and ACC (60) is taken from Figure 4.6.19 ACC_V=

23. Estimate the rms vertical secondary strokes

$$ST_V = ST\ (110) + \left(\frac{V-110}{60}\right)[ST\ (110) - ST\ (60)]$$

where ST (110) is taken from Figure 4.6.18

and ST (60) is taken from Figure 4.6.19 ST_v=

TABLE 4.6.1: (Concl'd)

24. Compare entry 22 to entry 17, and entry 23 to entry 18. If the actual indices exceed the desired values, repeat steps 19-24.

25. Compute dependent design parameters as indicated in Table 4.1.1.

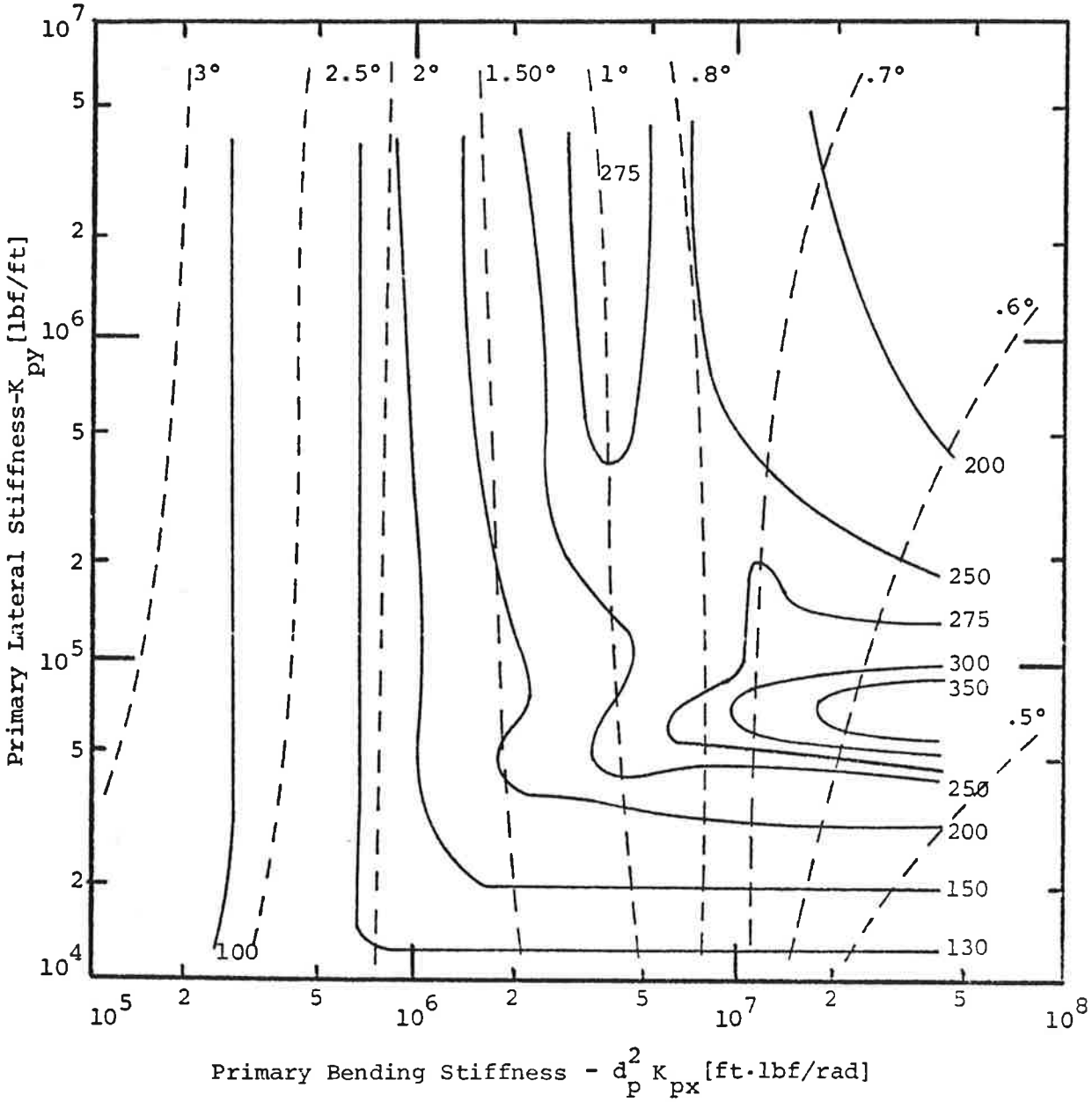

Primary Bending Stiffness - $d_p^2 K_{px}$ [ft·lbf/rad]

——— Lines of Constant Critical Speed [mph]

- - - -Lines of Constant Curving [Degrees]

FIGURE 4.6.1 : LINES OF CONSTANT CRITICAL SPEED AND CURVING FOR A CONVENTIONAL TRUCK WITH CONICAL WHEELS OF CONICITY $\lambda = 0.05$

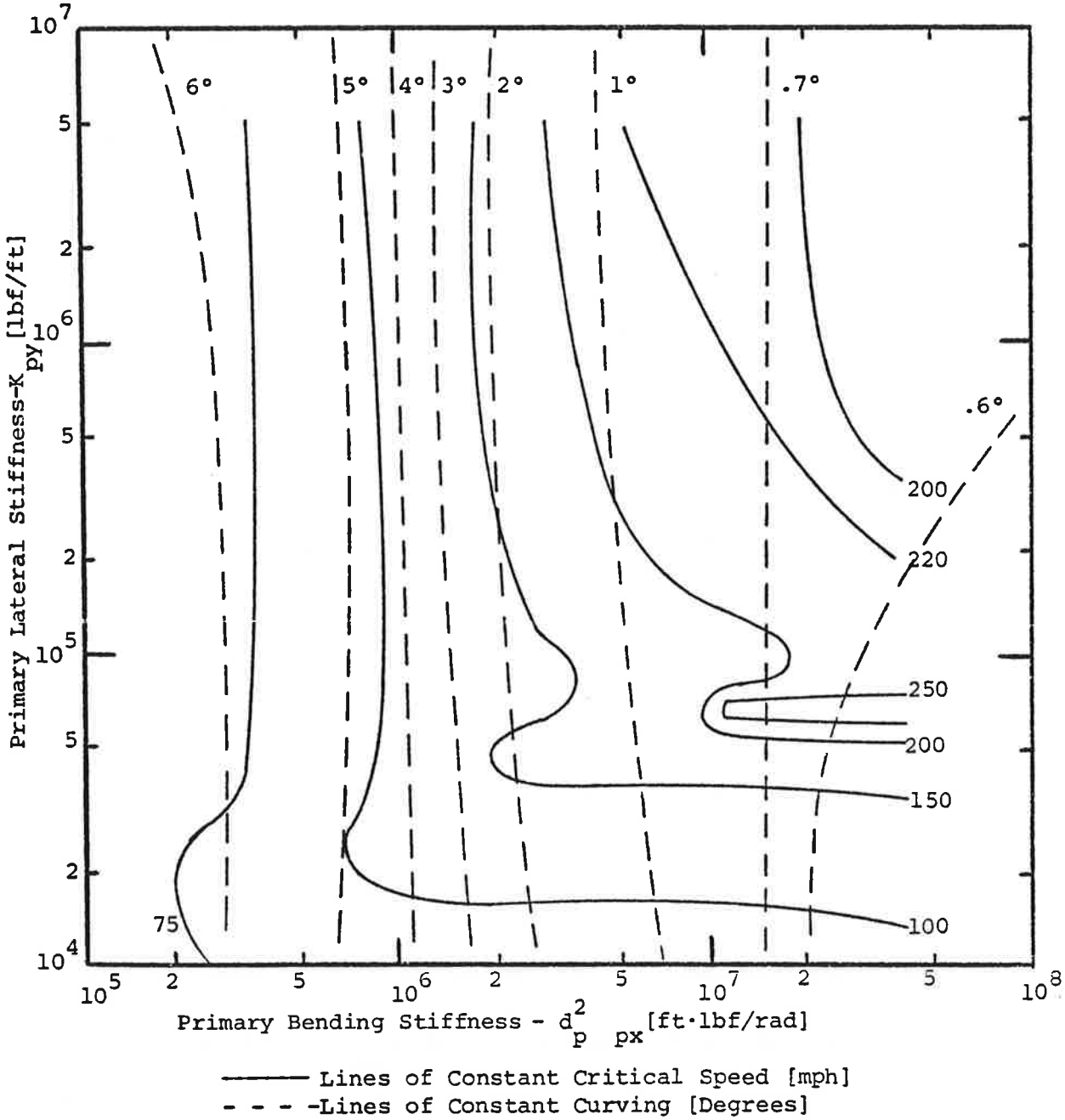

FIGURE 4.6.2 : LINES OF CONSTANT CRITICAL SPEED AND CURVING FOR A CONVENTIONAL TRUCK WITH PROFILED WHEELS OF CONICITY $\lambda = 0.10$

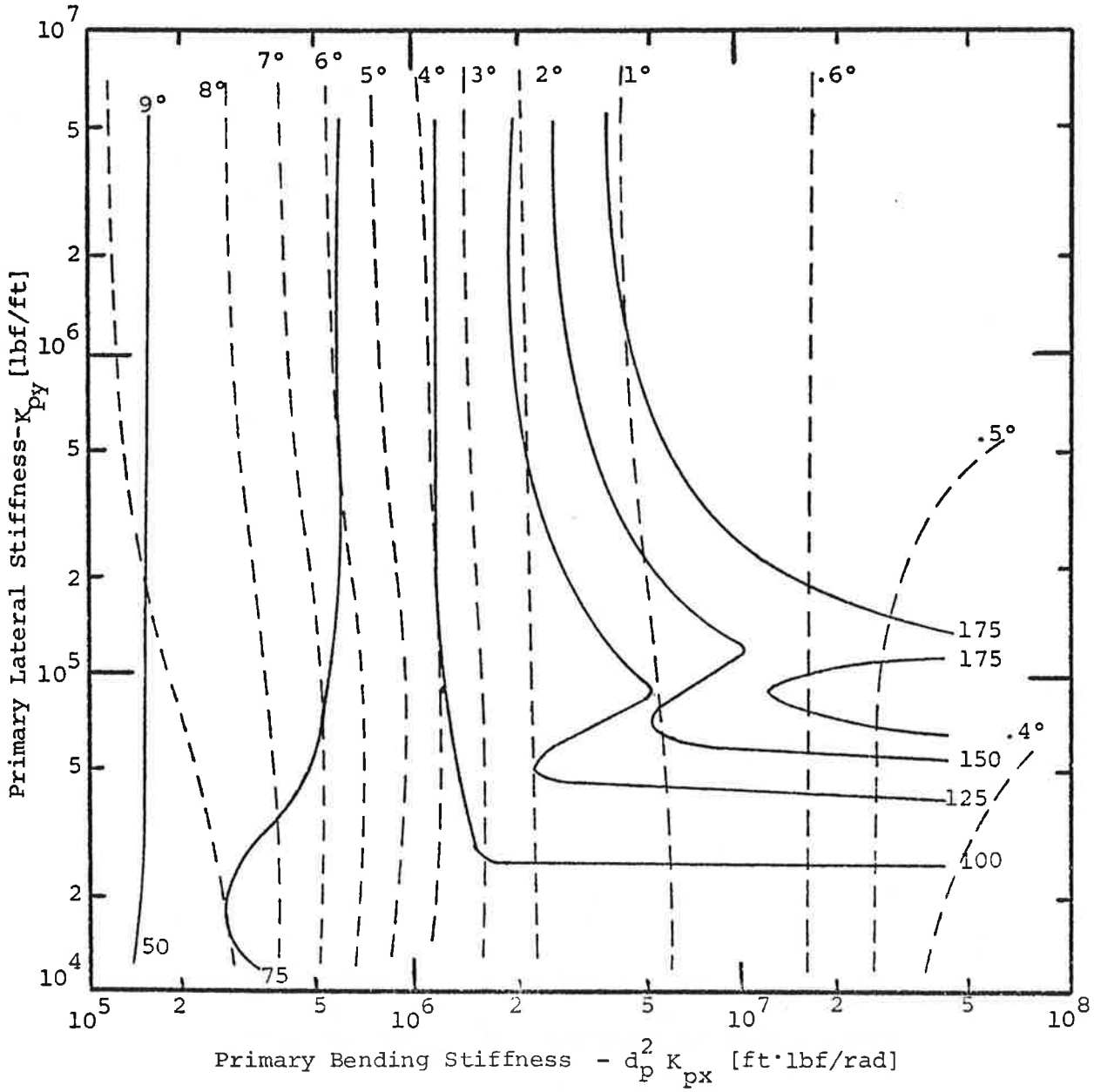

——— Lines of Constant Critical Speed [mph]

- - - -Lines of Constant Curving [Degrees]

FIGURE 4.6.3 : LINES OF CONSTANT CRITICAL SPEED AND CURVING FOR A CONVENTIONAL TRUCK WITH PROFILED WHEELS OF CONICITY $\lambda = 0.15$

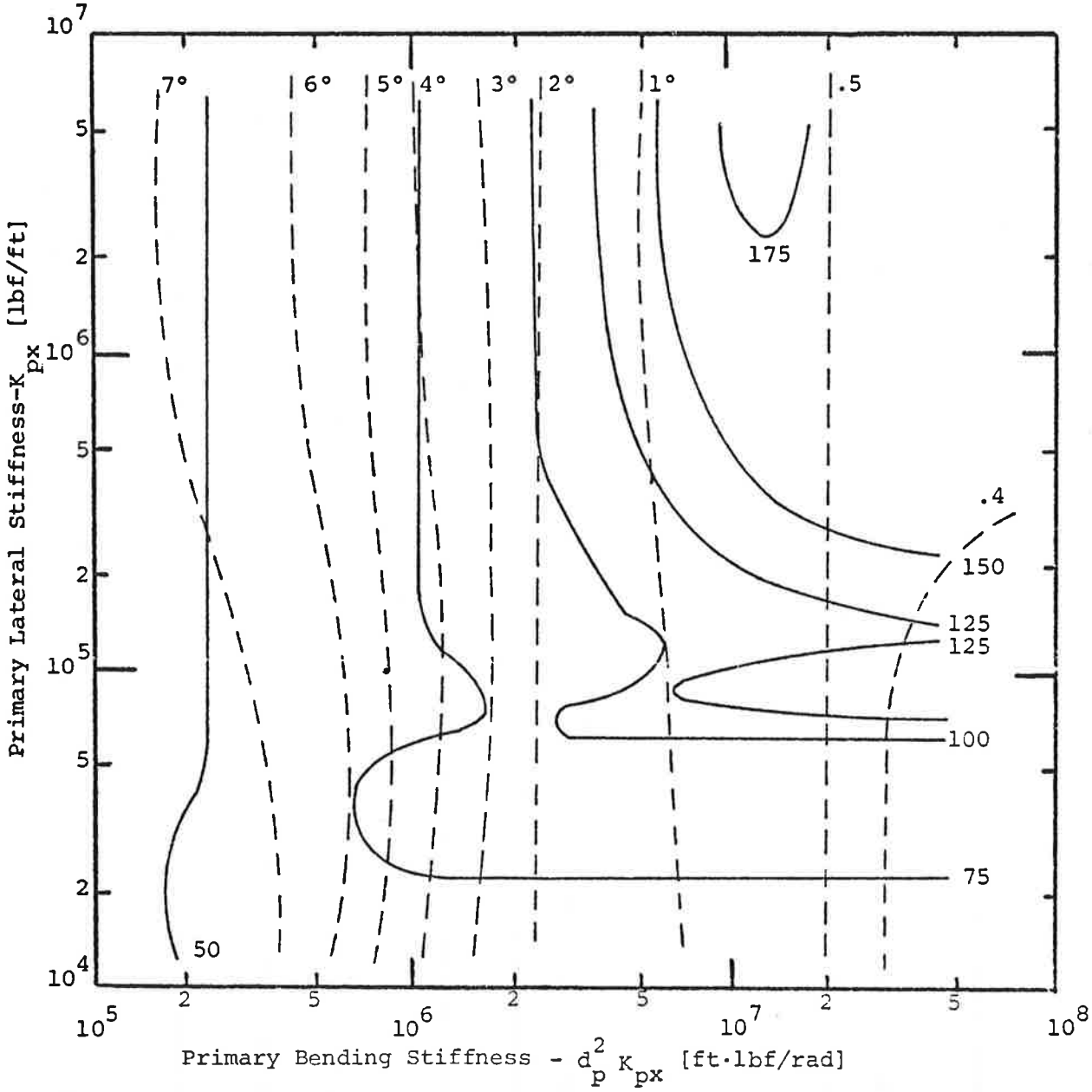

FIGURE 4.6.4 : LINES OF CONSTANT CRITICAL SPEED AND CURVING FOR A CONVENTIONAL TRUCK WITH PROFILED WHEELS OF CONICITY $\lambda = 0.25$

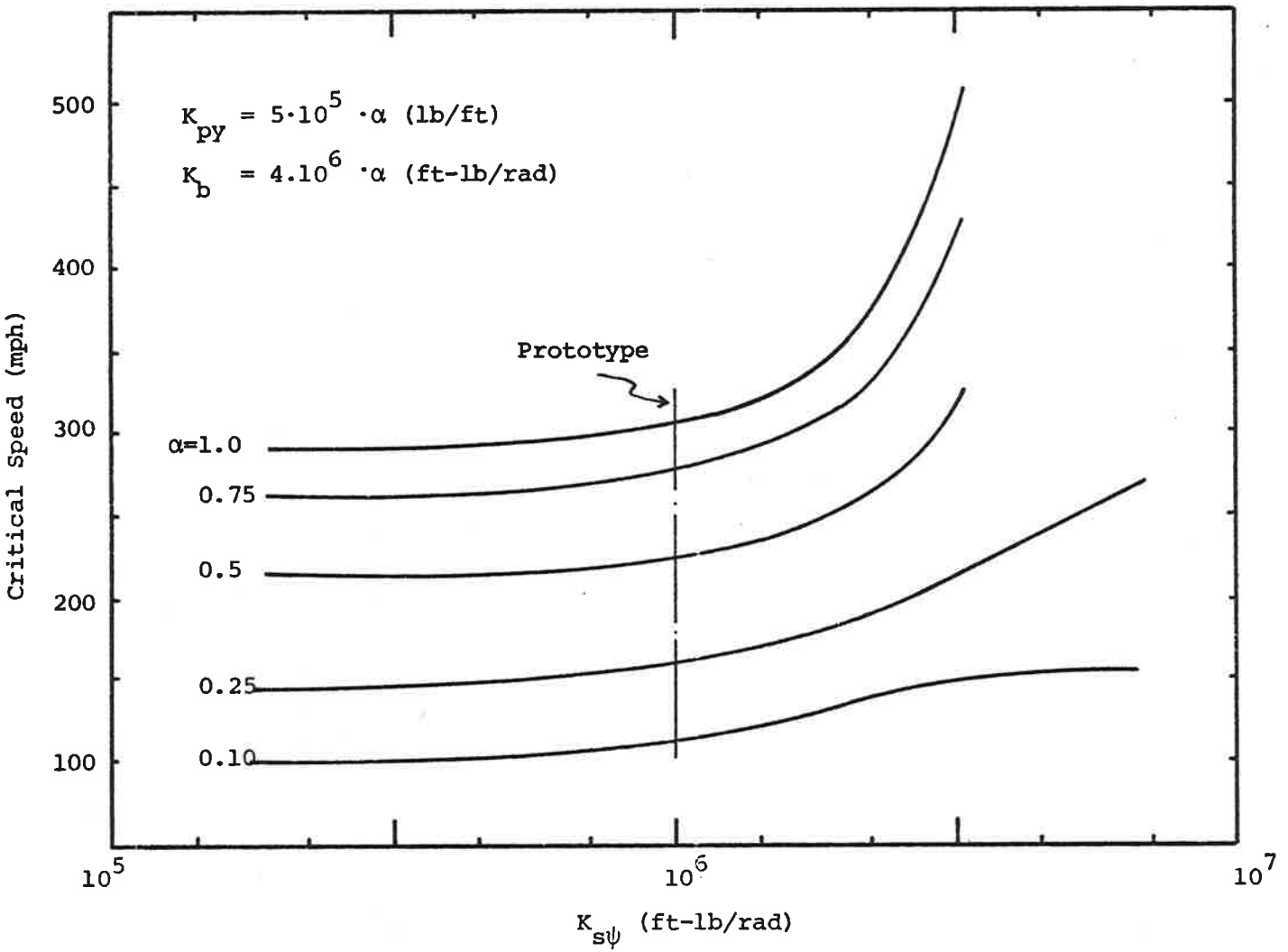

FIGURE 4.6.5: INFLUENCE OF THE SECONDARY YAW STIFFNESS ON THE CRITICAL SPEED OF THE PROTOTYPE VEHICLE

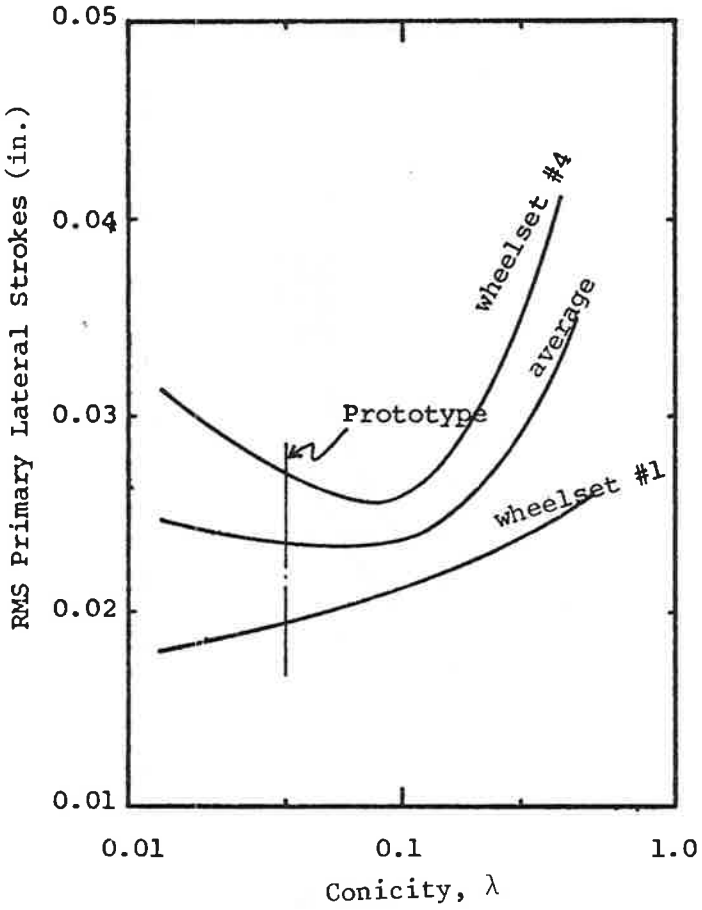

FIGURE 4.6.6: INFLUENCE OF THE CONICITY ON THE PRIMARY LATERAL SUSPENSION STROKES OF THE PROTOTYPE VEHICLE
(Wheelset #1 is the Leading Wheelset of the Leading Truck)

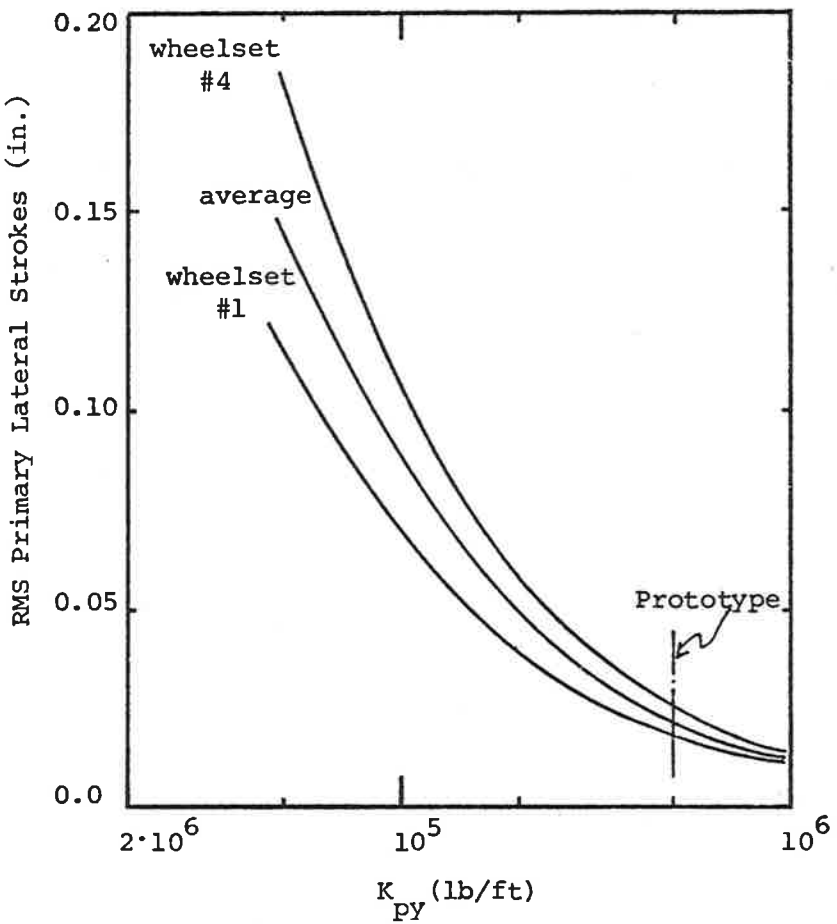

FIGURE 4.6.7: INFLUENCE OF THE PRIMARY LATERAL STIFFNESS ON THE PRIMARY LATERAL SUSPENSION STROKES OF THE PROTOTYPE VEHICLE

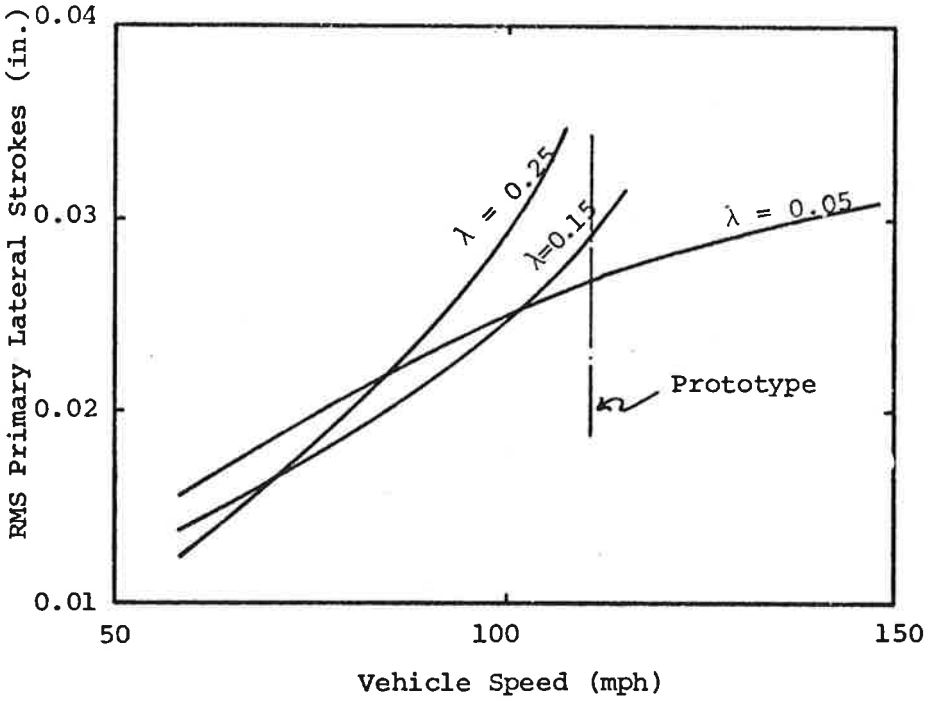

FIGURE 4.6.8: INFLUENCE OF VEHICLE SPEED ON PRIMARY SUSPENSION STROKES

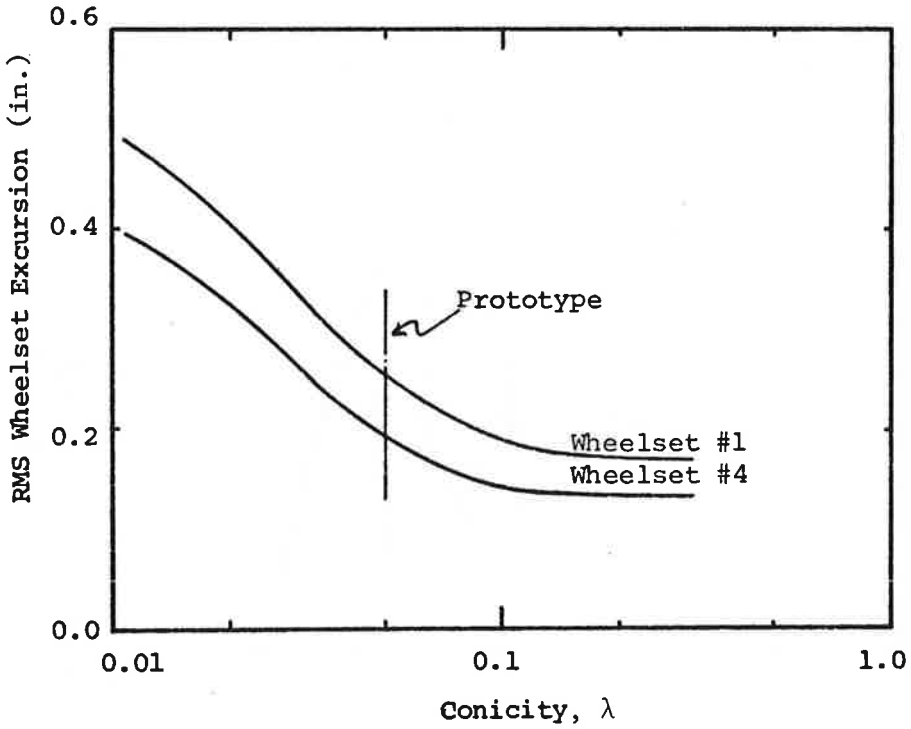

FIGURE 4.6.9: INFLUENCE OF CONICITY ON THE WHEELSET EXCURSIONS OF THE PROTOTYPE VEHICLE

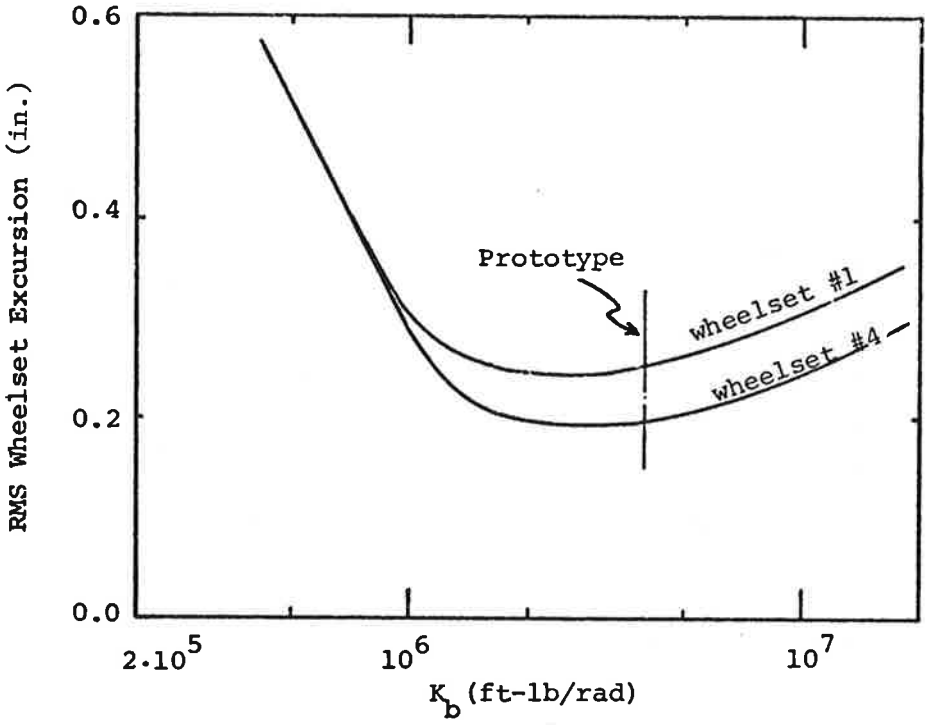

FIGURE 4.6.10: INFLUENCE OF PRIMARY BENDING STIFFNESS ON THE WHEELSET EXCURSIONS

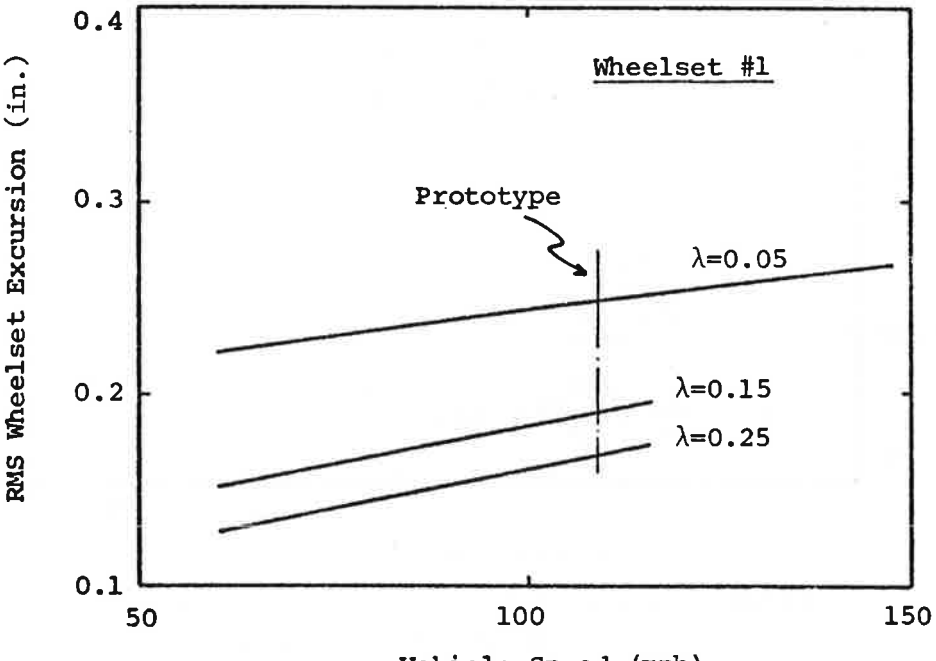

FIGURE 4.6.11: INFLUENCE OF VEHICLE SPEED ON WHEELSET EXCURSIONS

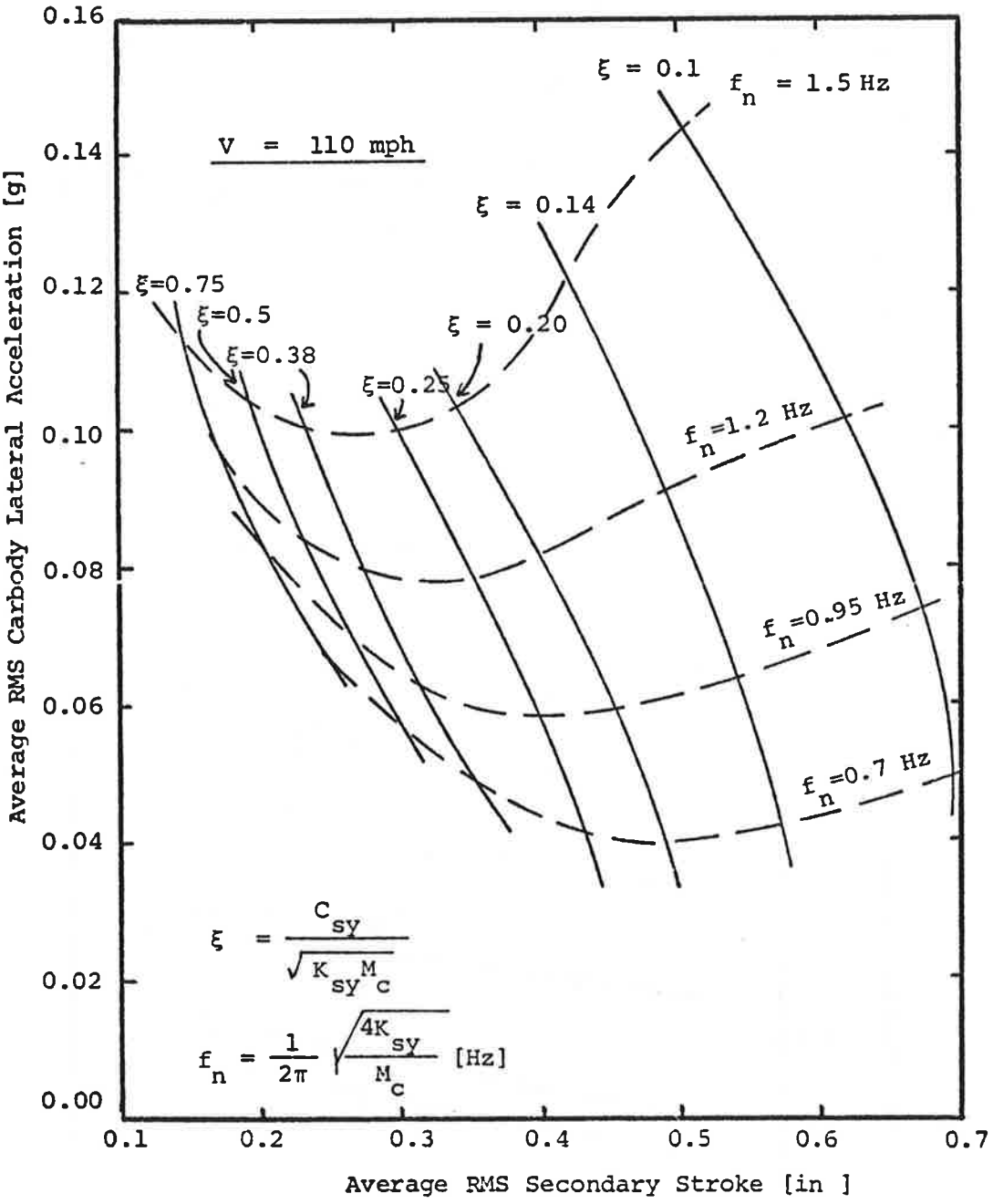

FIGURE 4.6.12: CARBODY LATERAL ACCELERATION-SECONDARY STROKE LENGTH TRADE-OFF PLOT, V=110 mph

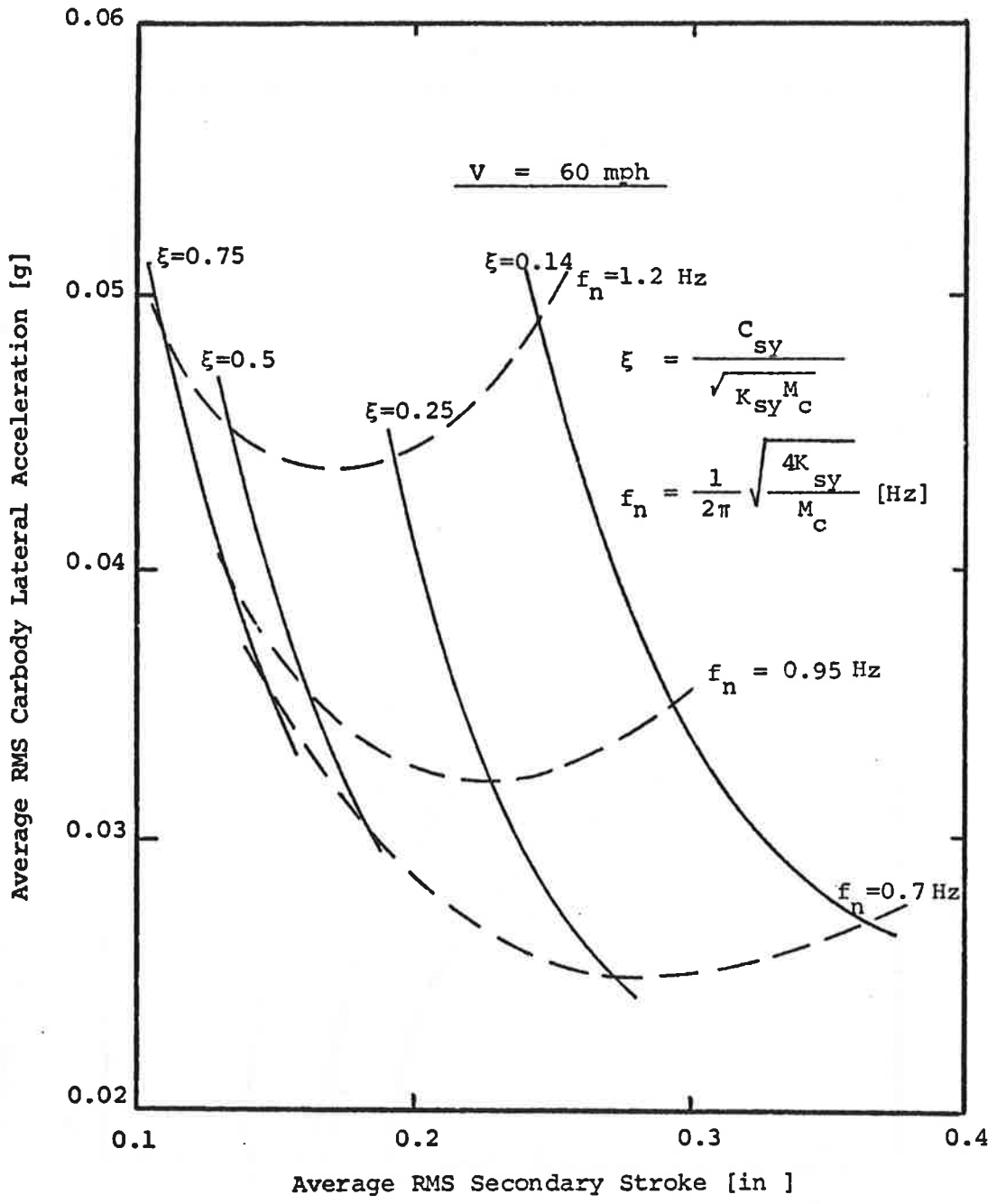

FIGURE 4.6.13 : CARBODY LATERAL ACCELERATION-SECONDARY STROKE LENGTH TRADE-OFF PLOT, V = 60 mph

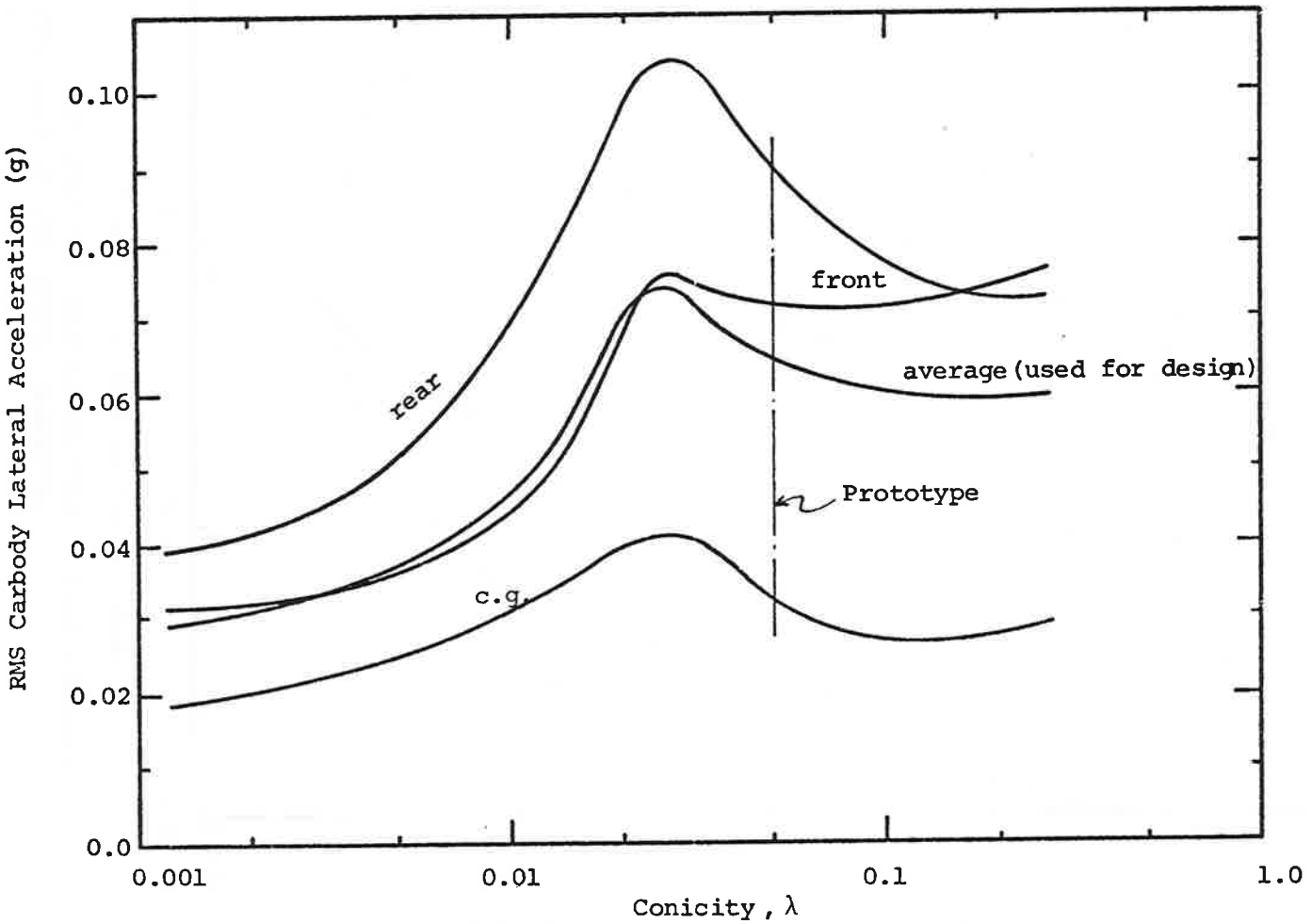

FIGURE 4.6.14: INFLUENCE OF CONICITY ON CARBODY LATERAL ACCELERATION

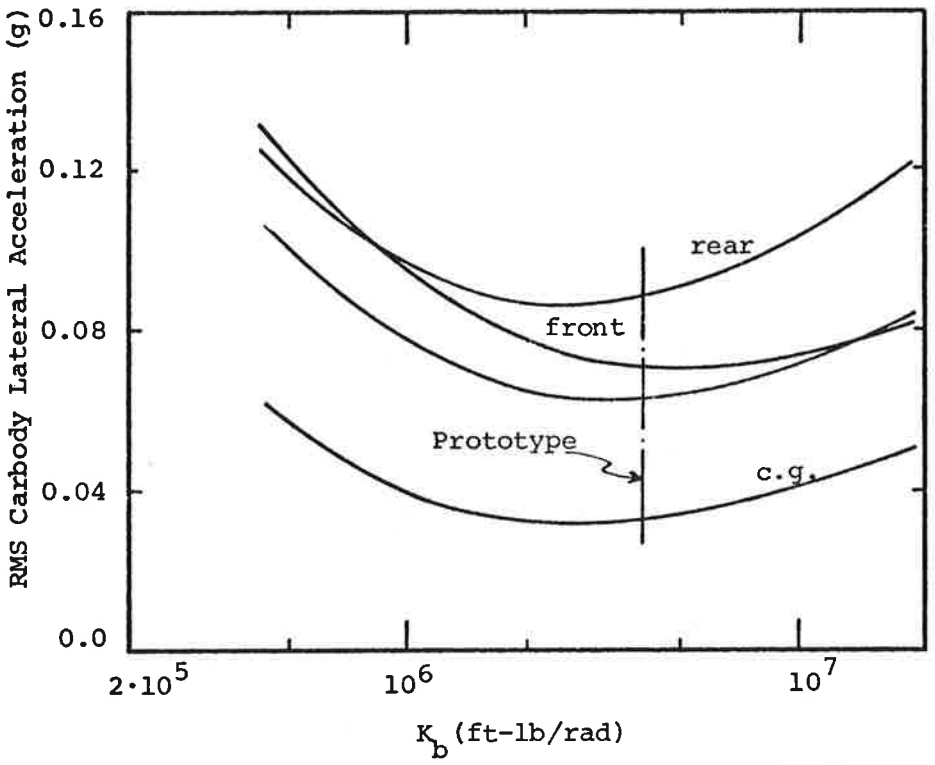

FIGURE 4.6.15: INFLUENCE OF PRIMARY BENDING STIFFNESS ON CARBODY LATERAL ACCELERATION

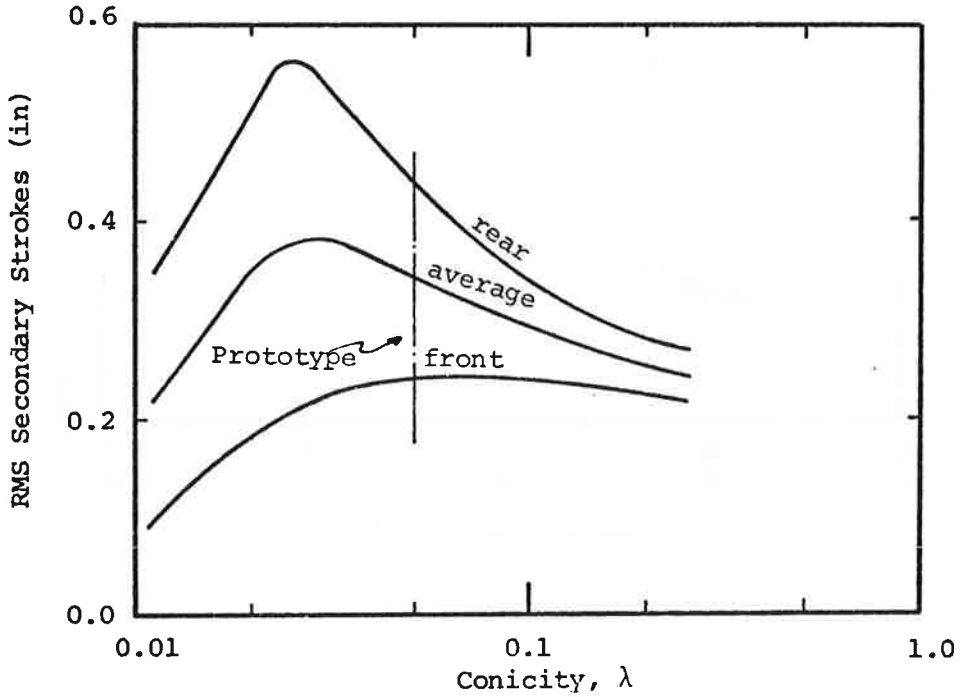

FIGURE 4.6.16: INFLUENCE OF CONICITY ON SECONDARY LATERAL SUSPENSION STROKE LENGTHS

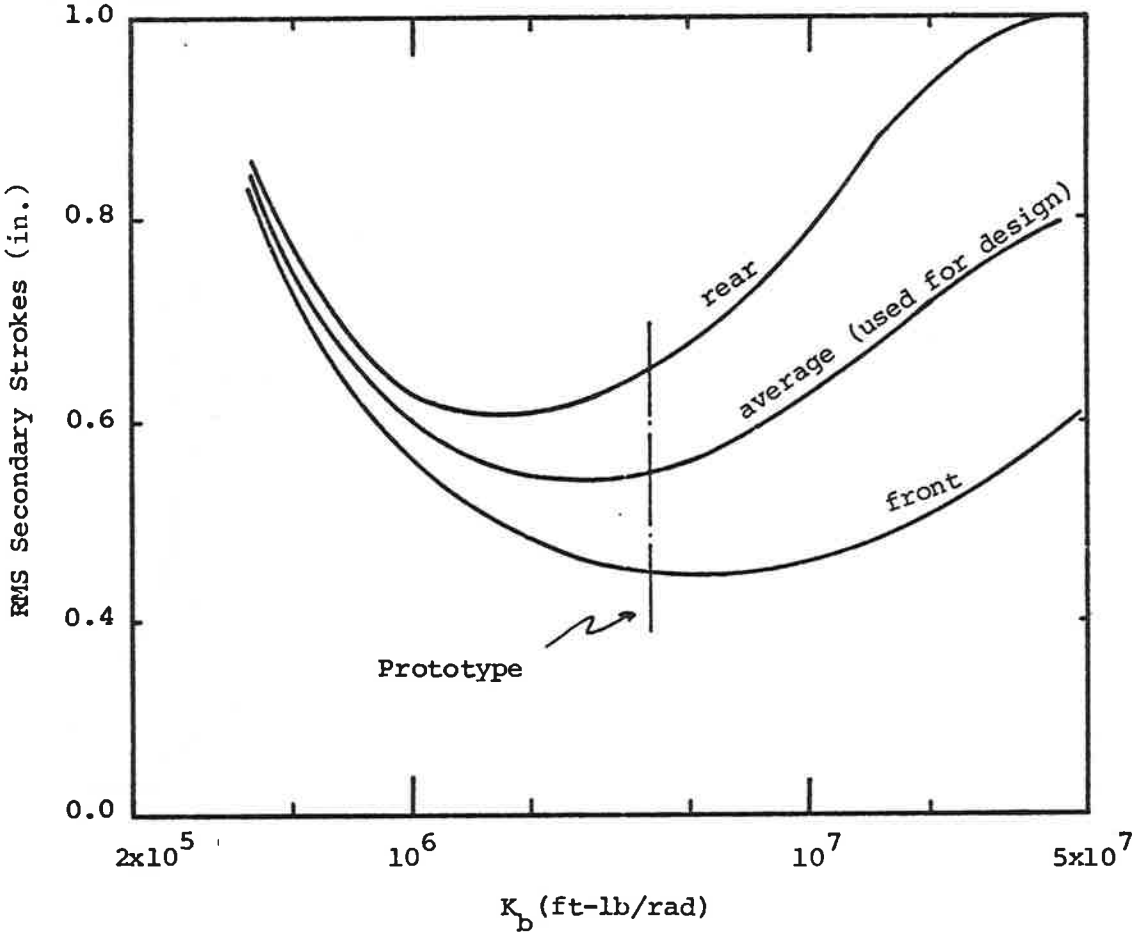

FIGURE 4.6.17: INFLUENCE OF PRIMARY BENDING STIFFNESS ON SECONDARY LATERAL SUSPENSION STROKES

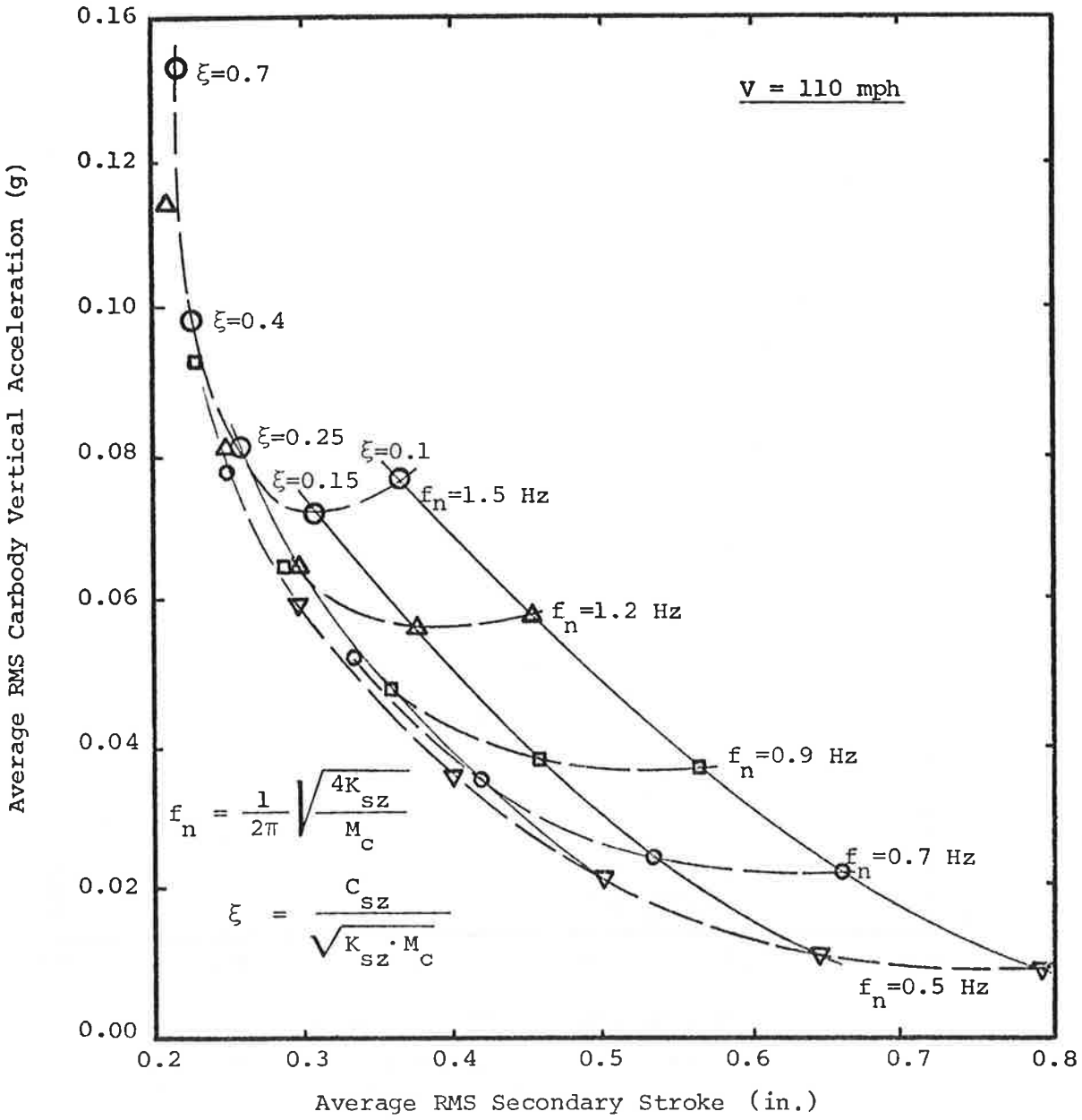

FIGURE 4.6.18: CARBODY VERTICAL ACCELERATION-SECONDARY STROKE LENGTH TRADE-OFF PLOT, V=110 mph

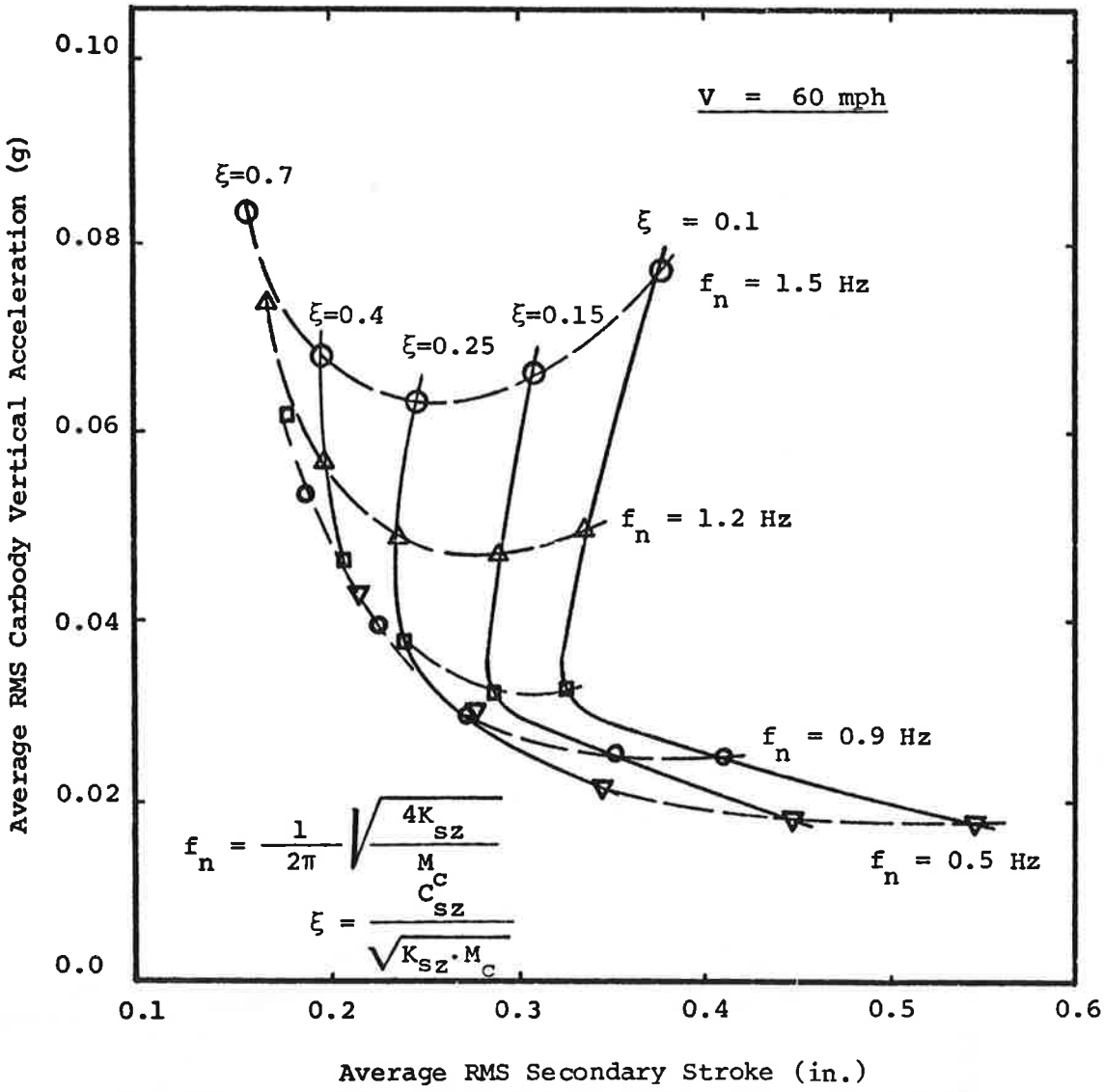

FIGURE 4.6.19: CARBODY VERTICAL ACCELERATION-SECONDARY STROKE LENGTH TRADE-OFF PLOT, V=60 mph

Steps 24 and 25

Follow the instructions in Table 4.6.1.

Once a design has been performed by following the steps, the detailed performance of the vehicle should be determined using the computer performance programs described in Chapter 3.

4.7 Design Examples

The use of the systematic design procedure is demonstrated with two design examples.

Example No. 1

The feasibility and performance of a high speed intercity rail vehicle which is to operate at 130 mph are evaluated. The carbody mass is given as 2500 slugs. It is assumed that the secondary yaw stiffness is $1 \cdot 10^6$ ft-lb/rad.

Design Procedure:

It is assumed that all the unspecified parameters of the vehicle will be close to the prototype vehicle values on which the design charts are based, so that no corrections are needed. To achieve a damping ratio of 0.1-0.2 of the kinematic mode at the operating speed it was estimated that a critical speed of 200 mph is needed. Since no curving performance is specified, the choice of the wheel profile is performed to maximize the degree curve index for V_{cr} = 200 mph. This leads to the choice of a conical profile with λ= 0.05 as indicated by Figure 4.5.13. The design continues as specified in

Table 4.7.3 (pp. 4-89). To evaluate the accuracy of the method all the estimated indices were computed using the full model computer programs [34] Table 4.7.2 summarizes the results of the two procedures.

TABLE 4.7.1: PERFORMANCE SUMMARY OF DESIGN EXAMPLE NO. 1
(For Operation at 130 mph)

	ESTIMATED	COMPUTED WITH FULL MODEL
RMS Primary Strokes, wheelset #4 (in)	0.060	0.068
RMS Wheelset Excursion, wheelset #1 (in)	0.26	0.335
RMS Secondary Lateral Suspension Strokes (in)	0.49	0.560
RMS Average Lateral Passenger Point Acceleration (g)	0.049	0.0618
RMS Secondary Vertical Suspension Strokes (in)	0.406	0.393
RMS Average Vertical Passenger Point Acceleration (g)	0.081	0.0853
Critical Speed (mph)	200	205
Degree Curve (°)	1.5	1.32
Kinematic Mode Damping Ratio	——	0.144

The agreement between the estimated and the computed indices is considered good. The largest errors occurred in the estimation of the lateral forced response performance indices. These values were underestimated, since the design charts were prepared for an intermediate value of the secondary yaw stiffness, $K_{s\psi} = 6 \times 10^6 \frac{\text{ft-lb}}{\text{rad}}$, and the evaluated vehicle has a $K_{s\psi}$ of 1×10^6 ft-lb/rad. There are three other sources of errors. First, errors are caused by reading values off the charts. Second, errors are caused by using the linearized

corrections for parameters' deviations from baseline values. Finally some errors are introduced by neglecting the fact that the vehicle weight, the secondary vertical suspension in the lateral response, and the creep coefficients are different from the baseline case. However, overall the design procedure has produced a vehicle with performance as estimated.

Example No. 2

Suppose it is decided to improve the curving performance of the vehicle in design No. 1 by reducing its critical speed. A new operating speed of 80 mph is adopted which requires a critical speed of about 140 mph. Following the design philosophy of Example No. 1, a worn profile with $\lambda = 0.1$ is chosen. The estimated design parameters are summarized in the design procedure form of Table 4.7.4 and are compared with computed results in Table 4.7.2.

TABLE 4.7.2: SUMMARY OF DESIGN EXAMPLE NO. 2
(for Operation at 80 mph)

	ESTIMATED	COMPUTED WITH FULL MODEL
RMS Primary Strokes, wheelset #4 (in)	0.048	0.0488
RMS Wheelset Excursion, wheelset #1 (in)	0.18	0.235
RMS Secondary Lateral Suspension	0.304	0.440
RMS Average Lateral Passenger Point Acceleration (g)	0.034	0.045
RMS Secondary Vertical Suspension Strokes (in)	0.291	0.282
RMS Average Vertical Passenger Point Acceleration (g)	0.0488	0.0507
Critical Speed (mph)	160	139
Degree Curve (°)	2.2	1.92
ξ-Kinematic mode	—	0.163

Now suppose that Design No. 2 is to be modified to increase its speed as much as possible, without decreasing its curving ability. Three methods are presented and evaluated.

•Reduction of wheelset's mass - Assume, 30% reduction of wheelsets' mass is possible from the baseline value of 120 slugs.

Using Equation 4.6.2

$$V_{cr} = 139\sqrt{\frac{250 + 2\cdot120}{250 + 2\cdot120\cdot0.7}} = 150.5 \text{ mph}.$$

The value obtained by a 6 DOF eigenvalue model is 151 mph.

•Reduction of wheelsets' and truck frame mass - Assume 30% total mass reduction is possible

$$V_{cr} = 139\sqrt{\frac{1}{0.7}} = 166 \text{ mph}.$$

The computed value is 169 mph.

•Use high secondary yaw stiffness - Assume the value $K_{s\psi} = 6\cdot10^6$ ft-lb/rad is used. From Figure 4.6.5, for the 0.5 primary stiffness case, the critical speed was increased by the factor of $\frac{270}{220} = 1.23$. Using Equation 4.6-3 the predicted speed is $V_{cr} = 139(\frac{270.}{220.}) = 171$ mph. The computed value is 164 mph.

The different methods lead to 10-30 mph critical speed improvement, indicating that the operating speed could possibly be increased by up to 20 mph without decreasing the curving performance.

Comparison and Evaluation of the Two Designs

Comparison of Table 4.7.2 with Table 4.7.4 shows that the high speed design (V_{cr} = 205 mph) has relatively low curving performance (D = 1.32°). The low speed design (V_{cr} = 139 mph) has a better curving performance (D = 1.92°). All the dynamic performance indices are higher for the high speed design, because of the speed dependence of the rail irregularities inputs as seen by the passing vehicle. The 3σ value of the primary stroke lengths for both designs are low compared with the strokes allowed by the primary suspension stops (3/8"). The 3σ values of the secondary suspension strokes are either close or less than the strokes allowed by the stops (1.5"). These results indicate that the linear suspension assumption is a good approximation for both cases.

The RMS values of the wheelset excursions are relatively high compared to the wayside clearance of 0.4". For the high speed case 1.2σ and for the low speed case 1.7σ correspond to flange contact, which means that 23% and 9% of the time, respectively, the linear assumption is violated. In practice the nonlinear wheel/rail geometry near the flange will generate restoring forces higher than those predicted by the linear models, so that performance close to the predicted is expected.

Reduction of primary mass was shown to be an effective way for increasing the critical speed, however it is limited by consideration other than the critical speed.

The use of secondary yaw stiffness for increasing the critical

speed was also demonstrated, however, the effectiveness of this method in practice is limited by the very low strokes developed by the secondary yaw suspension elements during operation. Since the strokes are of the order of 1-3mm, a clearance of similar size in the yaw suspension would result in loss of the stabilizing effect, and instability.

Finally, computed L/V ratios are less than 0.1 in both design examples, indicating a lack of hard flanging in curves.

TABLE 4.7.3: DESIGN PROCEDURE EXAMPLE NO. 1
(130 mph Vehicle)

1. Enter the Value of Desired V_{cr} (mph) If Not Specified Go to 2. — V_{cr}= 200

2. Enter the Value of Desired D (degrees) If Not Specified Go to 3 — D = 1.5

3. If the Wheel Profile is Specified, Enter the Following Wheel/Rail Parameters' Values

λ = 0.05 | Δ = 0.0 | δ = 0.05 | a_{11}= 0.05

$F_{11}=2.2\times10^{6}$ | F_{12}= 17500. | F_{22}= 160 | $F_{33}=2.3\times10^{6}$

4. Use Figures 4.6.1 throught 4.6.4 and Equations 4.6-2,4.6-3 to find K_{py} and K_b which satisfy or exceed V_{cr} and/or D, and enter the values. If only one index is specified, maximize the unspecified one. Complete the entries in lines 1 and 2. If the parameters in line 3 are not specified use the profile as a design parameter, i.e. choose values for the parameters in line 3. (Use Table 4.1.1)

$K_{py}= 2 \times 10^5$

$K_b= 1.8 \times 10^5$

5. Compute $K_{px} = K_b/d_p^2$ Enter the Value — $K_{px}=4.5 \times 10^5$

---

6. Estimate the primary suspension stroke lengths (use wheelset #4)

a. Determine the value of PS(Baseline,λ) from Figure 4.6.6 — 0.027

b. Determine the value of ΔPS(Baseline,K_{py}) from Figure 4.6.7 — + 0.030

c. Determine the value of ΔPS(Baseline,λ,V) From Figure 4.6.8 — + 0.003

d. Add entries a, b and c — PS= 0.060

TABLE 4.7.3: (Cont'd)

7. Estimate the wheelset excursions (use wheelset #1)

a. Determine the value of WE(Baseline,λ) from Figure 4.6.9	0.25
b. Determine the value of ΔWE(Baseline, K_b) from Figure 4.6.10	0.00
c. Determine the value of ΔWE(Baseline,λ,V) from Figure 4.6.11	0.01
d. Add entries a,b, and c	WE = 0.26

---

8. If entries 6d and 7d within reasonable limits, go to 9.
If not repeat steps 4 thru 8.

9. Enter the value of desired rms lateral acceleration	ACC_L^*= ——
10. Enter the value of desired rms secondary lateral strokes. If not specified go to 11.	ST_L^*= ——
11. Choose f_{n_L} and ξ_L to satisfy entries 9 and 10. Interpolate between Figure 4.6.12 (110 mph) and Figure 4.6.13 (60 mph) to get approximate values for speed V.	f_{n_L}= 0.7 ξ_L = 0.25
12. Compute the secondary lateral stiffness $K_{sy} = \pi^2 f_n^2 M_c$	K_{sy}= 12000.
13. Compute the secondary lateral damping $C_{sy} = \xi \sqrt{K_{sy} \cdot M_c}$	C_{sy}= 1370.

---

14. Estimate the rms lateral acceleration

a. Compute

$$ACC(Baseline, f_n, \xi, V) = ACC(110) + \left(\frac{V-110}{50}\right)[ACC(110) - ACC(60)]$$

0.046

TABLE 4.7.3: (Cont'd)

where ACC(110) is taken from Fig. 4.6.12

and ACC(60) is taken from Fig. 4.6.13

b. Determine the value of $\Delta ACC(Baseline,\lambda)$ from Figure 4.6.14 — + 0.000

c. Determine the value of $\Delta ACC(Baseline,K_b)$ from Figure 4.6.15 — + 0.003

d. Add Entries a,b and c — ACC_L = 0.049

---

15. Estimate the rms secondary lateral strokes

a. Compute

$$ST(Baseline, f_n, \xi, V) = ST(110) + \left(\frac{V-110}{50}\right)[ST(110)-ST(60)]$$ — 0.49

where ST(110) is taken from Figure 4.6.12
and ST(60) is taken from Figure 4.6.13

b. Determine the value of $\Delta ST(Baseline,\lambda)$ from Figure 4.6.16 — + 0.00

c. Determine the value of $\Delta ST(Baseline\ K_b)$ from Figure 4.6.17 — + 0.00

d. Add entries a,b, and c — ST_L = 0.49

---

16. Compare entry 14d to entry 9, and entry 15d to entry 10. If the actual indices exceed the desired values, repeat steps 11 through 15.

17. Enter the value of desired rms vertical acceleration. If not specified to to 18. — ACC_V* = ——

TABLE 4.7.3: (Cont'd)

18. Enter the value of desired rms secondary vertical stroke. If not specified go to 19.

ST_v*= ——

19. Choose f_{n_v} and ξ_v to satisfy entries 17 and 18. Interpolate between Figure 4.6.18 (110mph) and Figure 4.6.19 (60 mph) to get approximate values for speed V.

f_{n_v}= 0.9

ξ_v = 0.25

20. Compute the secondary vertical stiffness

$$K_{sz} = \pi^2 f_n^2 M_c$$

K_{sz}= 20000.

21. Compute the secondary vertical damping

$$C_{sz} = \xi_v \sqrt{K_{sz} \cdot M_c}$$

C_{sz}= 1800.

22. Estimate the rms vertical acceleration

$$ACC_v = ACC\ (110) + \left(\frac{V-110}{50}\right)[ACC\ (110) - ACC(60)]$$

where ACC (110) is taken from Figure 4.6.18

and ACC (60) is taken from Figure 4.6.19

ACC_v= 0.081

23. Estimate the rms vertical secondary strokes

$$ST_v = ST\ (110) + \left(\frac{V-110}{60}\right)[ST\ (110) - ST\ (60)]$$

where ST (110) is taken from Figure 4.6.18

and ST (60) is taken from Figure 4.6.19

ST_v= 0.406

TABLE 4.7.3: (Concl'd)

24. Compare entry 22 to entry 17, and entry 23 to entry 18. If the actual indices exceed the desired values, repeat steps 19-24.

25. Compute dependent design parameters as indicated in Table 4.1.1.

TABLE 4.7.4: DESIGN PROCEDURE EXAMPLE NO. 2
(80 mph Vehicle)

1. Enter the Value of Desired V_{cr} (mph) If Not Specified Go to 2. — V_{cr}= 160

2. Enter the Value of Desired D(degrees) If Not Specified Go to 3 — D = 2.2

3. If the Wheel Profile is Specified, Enter the Following Wheel/Rail Parameters' Values

λ = 0.1 | Δ = 9.0 | δ = 0.075 | a_{11}= 0.075

F_{11}= 2.37x10^6 | F_{12}= 17550 | F_{22}= 274 | F_{33}= 2.74x10^6

4. Use Figures 4.6.1 through 4.6.4 and Equations 4.6-2, 4.6-3 to find K_{py} and K_b which satisfy or exceed V_{cr} and/or D, and enter the values. If only one index is specified, maximize the unspecified one. Complete the entries in lines 1 and 2. If the parameters in line 3 are not specified use the profile as a design parameter, i.e. choose values for the parameters in line 3. (Use Table 4.1.1)

K_{py}= 2x10^5

K_b= 2x10^6

5. Compute $K_{px} = K_b/d_p^2$ Enter the Value — K_{px}= 5x10^5

---

6. Estimate the primary suspension stroke lengths (use wheelset #4)

a. Determine the value of PS(Baseline,λ) from Figure 4.6.6 — 0.026

b. Determine the value of ΔPS(Baseline,K_{py}) from Figure 4.6.7 — + 0.030

c. Determine the value of ΔPS(Baseline,λ,V) From Figure 4.6.8 — + -0.008

d. Add entries a, b and c — PS= 0.048

TABLE 4.7.4: (Cont'd)

7. Estimate the wheelset excursions (use wheelset #1)

a. Determine the value of WE(Baseline,λ) from Figure 4.6.9	0.19
b. Determine the value of ΔWE(Baseline, K_b) from Figure 4.6.10	0.00
c. Determine the value of ΔWE(Baseline,λ,V) from Figure 4.6.11	-0.01
d. Add entries a,b, and c	WE = 0.18

---

8. If entries 6d and 7d within reasonable limits, go to 9.
If not repeat steps 4 thru 8.

9. Enter the value of desired rms lateral acceleration — ACC_L^* = ——

10. Enter the value of desired rms secondary lateral strokes.
If not specified go to 11. — ST_L^* = ——

11. Choose f_{n_L} and ξ_L to satisfy entries 9 and 10. Interpolate between Figure 4.6.12 (110 mph) and Figure 4.6.13 (60 mph) to get approximate values for speed V.

f_{n_L} = 0.8

ξ_L = 0.2

12. Compute the secondary lateral stiffness

$$K_{sy} = \pi^2 f_n^2 M_c$$

K_{sy} = 16000.

13. Compute the secondary lateral damping

$$C_{sy} = \xi \sqrt{K_{sy} \cdot M_c}$$

C_{sy} = 1250.

---

14. Estimate the rms lateral acceleration

a. Compute

$$ACC(Baseline, f_n, \xi, V) = ACC(110) + \left(-\frac{V-110}{50}\right) [ACC(110) - ACC(60)]$$

0.036

TABLE 4.7.4: (Cont'd)

where ACC(110) is taken from Fig. 4.6.12

and ACC(60) is taken from Fig. 4.6.13

b. Determine the value of $\Delta ACC(Baseline,\lambda)$ from Figure 4.6.14 — $+$ -0.005

c. Determine the value of $\Delta ACC(Baseline,K_b)$ from Figure 4.6.15 — $+$ 0.003

d. Add Entries a,b and c — ACC_L=0.034

---

15. Estimate the rms secondary lateral strokes

a. Compute

$$ST(Baseline, f_n, \xi, V)=ST(110) + \left(\frac{V-110}{50}\right)[ST(110)-ST(60)]$$ — 0.353

where ST(110) is taken from Figure 4.6.12
and ST(60) is taken from Figure 4.6.13

b. Determine the value of $\Delta ST(Baseline,\lambda)$ from Figure 4.6.16 — $+$ -0.055

c. Determine the value of $\Delta ST(Baseline\ K_b)$ from Figure 4.6.17 — $+$ 0.000

d. Add entries a,b, and c — ST_L=-0.304

---

16. Compare entry 14d to entry 9, and entry 15d to entry 10. If the actual indices exceed the desired values, repeat steps 11 through 15.

17. Enter the value of desired rms vertical acceleration. If not specified to to 18. — ACC_v*= ——

TABLE 4.7.4: (Cont'd)

18. Enter the value of desired rms secondary vertical stroke. If not specified go to 19.

$ST_v^* =$ ——

19. Choose f_{n_v} and ξ_v to satisfy entries 17 and 18. Interpolate between Figure 4.6.18 (110mph) and Figure 4.6.19 (60 mph) to get approximate values for speed V.

$f_{n_v} = 0.9$

$\xi_v = 0.25$

20. Compute the secondary vertical stiffness

$$K_{sz} = \pi^2 f_n^2 M_c$$

$K_{sz} = 20000.$

21. Compute the secondary vertical damping

$$C_{sz} = \xi_v \sqrt{K_{sz} \cdot M_c}$$

$C_{sz} = 1800.$

22. Estimate the rms vertical acceleration

$$ACC_v = ACC\ (110) + \left(\frac{V-110}{50}\right)[ACC\ (110) - ACC(60)]$$

where ACC (110) is taken from Figure 4.6.18

and ACC (60) is taken from Figure 4.6.19

$ACC_v = 0.0688$

23. Estimate the rms vertical secondary strokes

$$ST_v = ST\ (110) + \left(\frac{V-110}{60}\right)[ST\ (110) - ST\ (60)]$$

where ST (110) is taken from Figure 4.6.18

and ST (60) is taken from Figure 4.6.19

$ST_v = 0.291$

TABLE 4.7.4: (Concl'd)

24. Compare entry 22 to entry 17, and entry 23 to entry 18. If the actual indices exceed the desired values, repeat steps 19-24.

25. Compute dependent design parameters as indicated in Table 4.1.1.

5. SUMMARY

The research described in this report has led to development of a design procedure for conventional passenger trucks. In the procedure the fifty inertial, damping, stiffness and geometric parameters that characterize a vehicle are divided into three categories.

1) Fixed design parameters such as vehicle length and weight set by overall vehicle size and service requirements.

2) Dependent design parameters such as wheel/rail profile geometry and damping in primary suspension elements which depend directly upon the values of free design parameters.

3) Free design parameters such as primary and secondary suspension parameters and wheel conicity which are selected by the design procedure.

The procedure selects the values of the free design parameters to meet the following dynamic performance indices:

- Ride Quality represented by the acceleration environment in the car
- Stability represented by the critical speed of the vehicle
- Curve negotiation represented by the maximum degree curve traversed without slipping or flanging.

These indices are met while satisfying constraints represented in terms of secondary strokes to limit the carbody dynamic envelope and wheel excursions to limit wheel-rail forces. The procedure consists of a set of steps which lead to selection of the free design parameters using paper and pencil calculations.

The procedure is based upon partitioning the design task into three basic trade-off studies.

a) The vertical ride quality versus vertical suspension stroke trade-off which sets the secondary vertical suspension parameters.

b) The lateral ride quality versus suspension stroke trade-off which sets the lateral secondary suspension parameters.

c) The stability versus curving trade-off which sets the primary suspension and wheel conicity parameters as well as the secondary yaw suspension parameters.

Data in the form of design charts have been prepared using a linear rail vehicle model for each of these basic trade-offs so that design parameters may be selected directly from the charts. The basic design is performed for a fixed vehicle inertial and geometric characteristics, and correction equations are provided for wheelset of track masses (which are altered from reference values). The detailed charts provided with the design procedure are applicable to vehicles with a conventional primary suspension connecting the wheelsets to the truck frame. The procedure may be extended directly to radial truck designs by preparing design charts similar to those provided with the methods described in reference [39]. The procedure considers a secondary vertical suspension consisting of a conventional spring and damper. It may be extended directly to include combined pneumatic-orifice damping suspensions using trade-off data generated with the model in reference [39]. The detailed trade-off charts for the vehicle are referenced to 110 mph operation on class 6 track.

The design procedure has been illustrated with two design examples. The first example is an intercity vehicle with a maximum operating speed of 130 mph and designed to have a critical speed of 200 mph.

The vehicle is of conventional geometry and has conventional values of vehicle, truck and wheelset mass. A design value of wheel conicity of 0.05 was found to result in primary suspension stiffness parameters which provide the desired critical speed and, result in a maximum curving capability of 1.3° without slipping and flanging. The design results in rms secondary stroke lengths during operation at 110 mph on class 6 track which are one third of the total clearance provided by bump stops and has an rms acceleration of 0.081 g's.

The second design example considered an urban vehicle operating at 80 mph. For this vehicle a design critical speed of 140 mph was selected. A wheel conicity of 0.1 was found to provide primary suspension stiffness parameters which provide the required critical speed and result in a maximum curving capability of 2.2° without slipping and flanging. The performance of the vehicle operating at 80 mph on class 6 track results in rms secondary strokes less than one third of bump stop clearances and provides an rms passenger compartment acceleration of 0.05 g's. For this urban design it was also shown that a reduction of wheelset and truck frame mass by 30% could result in increasing the vehicle critical speed to 160 mph.

The design procedure developed provides a systematic method of selecting conventional passenger truck design parameters to meet dynamic performance indices. The procedure has been developed using linear models of rail passenger vehicles which have not been validated with experimental test data. The validation of rail passenger vehicle

models with experimental data is of high priority and is strongly recommended. While the linear models employed in the design process reflect the dominant characteristics of vehicle performance, in two areas, these models can be improved to provide a more accurate representation of performance. An improved representation of the secondary yaw suspension in terms of its nonlinear breakaway characteristics and of the wheel-rail nonlinear forces, as influenced by track irregularities, would provide an improved capability to estimate vehicle stability and wheelset motions. These extensions to the design procedure would result in an ability to more accurately select suspension design parameters.

The design charts utilized in the procedure have been prepared for smooth curved track and class 6 tangent track. The computer programs cited in Section 3.4 may be used to prepare data for other classes of track and alternate values of creep coefficients. Thus the procedure may be extended directly to track classes 4 and 5 and to alternate values of coefficients. The design procedure does not include the influence of spiral track curve entries and exits. An extension of the analysis is recommended to include spiral entry and exit design constraints.

The procedure in its present form is restricted to selection of truck design parameters based upon dynamic performance indices. Extension of truck design procedures to include static design constraints based upon strength and fatigue factors, maintainability considerations, i.e., performance with deteriorated and/or worn parts and the resulting performance at the end of a maintenance cycle, and to include braking functions and powered truck design factors should be considered.

6. REFERENCES

1. Aronson, R., "Amtrak to Roll," Machine Design, January 22, 1976, p. 18-24.

2. Scheffel, H., "The Hunting Stability and Curving Ability of Railway Vehicles," Rail International, No. 2, February 1974, p. 154-177.

3. List, H.A., Caldwell, W.N., Marcotte, P., "Proposed Solutions to the Freight Car Truck Problems of Flange Wear and Truck Hunting," ASME Paper No. 75-WA-RT-8, 1976.

4. Klinger, D., Cooperrider, N.K., Hedrick, J.K., and White, R.H., "Guideway-Vehicle Cost Reduction," Final Report, U.S. DOT, Report No. DOT-TST-76-95, June 1976.

5. Hedrick, J.K. and Wormley, D.N., "Active Control for Ground Transportation Vehicles: A State of the Art Review," ASME, AMD Monograph, AMD-Vol. 15, 1975.

6. "Dynamics and Control of Rail Vehicle Systems," M.I.T. Short Course, 2.02S, Cambridge MA, 1976.

7. Law, E.H., and Cooperrider, N.K., "A Survey of Railway Dynamics Research," ASME Transactions, Vol. 98, Series G, No. 2, June 1974, p. 132-146.

8. Nathanson, W., "Parametric Study Bibliography: Literature Survey for Rail System Dynamics Parametric Study," TSC RFP No. TSC/612-0368-GF, July 1976.

9. Wickens, A.H., "The Dynamic Stability of Railway Vehicle Wheelsets and Bogies Having Profiled Wheels," International Journal of Solids and Structures, Vol. 1, 1965, p. 319-341.

10. Wickens, A.H., "General Aspects of the Lateral Dynamics of Railway Vehicles," Journal of Engineering for Industry, Trans. ASME, Series B. Vol. 91, No. 3, August 1969, p. 868-878.

11. Wickens, A.H., "Vehicle Dynamics and Wheel-Rail Interace Problems," Proceedings of the Carnegie-Mellon Conference on High-Speed Ground Transportation, Pittsburgh, Pa. 1969, p. 157-171.

12. Newland, D.E., "Steering a Flexible Railway Truck on Curved Track," Journal of Engineering for Industry, Trans. ASME Series B, Vol. 91, No. 3, August 1969, p. 908-918.

13. Boocock, D., "Steady State Motion of Railway Vehicles on Curved Tracks," Journal of Mechanical Engineering Science, Vol. II, No. 6, 1969, p. 556-566.

14. White, R.W., et.al., "Guideway-Suspension Trade-offs In Rail Vehicles Systems," Final Report, U.S. DOT, Contract DOT-OS-50107, January 1978.

15. Shapiro, S.M., "Engineering Data on Selected High Speed Passenger Trucks," Final Technical Report, Report No. 0391, The Budd Technical Center, Fort Washington, PA, May 1977.

16. Kar, A.K., "A Survey for Trucks of Passenger Rail Vehicles," Term Project for Course 1.290J, M.I.T., May 1977.

17. Bullock, R.L., "Modified Three-Piece Truck Reduces Hunting and Improves Curving-Status Report," 12th Annual Railroad Engineering Conference on the Effect of Heavy Axle Loads on Track, 1975, p. 85.

18. Scheffel, H., "Wheelset Suspensions Designed to Eliminate the Detrimental Effects of Wheel Wear on the Hunting Stability of Railroad Vehicles," ASME Symposium on Railroad Equipment Dynamics, Chicago, 1976.

19. Wickens, A.H., "Steering and Dynamic Stability of Railway Vehicles," Vehicle System Dynamics, Vol. 5, 1975/1976, p. 15.

20. Scales, B.T., "Behavior of Bogies on Curves," Railway Engineering Journal, Vol. 1, No. 4, 1972, p. 12.

21. Scheffel, H., "A New Design Approach for Railway Vehicle Suspension," Rail International, October 1974, p. 638.

22. Scheffel, H., "Self-Steering Wheelsets will Reduce Wear and Permit Higher Speeds," Railway Gazette International, December 1976, p. 453.

23. List, H.A., "Design System Approach to Problem Solving," 12th Annual Railroad Engineering Conference on the Effects of Heavy Axle Loads on Track, 1975, p. 79.

24. Hawthorne, V.T., "Truck Design-A System Approach to Solving Problems," 12th Annual Railroad Engineering Conference on the Effects of Heavy Axle Loads on Track, 1975, p. 74.

25. List, H.A., "Means for Improving the Steering Behavior of Railway Vehicles," Presented to the Annual Meeting of the Transportation Research Board, January 22, 1976.

26. Hanes, R.N., "Human Sensitivity to Whole-Body Vibrations in Urban Transportation Systems: A Literature Review: The Johns Hopkins University Applied Physics Lab., Report No. APL/JK/U TPR 004, May 1970.

27. Jankovitch, J.P., "Ride Quality-A Review," Report prepared for U.S. Department of Transportation, Office of the Secretary, 1976.

28. Anon., "Guide for the Evaluation of Human Exposure to Whole-Body Vibration," I.S.O. 2631, International Organization for Standardization, 1977.

29. Leatherwood, J.D. and Dempsey, T.K., "A Model for Prediction of Ride Quality in a Multifactor Environment," NASA TMX-72842, April 1976.

30. Anon., "Track Safety Standards," DOT-FRA Office of Safety, March 1975.

31. Bumgardner, H.M., Dean, F.E., and Hall, V.W., "LTV/SIG Metroliner Truck-Final Design Report," U.S. Department of Transportation Final Report, Report No. FRA OR&D 76-250, 1975.

32. Koci, L.F. and Marta, H.A., "Lateral Loading Between Locomotive Truck Wheels and Rail Due to Curve Negotiation," Axle, Wheels, and Interaction, Anthology of Rail Vehicle Dynamics, ASME, Vol. 3, 1973.

33. Rice, S.O., "Mathematical Analysis of Random Noise," Bell System Tech., Vol. 23, 1944, pp. 282-332, Vol. 24, 1945, p. 46-156.

34. Anis, Z., and Hedrick, J.K., "Characterization of Rail Track Irregularities," Final Report U.S. Department of Transportation Contract No. DOT-TSC-1206, September 1977.

35. Corbin, J., Statistical Representations of Track Geometry," Technical Report Federal Railroad Administration, FRA/ORD-80/22-1, 1980.

36. Kalker, J.J., "On the Rolling Contact of Two Elastic Bodies in the Presence of Dry Friction," Doctoral Dissertation, 1967, Technische Hogeshoul, Delft, Netherlands, 1967.

37. Sayers, M.W., "Analytical Methods to Reduce the Combined Track/Vehicle Suspension Costs of Rail Systems," M.S. Thesis, Dept. of Mechanical Engineering, M.I.T., 1976.

38. System/360 Scientific Subroutine Package, IBM Publication, H20-0205-3, 1968.

39. Hedrick, J.K. et al., "Performance Limits of Rail Passenger Vehicles: Evaluation and Optimization," Technical Report Prepared under U.S. Department of Transportation Control DOT-OS-70052, August 1978.

40. Lewin, B., "Loads Due to Forced Response of Random Inputs on Radial Trucks of Rail Passenger Vehicles," S.M. Thesis, Massachusetts Institute of Technology, October 1979.

41. Weinstock, H.,"Analyses of Rail Vehicle Dynamics in Support of the Wheel Rail Dynamics Research Facility," U.S. Department of Transportation Interim Report No. UMTA-MA-06-0025-73, June 1973.

42. Weinstock, H. and Greif, R., "Analysis of Wheel Rail Force and Flange Force During Steady State Curving of Rigid Trucks," DOT-TSC-UMTA-80-26/UMTA-MA-06-0025-80-8, September 1980.

APPENDIX A: DERIVATION OF SIMPLIFIED CURVING EXPRESSIONS

The following simplified treatment of curving mechanics is based on the vehicle models developed in ref. [39]. By assuming purely conical wheel treads and negligible secondary yaw suspension torque, each truck of the full 15 D.O.F. model may be represented accurately by the reduced 4 D.O.F. truck model shown in Figure A.1. The simplified truck model consists of two wheelsets interconnected by relative shear and bending stiffnesses, K_s and K_b, which represent the total effective static shear and bending stiffnesses acting between the wheelsets, respectively. For a conventional truck with primary stiffnesses K_{px} and K_{py}, the effective interconnection stiffnesses are given by:

$$K_s = \frac{d_p^2 K_{px} K_{py}}{d_p^2 K_{px} + b^2 K_{py}} \qquad \text{(A-1)}$$

$$K_b = d_p^2 K_{px} \qquad \text{(A-2)}$$

Use of K_s and K_b instead of K_{px} and K_{py} simplifies the analysis which follows.

A further simplification is achieved by assuming that the spin components of creep force are small, and that the lateral and longitudinal creep force coefficients are equal:

---

*Similar developments are given in Refs. [12,13,41,42].

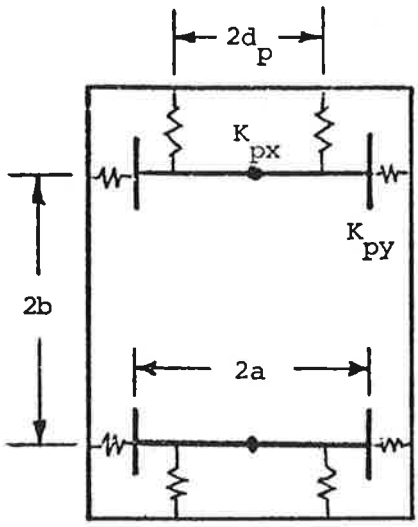

Conventional Truck Configuration

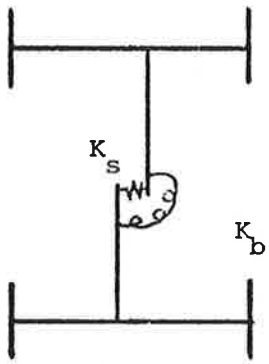

Equivalent Shear and Bending Stiffnesses

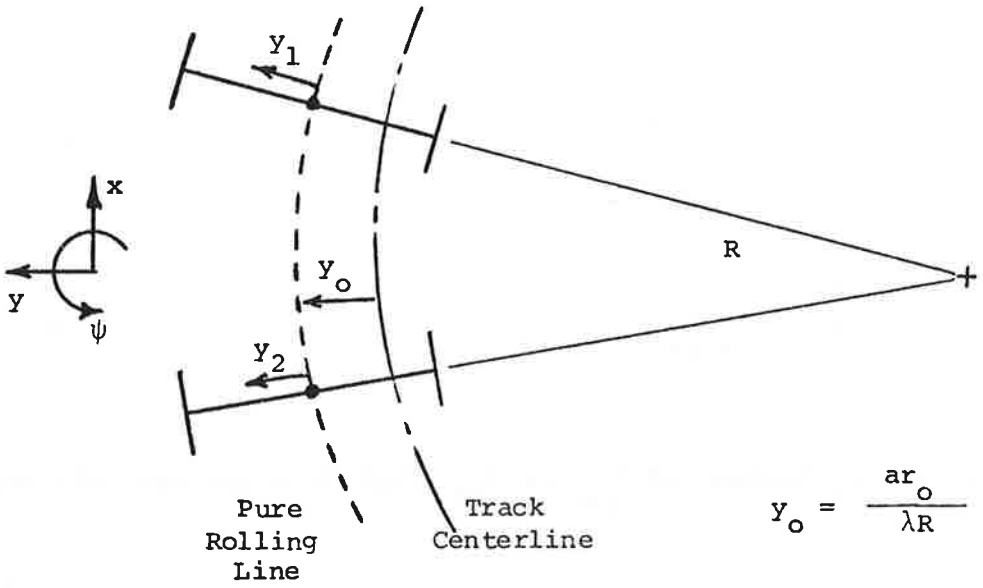

y_1, y_2: Lateral wheelset displacement from pure rolling line.

ψ_1, ψ_2: Angular wheelset displacement from radial alignment.

FIGURE A.1: SIMPLIFIED 4 D.O.F. CURVING MODEL AND COORDINATE DEFINITIONS

$$f_{11} = f_{33} = f \qquad \text{(A-3)}$$

$$f_{12} \approx f_{22} \approx 0 . \qquad \text{(A-4)}$$

The 4x4 simplified curving equations may be written as shown below in terms of the lateral and yaw wheelset displacments for a vehicle negotiating a constant radius curve at balance speed.

$$\begin{bmatrix} -K_s & +bK_s+2f & +K_s & +bK_s \\ +bK_s-2f\frac{\lambda a}{r_o} & -b^2K_s-K_b & -bK_s & -b^2K_s+K_b \\ +K_s & -bK_s & -K_s & -bK_s+2f \\ +bK_s & -b^2K_s+K_b & -bK_s-2f\frac{\lambda a}{r_o} & -b^2K_s-K_b \end{bmatrix} \begin{bmatrix} y_1 \\ \psi_1 \\ y_2 \\ \psi_2 \end{bmatrix} = \begin{bmatrix} 0 \\ -2\frac{b}{R}K_b \\ 0 \\ +2\frac{b}{R}K_b \end{bmatrix}$$

These equations are solved for the wheelset displacements:

$$\psi_1 = -\psi_2 = \frac{K_s\lambda a}{K_s b r_o + f\lambda a} \qquad y_1 = \frac{b}{R}\,\frac{1}{1+\frac{f^2}{K_bK_s}\,\frac{\lambda a}{r_o}} \qquad \text{(A-5)}$$

$$y_1 = \frac{b}{R}\,\frac{bK_sK_b\,\frac{r_o}{\lambda a} + K_bf}{K_sK_b + f^2\,\frac{\lambda a}{r_o}} \qquad \text{(A-6)}$$

$$y_2 = \frac{K_s b r_o - f\lambda a}{K_s b r_o + f\lambda a} y_1 \quad . \qquad \text{(A-7)}$$

The curving indices [39] of flange contact and slip are evaluated using Equations (A-5) through (A-7) as follows. Note that curve radius is related to curvature in degrees by the expression

$$D = 2 \sin^{-1}\left(\frac{50}{R}\right) \cdot \frac{360}{2\pi} \quad , \qquad \text{(A-8)}$$

which may be approximated reasonably well for curvatures less than about 10 degrees by

$$D = \frac{5730}{R} \quad . \qquad \text{(A-9)}$$

Flange Contact Index

A simplified expression for the tightest curve which can be negotiated without flange contact is obtained by solving for the track curvature at which the greatest wheelset excursion from the track centerline is equal to the flange clearance available to a centered wheelset; the condition given by

$$y_1 + y_o = y_{fc} \quad . \qquad \text{(A-10)}$$

Solving Equation (A-6) subject to Equation (A-10) yields

$$D_{flange} = 5730\, y_{fc} \; \frac{K_b K_s + f^2 \frac{\lambda a}{r_o}}{b^2 K_b K_s \frac{r_o}{\lambda a} + b K_b f + \frac{a r_o}{\lambda} K_b K_s + f^2 a^2} \qquad \text{(A-11)}$$

Slip Index

A corresponding simplified expression for the tightest curve which can be negotiated without "wheel slip" is obtained by setting the worst-case resultant creep force equal to the limit of adhesion at a wheel, μN.

$$\sqrt{(F_{long.})^2 + (F_{lat.})^2} = \mu N \qquad \text{(A-12)}$$

The creep forces are given in terms of wheelset displacements by [39]:

$$\sqrt{(f \frac{\lambda}{r_o} y_1)^2 + (f\psi_1)^2} = \mu N \,. \qquad \text{(A-13)}$$

Substituting Equations (A-5) and (A-6) for y_1 and ψ_1 and solving for the track curvature yields:

$$D_{slip} = 5730 \frac{\mu N}{bf} \sqrt{\frac{(1 + \frac{f^2 \lambda a}{K_b K_s r_o})^2}{(\frac{b}{a} + \frac{f\lambda}{K_s r_o})^2 + 1}} \,. \qquad \text{(A-14)}$$

External Lateral Forces

Equations (A-4) through A-7) and Equation (A-11) can be readily extended to consider a static flanging force, F_f, on the front wheelset and a static lateral load, F_c, at the centerpin of the truck as shown below.

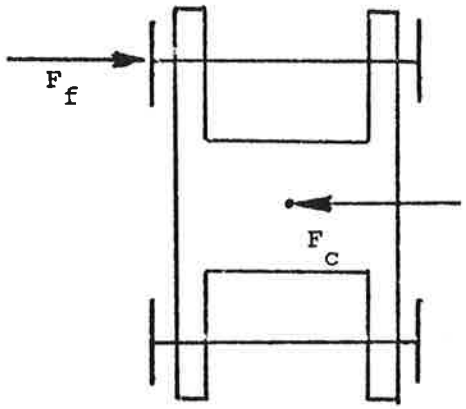

Equation (A-4) becomes:

$$\begin{bmatrix} -K_s & +bK_s+2f & +K_s & +bK_s \\ +bK_s-2f\frac{\lambda a}{r_o} & -b^2K_s-K_b & -bK_s & -b^2K_s+K_b \\ +K_s & -bK_s & -K_s & -bK_s+2f \\ +bK_s & -b^2K_s+K_b & -bK_s-2f\frac{\lambda a}{r_o} & -b^2K_s-K_b \end{bmatrix} \begin{bmatrix} y_1 \\ \psi_1 \\ y_2 \\ \psi_2 \end{bmatrix} = \begin{bmatrix} F_f-\frac{F_c}{2} \\ -2\frac{b}{R}K_b \\ -\frac{F_c}{2} \\ +2\frac{b}{R}K_b \end{bmatrix}$$

Equations (A-5) through (A-7) and Equation (A-11) become:

$$\psi_1 = -\psi_2 + \frac{F_f}{2f} - \frac{F_c}{2f}$$

$$= \frac{[K_s\lambda a]y_1 - \frac{F_f}{4f}[K_s b\lambda a - 2f\lambda a - 2K_s br_o] + \frac{F_c}{4f}[K_s b\lambda a - f\lambda a - K_s br_o]}{K_s br_o + f\lambda a} \quad \text{(A-15)}$$

$$y_1 = \frac{[\frac{b}{R}[bK_sK_b\frac{r_o}{\lambda a} + K_bf] - \frac{F_f}{4f}[b^2fK_s + K_bf + bK_sK_b(\frac{r_o}{\lambda a} - 1)] + \frac{F_c}{4f}[b^2fK_s - bK_sK_b]}{K_sK_b + f^2\frac{\lambda a}{r_o}} \quad \text{(A-16)}$$

$$y_2 = \frac{[K_s br_o - f\lambda a]y_1 - \frac{F_f}{4f}[2K_s b^2 r_o] + \frac{F_c}{4f}[2K_s b^2 r_o]}{K_s br_o + f\lambda a} \quad \text{(A-17)}$$

$$D_{flange} = 5730\,\frac{y_{fc}[K_bK_s + f^2\frac{\lambda a}{r_o}] + \frac{F_f}{4f}[b^2fK_s + K_bf + bK_sK_b(\frac{r_o}{\lambda a} - 1)] - \frac{F_c}{4f}[b^2K_sf - bK_sK_b]}{b^2K_sK_b\frac{r_o}{\lambda a} + bK_bf + \frac{ar_o}{\lambda}K_bK_s + f^2a^2} \quad \text{(A-18)}$$

Rearranging Equation A-18 yields an expression for estimating the flanging force levels encountered when a vehicle negotiates a track curvature which exceeds that given by Equation A-18 with $F_f = 0$.

$$F_f \approx 4f\,\frac{\frac{1}{R}(b^2K_sK_b\frac{r_o}{\lambda a} + bK_bf + \frac{ar_o}{\lambda}K_bK_s + a^2f^2) + \frac{F_c}{4f}(b^2fK_s - bK_sK_b) - y_{fc}(K_bK_s + f^2\frac{\lambda a}{r_o})}{b^2fK_s + K_bf + bK_sK_b(\frac{r_o}{\lambda a} - 1)} \quad \text{(A-19)}$$

The lateral load F_c can represent an outboard cant deficiency load, although the above simplified expressions do not include the overturning effect of cant deficiency loading in terms of vertical wheel load shifts [39]. The force F_c represents only the lateral component of cant deficiency loading.

The simplified expressions derived in this appendix are accurate representations of the full 15 D.O.F. model when secondary yaw torques are relatively small, say below 5000 ft-lb. As secondary yaw torque increases, curving performance tends to be degraded by an amount proportional to the magnitude of the torque over the range of practical truck parameter values. An estimate of the reduction in curving performance for given values of secondary yaw torque can be obtained from Figure A.2.

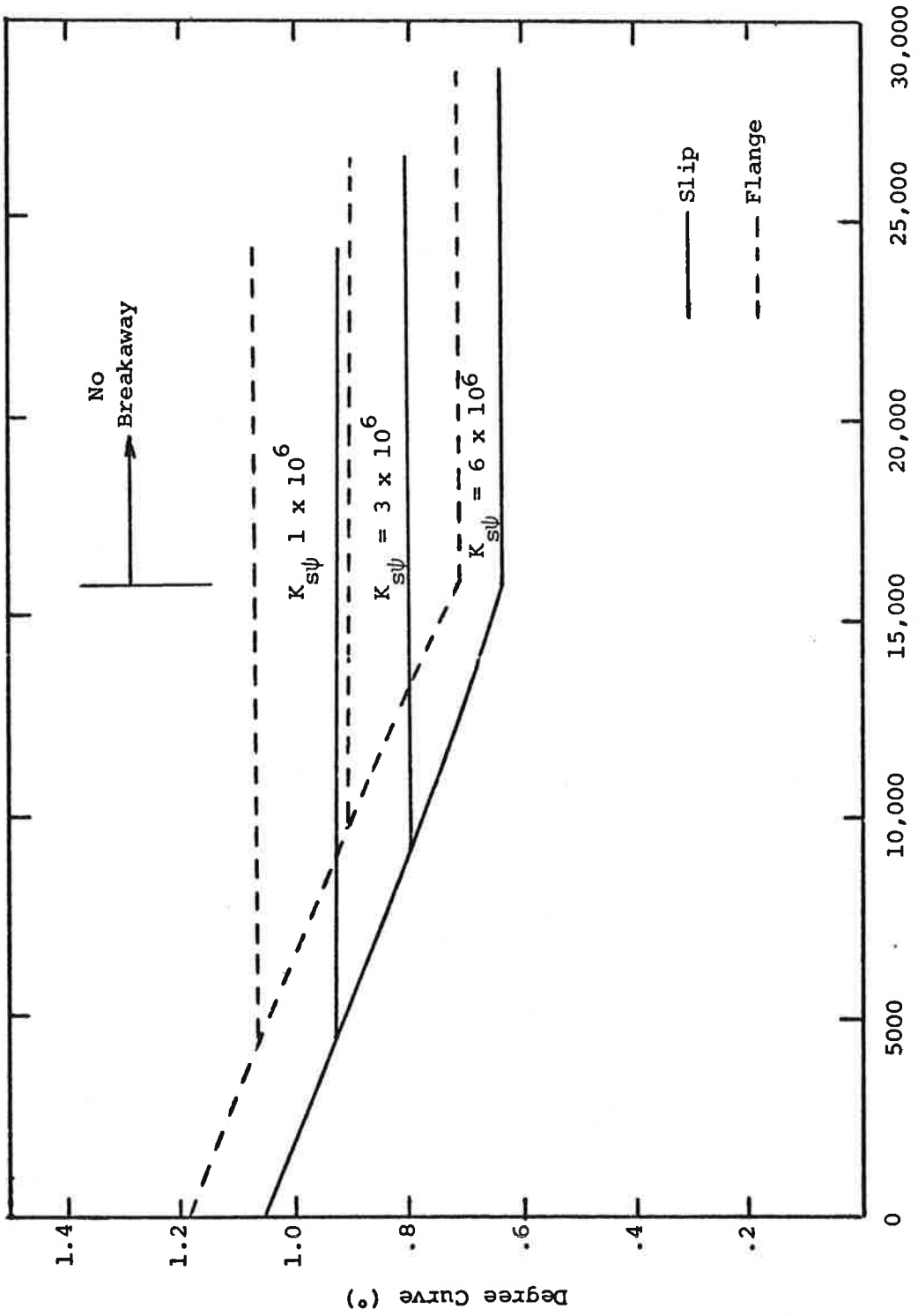

FIGURE A.2: DEGREE CURVE vs $T_{s\psi}$ FOR THREE VALUES OF $K_{s\psi}$

APPENDIX B: REPORT OF NEW TECHNOLOGY

This report describes the development of a design procedure for powered and unpowered rail passenger vehicles. Included in the procedure is a methodology for selecting truck design parameters for satisfying dynamic performance indices, such as ride quality, stability and curve negotiation. These performance indices are evaluated for a vehicle traveling at constant speed using dynamic computer models. Details of these innovative design procedures are described in Section 4.

☆ U. S GOVT. PRINTING OFFICE 1981 700-755 #338